

Photocatalytic Growth and Chemical Dissolution of Gold Structures for Advanced Neuromorphic Systems

Dissertation

for the degree of Doctor of Engineering
(Dr.-Ing)



Faculty of Engineering
Kiel University

by
Fatemeh Abshari

March, 2025

1st Referee: Prof. Dr. Martina Gerken
2nd Referee: Prof. Dr. Rainer Adelung

Date of oral examination: 28.03.2025

Journal Publications

F. Abshari, S. Veziroglu, B. Adejube, A. Vahl, and M. Gerken, “Photocatalytic Edge Growth of Conductive Gold Lines on Microstructured TiO₂-ITO Substrates,” *Langmuir*, vol. 40, p. 22, 2024, doi: 10.1021/acs.langmuir.4c02106.

F. Abshari, M. Paulsen, S. Veziroglu, A. Vahl, and M. Gerken, “ITO-TiO₂ Heterojunctions on Glass Substrates for Photocatalytic Gold Growth Along Pattern Edges,” *Catalysts*, vol. 14, no. 12, p. 940, 2024, doi: 10.3390/CATAL14120940.

F. Abshari, M. Paulsen, S. Veziroglu, A. Vahl, and M. Gerken, “Mimicking Axon Growth and Pruning by Photocatalytic Growth and Chemical Dissolution of Gold on Titanium Dioxide Patterns,” *Molecules*, vol. 30, no. 1, p. 99, 2024, doi: 10.3390/MOLECULES30010099.

Conference Contributions

F. Abshari, M. Paulsen, J. Schardt, and M. Gerken, “Photocatalytic Conductive Gold Deposition on Titanium Dioxide Templates Mimicking Axonal Growth”. *MRS Conference*, 2023.

J. Schardt, M. Paulsen, F. Abshari, S. Pei, and M. Gerken, “Optical Probes for Resonance-Enhanced Gold Growth on Nanooptical Substrates”. *ECS Meeting*, 2024.

F. Abshari, S. Veziroglu, A. Vahl, and M. Gerken, “Mimicking Axons by Conductive Metal Lines Formed by Photocatalytically Grown Gold”. *ECS Meeting Abstracts*, 2024.

F. Abshari, M. Paulsen, A. Vahl, S. Veziroglu, and M. Gerken, “Photocatalytic Growth and Chemical Dissolution of Gold Nanoparticles on TiO₂ Patterns”. *FMNT&NIBS Conference*, 2024.

Acknowledgements

First and foremost, I extend my deepest gratitude to my doctoral supervisor, Prof. Dr. Martina Gerken. Over the past three years, I have learned so much under her guidance. She has been a true source of inspiration, both professionally and personally, supporting me not only as an exceptional mentor but also with the warmth and care of a mother. Her unwavering encouragement and invaluable advice have been instrumental in shaping both my academic and personal growth.

I would like to express my heartfelt thanks to my beloved parents, Noor and Mojtaba, for their endless support and unconditional love. Even though we were separated by distance, they were always close to my heart, providing me with strength and motivation to overcome every challenge.

I am deeply grateful to my colleagues at the Integrated Systems and Photonics Group: Moritz, Igor, Jan, Fabio, Markus, Giuseppe, Jülf, Heike, Nathalie, Lucas, and the rest of the team. Working with them has been a truly enjoyable experience filled with great memories and an exceptional working atmosphere. A special thank you goes to Mohsen, whose guidance and support has been invaluable and who has inspired me in my personal life and professional career. I am also deeply appreciative of the friendship and unwavering support of my best friend, Nazanin.

I sincerely appreciate the support from the Deutsche Forschungsgemeinschaft (DFG, German Research Foundation) for funding my PhD project under Project-ID 434434223 – SFB 1461. Being part of the Collaborative Research Center 1461 has been a valuable opportunity to collaborate with experts from various fields and to further develop my research in a supportive and inspiring environment.

Finally, I would like to thank myself for persevering through challenges and hardships, for continuing on this journey despite the obstacles, and for finding joy in the meaning of life while striving for growth and progress.

The strength of a woman lies in her wisdom, not necessarily in physical force.

Abstract

This dissertation explores the photocatalytic growth and chemical dissolution of gold structures on titanium dioxide (TiO_2) substrates, focusing on their potential as foundational building blocks for neuromorphic systems. Neuromorphic engineering aims to replicate the adaptability and connectivity of biological neural networks, with the goal of advancing bio-inspired computing architectures.

The research investigates UV-stimulated photocatalytic processes to drive the localized growth of conductive gold lines on TiO_2 templates, offering a method to form axon-like connections. Complementarily, chemical dissolution using potassium iodide (KI) enables selective pruning of these structures, providing a framework for adaptive reconfiguration. By alternating growth and pruning, the study introduces a material-based approach to mimic neural plasticity, laying groundwork for future neuromorphic devices.

Key findings include the identification of critical parameters such as UV intensity, precursor concentration, and substrate architecture, which govern the morphology and connectivity of the gold structures. Advanced configurations, including patterned TiO_2 templates and microfluidic systems, were explored to enhance precision and functionality. These developments demonstrate the potential for creating adaptive and reconfigurable structures, contributing to the broader field of neuromorphic engineering.

This dissertation contributes to the understanding of photocatalytic growth and dissolution processes, providing insights that could contribute to the development of neuromorphic systems. The findings highlight the importance of dynamic material systems as building blocks for adaptive networks, advancing the exploration of bio-inspired computing architectures.

Zusammenfassung

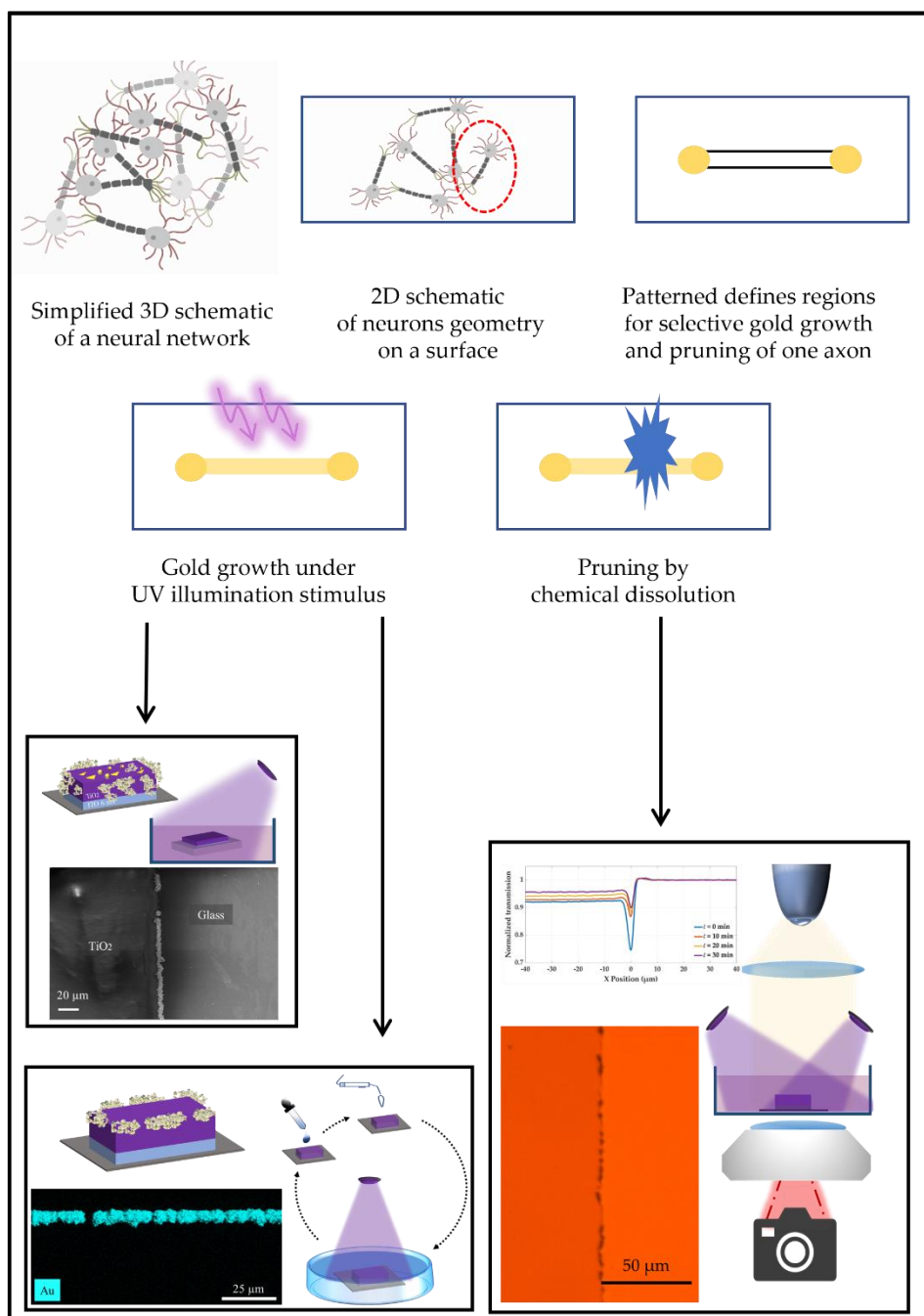
Diese Dissertation untersucht das photokatalytische Wachstum sowie die chemische Auflösung von Goldstrukturen auf Titandioxid (TiO_2)-Substraten und konzentriert sich dabei auf ihr Potenzial als grundlegende Bausteine für neuromorphe Systeme. Die neuromorphe Technik zielt darauf ab, die Anpassungsfähigkeit und Konnektivität biologischer neuronaler Netzwerke nachzubilden, um bioinspirierte Rechenarchitekturen voranzubringen.

Im Rahmen dieser Arbeit werden UV-stimulierte photokatalytische Prozesse erforscht, mit denen sich leitfähige Goldlinien lokal auf TiO_2 -Templates wachsen lassen – ein Verfahren zur Bildung axonähnlicher Verbindungen. Ergänzend ermöglicht die chemische Auflösung mittels Kaliumiodid (KI) eine gezielte Entfernung dieser Strukturen, wodurch ein Ansatz zur adaptiven Reorganisation entsteht. Durch den Wechsel von Wachstum und Abbau wird ein materialbasierter Mechanismus zur Nachbildung neuronaler Plastizität vorgestellt, der eine Grundlage für zukünftige neuromorphe Bauelemente bietet.

Zu den zentralen Ergebnissen zählen die Identifikation entscheidender Parameter – wie UV-Intensität, Vorläuferkonzentration und Substratarchitektur – die die Morphologie und Konnektivität der Goldstrukturen maßgeblich beeinflussen. Erweiterte Konzepte, darunter strukturierte TiO_2 -Templates und mikrofluidische Systeme, wurden untersucht, um die Präzision und Funktionalität zu steigern. Diese Entwicklungen verdeutlichen das Potenzial zur Realisierung adaptiver und rekonfigurierbarer Strukturen und leisten einen Beitrag zur Weiterentwicklung der neuromorphen Technik.

Die Arbeit liefert neue Erkenntnisse über photokatalytische Wachstums- und Auflösungsprozesse und eröffnet Perspektiven für die Entwicklung neuromorpher Systeme. Die Ergebnisse unterstreichen die Relevanz dynamischer Materialsysteme als Bausteine adaptiver Netzwerke und fördern die Erforschung bioinspirierter Rechenarchitekturen.

Graphical Abstract



Declaration

I hereby declare that I have written this dissertation entitled

Photocatalytic Growth and Chemical Dissolution of Gold Structures on Titanium Dioxide Substrates for Advanced Neuromorphic Systems

independently and without improper external assistance and that I have identified all quotations of other authors. Furthermore, this thesis has not been, partially or completely, submitted to any other university or institute in the context of an examination procedure. Parts of the content of the work have already been published in my scientific publications and are stated accordingly. I declare that the following work has been written in compliance with the rules of good scientific practice established by the German Research Foundation. AI tools were used solely for grammar correction and language refinement. I also declare that an academic degree has never been withdrawn and no relevant grounds for this are present.

14.04.2025, Kiel

Date, Place



Fatemeh Abshari

Contents

1. Introduction	1
1.1. Motivation	1
1.2. Specific Aims	4
1.3. Outline	5
2. Fundamentals.....	8
2.1. Neuromorphic Engineering and Bio-inspired System Design	10
2.1.1. Principles of Neuromorphic Engineering	11
2.1.2. Mechanisms of Synaptic Plasticity	13
2.2. Methods for Mimicking Brain Networks in Neuromorphic Engineering .	14
2.2.1. Overview of Current Techniques	15
2.2.2. Advantages of Photocatalysis for Adaptive Networks	17
2.3. Photocatalysis as a Method for Dynamic Network Formation	19
2.3.1. Photocatalytic Process and Mechanisms	20
2.3.2. Applications of Photocatalysis in Neuromorphic Systems.....	21
2.4. Components of the Photocatalytic System	22
2.4.1. Titanium Dioxide (TiO ₂) as the Photocatalytic Substrate	24
2.4.2. Gold Precursor Solution.....	25
2.4.3. UV Light Source and Illumination Conditions	27
2.4.4. Environmental and External Parameters.....	28
2.5. Photocatalytic Deposition and Control of Gold Nanostructures.....	31
2.5.1. Mechanism of Gold Nanoparticle Formation.....	32
2.5.2. Patterned Growth Using Lithography	33
2.6. Role of Indium Tin Oxide (ITO) in Directing Gold Growth	34
2.6.1. Formation of Schottky Barrier at TiO ₂ -ITO Interface	35
2.6.2. Heterojunctions in ITO-TiO ₂ Interfaces: Theoretical Insights and Applications.....	36
2.6.3. Influence of ITO Layer Thickness on Growth Patterns.....	38
2.7. Controlled Pruning of Grown Nanostructures for Neuromorphic Systems	38
2.7.1. Pruning of Axonal Structures in Neuromorphic Systems.....	40

2.7.2. Techniques for Mimicking Pruning in Neuromorphic Engineering	41
2.7.3. Chemical Dissolution for Pruning Using Potassium Iodide (KI)...	42
2.7.4. Parameters Affecting the KI Dissolution Process	44
2.8. Sequential Growth and Pruning Cycles for Adaptive Neuromorphic Networks.....	45
2.8.1. Integration of Growth and Pruning for Dynamic Networks.....	46
2.8.2. Balancing Photocatalytic Growth with KI Dissolution	47
2.8.3. Simulating Adaptive Neural Processes through Sequential Cycles	48
2.9. Flowchart of Lithography Process	49
3. Publications in Peer-Reviewed Journals.....	51
3.1. Photocatalytic edge growth of conductive gold lines on microstructured TiO ₂ -ITO substrates	53
3.1.1. Published Paper	54
3.2. ITO-TiO ₂ Heterojunctions on Glass Substrates for Photocatalytic Gold Growth along Pattern Edges	73
3.2.1. Published Paper	74
3.3. Mimicking Axon Growth and Pruning by Photocatalytic Growth and Chemical Dissolution of Gold on Titanium Dioxide Patterns	91
3.3.1. Published Paper	92
4. Conference Contributions.....	109
4.1. Photocatalytic Conductive Gold Deposition on Titanium Dioxide Templates Mimicking Axonal growth.....	109
4.1.1. Abstract.....	109
4.1.2. Presented Poster	111
4.2. Optical Probes for Resonance-Enhanced Gold Growth on Nano optical Substrates.....	112
4.2.1. Abstract.....	112
4.3. Mimicking Axons by Conductive Metal Lines Formed by Photocatalytically Grown Gold.....	114
4.3.1. Abstract.....	114
4.4. Photocatalytic Growth and Chemical Dissolution of Gold Nanoparticles on TiO ₂ Patterns	116

4.4.1. Abstract.....	116
5. Conclusion and Proposed Future Research	118
5.1. Summary and Conclusions.....	118
5.2. Proposed Improvements	120
6. Bibliography	122

Chapter 1

1. Introduction

In this chapter, the foundation and context of this research are established by exploring the driving motivations, defining the specific aims, and outlining the structure of the thesis. The content begins with a discussion of the motivation for investigating photocatalytic growth and chemical dissolution processes for gold structures on titanium dioxide (TiO_2) substrates, highlighting their relevance to advancing neuromorphic systems. The chapter further presents the aims of the thesis, emphasizing its contribution to the field of neuromorphic engineering. Finally, the structure of the thesis is outlined, providing an organized framework for the discussions and findings presented in subsequent chapters.

1.1. Motivation

Neuromorphic systems aim to emulate the complex functionality of biological neural networks, where neurons are interconnected by synaptic pathways to transmit and process information. In biological systems, neurons communicate via axons and dendrites, forming highly dynamic and adaptive networks capable of learning, memory retention, and signal modulation. Mimicking these processes in artificial systems requires precise engineering of network connectivity and adaptability [1]. Unlike conventional computing systems, neuromorphic systems rely on real-time reconfigurability, demanding innovative approaches to construct artificial networks that replicate these biological phenomena.

As the demand for energy-efficient, adaptive computing architectures grows, neuromorphic systems have emerged as a potential solution. These systems are essential for applications such as artificial intelligence, robotics, and sensory devices, where dynamic reconfiguration and efficient information processing are critical. However, existing methods for fabricating and controlling neural networks in these systems often lack the precision and adaptability needed to meet the growing complexity of real-world applications. Developing advanced techniques that mimic the adaptability and resilience of biological neural networks is, therefore, a pressing need [2].

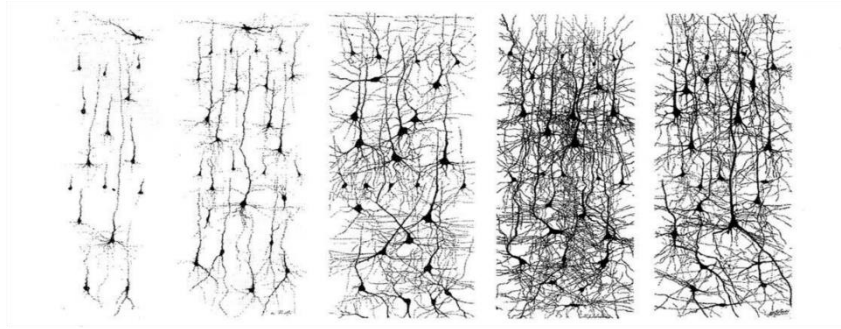
Photocatalytic growth and chemical dissolution represent innovative approaches for creating adaptive and reconfigurable networks in neuromorphic systems. Photocatalytic processes enable the controlled deposition of gold structures on substrates, forming pathways with tunable connectivity. Chemical dissolution, on the other hand, allows for the selective removal of these pathways, mirroring the natural processes of synaptic pruning in biological networks [3]. Together, these methods provide the precision, scalability, and adaptability required to fabricate networks capable of mimicking neural plasticity.

Integrating controlled growth and chemical pruning into neuromorphic engineering is a significant advancement toward creating brain-like adaptability in artificial systems. These processes mimic the neurobiological principles of growth and pruning, essential for learning and memory [4]. The ability to dynamically reconfigure networks by sequentially adding and removing connections introduces plasticity into neuromorphic devices enhancing their capability to respond to environmental stimuli and process complex information efficiently.

The dynamic plasticity of neural systems in biological organisms serves as a cornerstone for the development of neuromorphic systems, which aim to replicate this adaptability in artificial networks. The maturation of neuronal networks, as shown in Figure 1, exemplifies the intricate progression of connectivity and complexity that underpins learning, memory, and adaptability in the brain. Starting with sparse and linear connections in newborns, these networks

grow through branching and densification over time, achieving extensive dendritic arborization and synaptic complexity by four years of age. This natural process of network formation and refinement highlights the importance of adaptability and connectivity in achieving efficient and robust information processing.

In neuromorphic engineering, mimicking this dynamic progression is crucial for creating systems capable of self-organization and real-time reconfiguration. The ability to grow and adapt conductive pathways, akin to the biological processes depicted in Figure 1, forms the foundation of this research. By leveraging photocatalytic growth and selective pruning of gold nanostructures, this work seeks to emulate the developmental principles of neural plasticity, advancing the capabilities of neuromorphic systems for bio-inspired computing applications [5].



Newborn 1 Month 2 Months 2 Years 4 Years

Figure 1. Progressive development of neuronal networks from birth to four years of age. The images depict the increasing complexity and connectivity of dendritic and synaptic structures: (Newborn) Sparse and linear connections; (1 Month) Emergence of branching patterns; (2 Months) Enhanced dendritic density and synaptic connections; (2 Years) Extensive dendritic arborization and network complexity; and (4 Years) Fully interconnected and mature neuronal network. This progression exemplifies the plasticity of biological neural systems and serves as inspiration for developing adaptive neuromorphic architectures. This figure is used with permission from [5].

1.2. Specific Aims

The overarching aim of this thesis is to develop and refine methods for constructing and dynamically reconfiguring gold conductive pathways on TiO_2 substrates, tailored to the unique demands of advanced neuromorphic systems. By leveraging the dual processes of photocatalytic growth and chemical dissolution, this research seeks to emulate biological neural plasticity, enabling the creation of adaptive, reconfigurable networks for applications in neuromorphic engineering.

Central to this research is the development of innovative techniques for the photocatalytic growth of gold structures. This involves investigating the influence of key experimental parameters such as ultraviolet (UV) light intensity, precursor concentration, and reaction time on the morphology and connectivity of the deposited gold. The goal is to achieve precise, localized growth patterns that support high resolution conductive pathways, critical for emulating the functionality of biological synaptic connections.

Another critical aim is to establish chemical pruning methods for selective removal of gold structures, enabling the dynamic reconfiguration of neuromorphic networks. Using agents such as potassium iodide (KI), this research will explore how controlled dissolution processes can refine and adapt network connectivity, mirroring the biological mechanisms of synaptic pruning. The integration of these two processes growth and pruning forms the foundation for constructing dynamic, reconfigurable networks that respond to changing functional demands, much like biological neural systems.

This thesis also aims to implement sequential cycles of growth and pruning to simulate the dynamic processes observed in adaptive neural networks. By balancing the deposition and dissolution processes, it seeks to demonstrate how neuromorphic systems can achieve the flexibility and efficiency required for real-world applications, such as adaptive computing and memory storage. These processes will highlight the potential of photocatalytic and chemical methods to mimic the plasticity of biological networks, pushing the boundaries of current neuromorphic engineering capabilities.

Ultimately, this work aspires to advance the field of neuromorphic engineering by providing scalable, efficient methods for creating adaptive networks. The combination of innovative photocatalytic techniques and chemical dissolution processes addresses the challenges of replicating biological neural processes, paving the way for next-generation computing systems capable of real-time adaptability and reconfiguration. This research not only contributes to fundamental knowledge but also offers practical solutions for developing robust, cost-effective neuromorphic devices.

The central hypothesis of this thesis is that photocatalysis and chemical dissolution can be employed to mimic the processes of long-range connection growth and pruning observed in biological neural networks. This hypothesis is grounded in the idea that adaptive, reconfigurable networks are fundamental for neuromorphic systems to emulate the plasticity and functionality of biological brains.

To test this hypothesis, a series of experiments were conducted focusing on the photocatalytic growth of gold structures on TiO_2 substrates and their selective pruning using chemical dissolution with KI. These experiments aimed to evaluate whether these processes could effectively mimic the dynamic adaptability of axonal growth and pruning.

The overarching evaluation of this hypothesis is presented in the concluding sections of the thesis, where the experimental findings are analyzed to determine the validity of this approach. By integrating material-based techniques with biological principles, this thesis explores the extent to which photocatalysis and chemical dissolution can serve as building blocks for adaptive neuromorphic networks, bridging the gap between material science and neural engineering.

1.3. Outline

This thesis is organized to provide a thorough exploration of the development and application of photocatalytic growth and chemical dissolution techniques for neuromorphic systems. It begins with a foundational discussion of the principles and methodologies that form the scientific basis of the research,

followed by an in-depth presentation of the original contributions made through peer-reviewed publications, and concludes with a synthesis of findings and proposals for future work.

Chapter 2 focuses on the fundamental principles underlying this research. It introduces the key concepts of photocatalytic growth on TiO_2 substrates and chemical dissolution processes, highlighting their relevance to neuromorphic systems. The theoretical frameworks discussed in this chapter provide the foundation for understanding the experiments and analyses presented in subsequent sections, with emphasis on the interplay between controlled growth and pruning in creating adaptive networks.

In Chapter 3, the thesis showcases the original contributions of the research, as published in peer-reviewed journals. This chapter details the experimental approaches, methodologies, and findings, demonstrating the progression of the work. Each publication highlights a distinct aspect of the research, such as advancements in photocatalytic techniques, innovations in chemical pruning methods, and the integration of these approaches for dynamic and reconfigurable network formation.

Chapter 4 presents the key results and provides a detailed discussion of their implications. This chapter links the experimental findings to the broader goals of neuromorphic system development, emphasizing their significance in creating adaptive networks. The analyses presented here address the practical and theoretical advancements achieved through the research, offering insights into the role of photocatalytic and dissolution techniques in enhancing neuromorphic architectures.

Chapter 5 concludes the thesis with a summary of the main findings and a discussion of potential future research directions. The first section, Summary and Conclusions, highlights the contributions of the work and their relevance to advancing neuromorphic systems. The second section, Proposed Improvements, outlines recommendations for refining current methods and expanding the scope of the research, with an emphasis on scalability and real-world applications.

Finally, the thesis concludes with a comprehensive bibliography, documenting all the references used throughout the work. This section not only provides scientific context but also serves as a resource for further exploration by readers. Together, these chapters form a cohesive narrative, guiding the reader through the motivations, methodologies, and contributions of this research, and its potential impact on the field of neuromorphic systems.

Chapter 2

2. Fundamentals

The Fundamentals section of this thesis lays the scientific groundwork essential for understanding the methodologies and theoretical principles that inform this research. Neuromorphic engineering, inspired by the structure and adaptability of biological neural networks, is an evolving field aimed at developing bio-inspired computational systems with enhanced flexibility and efficiency. The goal of such systems is to replicate the brain's synaptic dynamics, including the formation, strengthening, and pruning of connections in response to external stimuli and internal demands, thus enabling artificial systems to process information in more sophisticated ways than conventional computers [6].

In biological neural networks, adaptability is achieved through a balance of synaptic plasticity mechanisms, which include both fast, localized changes and slower, global structural modifications within the network. Synaptic plasticity is a fundamental concept in neuromorphic engineering, as it provides the basis for creating artificial systems capable of real-time reconfiguration [7], which is critical for applications ranging from learning algorithms to adaptive signal processing.

To mimic these adaptive qualities, various methods have been explored within neuromorphic engineering. Among the promising approaches is photocatalysis, which enables precise control over the growth and dissolution of nanoscale structures through light-induced chemical reactions. Photocatalytic processes allow the emulation of synaptic dynamics by enabling both the controlled growth of conductive pathways and the selective pruning of these

connections [8]. This dual capability has positioned photocatalysis as a powerful tool for achieving the dynamic reconfigurability essential in neuromorphic networks.

This section begins by exploring the principles of neuromorphic engineering, emphasizing the key processes of synaptic plasticity that form the basis of biological adaptability. Following this, an overview of methods for mimicking brain networks in artificial systems is presented, with a focus on the advantages of photocatalysis as a mechanism for adaptive connectivity.

The components of the photocatalytic system are then analysed in detail, starting with TiO_2 , a semiconductor widely used for its stability, non-toxicity, and capacity to generate electron-hole pairs upon UV light exposure. TiO_2 is instrumental in this research as a substrate for gold nanoparticle growth [9], providing a controllable platform for structuring conductive paths. The role of gold precursor solutions, such as HAuCl_4 , is also discussed, with attention to how factors like solution concentration, pH, and additive presence influence nanoparticle morphology and growth kinetics.

Additionally, the influence of UV light and illumination conditions is investigated, as UV exposure is a fundamental aspect of photocatalytic activity. Factors such as UV intensity, exposure duration, and patterning techniques are analyzed to illustrate their effects on nanoparticle growth and morphology. Beyond illumination, environmental and external parameters such as temperature, ambient atmosphere [10], and applied electrical bias are explored to provide insight into the controllability and adaptability of these systems for neuromorphic applications.

Finally, attention is given to the controlled pruning of nanostructures, a process which emulates the selective elimination of neural connections observed in biological networks. In this work, pruning is achieved through chemical dissolution using KI, where conditions such as KI concentration and exposure time are modulated to allow precise control over the removal of gold structures. These processes, when applied sequentially with photocatalytic growth, create a dynamic cycle of growth and pruning, simulating the adaptive

processes inherent to neural networks and establishing a foundation for reconfigurable, neuromorphic networks.

In summary, this section provides a comprehensive foundation on neuromorphic engineering principles, photocatalytic processes, and dynamic nanostructure control methods, forming the basis for the experimental and analytical components of this thesis.

2.1. Neuromorphic Engineering and Bio-inspired System Design

Neuromorphic engineering is an interdisciplinary field that aims to replicate the structure and functional dynamics of biological neural networks within artificial systems. By emulating the brain's efficiency and adaptability, neuromorphic engineering provides a pathway toward computing architectures that can perform tasks such as pattern recognition, adaptive learning, and autonomous decision-making with a level of efficiency and flexibility unattainable by traditional computing systems [2], [11].

One of the central challenges in this field is achieving the kind of adaptive connectivity found in biological systems, where neural networks reorganize in response to stimuli through processes such as synaptic plasticity. This plasticity enables networks to form, strengthen, or remove connections, supporting learning and memory formation at both local and network-wide levels [12]. Mimicking these processes within artificial systems allows neuromorphic devices to dynamically reconfigure, adapting to new inputs and evolving with use, thereby establishing a foundation for robust and versatile bio-inspired computing systems [13].

While numerous approaches, including memristive devices, nanowire networks, and electrolyte gating, have been investigated to replicate these adaptive qualities, photocatalytic methods present a distinctive advantage. Photocatalysis enables precise, controlled growth and dissolution of microscale conductive pathways, simulating the processes of synaptic formation and pruning observed in biological networks. This research employs photocatalytic techniques to grow and selectively remove gold nanostructures on TiO_2 substrates,

forming dynamically reconfigurable networks that closely mimic adaptive neural connectivity [14], [15].

This thesis builds upon these principles of neuromorphic engineering by implementing a photocatalytic system that supports cyclic growth and pruning of conductive pathways. This capability is fundamental for creating bio-inspired computing systems capable of self-organization, reconfiguration, and adaptability in real-time. In the following sections, we will further explore the core principles of neuromorphic engineering, including an in-depth look into synaptic plasticity and its role in establishing adaptable neural networks.

2.1.1. Principles of Neuromorphic Engineering

Neuromorphic engineering, as a concept, is rooted in the ambition to replicate the computational principles observed in biological neural networks, aiming to achieve brain-like efficiency, adaptability, and robustness. At its core, neuromorphic engineering seeks to bridge the gap between the human brain's capacity for complex cognitive tasks and the rigid architectures of conventional computing systems. Traditional von Neumann architectures, where data storage and processing are separate, face significant limitations when attempting to emulate the brain's highly interconnected and adaptive network. By contrast, neuromorphic architectures integrate storage and processing, enabling real-time adaptability and localized learning, key characteristics that define biological neural networks [2], [11].

In neuromorphic systems, one essential principle is the ability to mimic synaptic plasticity, where connections between nodes (analogous to synapses between neurons) are dynamically reconfigured based on learning processes. This adaptability is fundamental to functions such as memory formation, recognition, and decision-making, allowing the system to evolve with each new piece of information. Synaptic plasticity within neuromorphic devices can be achieved through memristive elements, which emulate the behavior of biological synapses by changing their resistance states in response to electrical stimuli, thereby “remembering” past interactions [16]. Memristors, first theorized and later demonstrated by Strukov et al., act as resistive memory components

that adjust their resistance based on previous electrical activity, making them ideal candidates for neuromorphic computing systems [17].

Moreover, the design of neuromorphic architectures goes beyond hardware components and seeks to emulate neural processes at various scales, from individual synaptic connections to complex, network-wide behaviors. In this framework, brain-inspired architectures provide models that leverage connectivity patterns and computational efficiency found in the brain, such as hierarchical processing, parallelism, and redundancy, to achieve advanced functions with low energy consumption [18]. The work of Kendall and Kumar on brain-inspired computing explores how these principles can be translated into electronic circuits, presenting a foundation for neuromorphic devices that not only replicate structural aspects but also emulate functional behaviors seen in biological networks [6].

Neuromorphic engineering also incorporates advanced materials and device architectures designed to simulate the complex signaling and learning dynamics of neurons and synapses. Sangwan and Hersam's research into neuromorphic nanoelectronic materials has shown how materials with specialized properties can replicate synaptic functions, enabling localized adaptability and high-density storage in compact systems [7]. The field has also seen developments in devices utilizing nanoionic materials, which leverage ionic movement within the material to produce resistive switching, thereby allowing controlled changes in connectivity that are critical for adaptive, reconfigurable systems [8].

In summary, the principles of neuromorphic engineering emphasize creating systems capable of adaptive learning, low-energy computation, and structural flexibility. These systems are intended to emulate the functional organization and efficiency of the brain, thereby offering promising advancements in fields such as artificial intelligence, sensory processing, and autonomous decision-making. The next section will delve into the mechanisms of synaptic plasticity, a foundational concept that enables the adaptability essential for neuromorphic systems to perform complex, dynamic computations.

2.1.2. Mechanisms of Synaptic Plasticity

Synaptic plasticity is a core mechanism that enables the adaptability and learning capabilities of biological neural networks, allowing connections between neurons (synapses) to strengthen or weaken in response to experience. This adaptability supports processes like memory formation, learning, and decision-making, and is a crucial concept for neuromorphic engineering, where the goal is to emulate the brain's functionality. Research has shown that neuromorphic systems can replicate synaptic plasticity by using adaptable materials and architectures, which enable real-time reconfiguration based on previous interactions [19].

Plasticity in biological systems is generally divided into short-term plasticity and long-term plasticity. Short-term plasticity involves temporary adjustments in synaptic strength, typically on the order of milliseconds to minutes, which are essential for immediate signal processing. In contrast, long-term plasticity results in sustained changes that can last from hours to a lifetime, forming the basis for long-term memory and learning. Advanced neuromorphic devices are designed to emulate these two types of plasticity through different materials and mechanisms. For instance, short-term plasticity can be achieved through volatile switching in nanoionic devices, where ionic movement temporarily alters conductivity [20]. Long-term plasticity, on the other hand, is often achieved in non-volatile devices that retain their state over extended periods, which is fundamental for applications requiring stable memory [20].

Recent innovations in memristive materials and nanoionic devices have provided a platform to mimic these plasticity mechanisms effectively. Memristive devices, known for their ability to “remember” previous states, exhibit resistance changes in response to electrical stimuli, similar to synaptic adjustments in biological systems. For instance, a previous study [21] demonstrated that by modulating ionic diffusion within memristive devices, it is possible to emulate both fast and slow changes in synaptic strength, enabling neuromorphic systems to replicate short-term and long-term plasticity in one device.

In addition to memristive materials, neuromorphic research has explored heterosynaptic plasticity, a form of plasticity where changes in one synapse

influence neighboring synapses. This property is vital for associative learning, where related information becomes linked through experience, a function that is fundamental to human cognition. Recent studies [22] have demonstrated heterosynaptic plasticity in artificial synaptic networks, showing that neuromorphic devices can achieve complex, biologically realistic behaviors through interconnected memristive arrays.

Architectural designs in neuromorphic systems also play a crucial role in accurately replicating synaptic plasticity. Many neuromorphic devices now incorporate layered or hierarchical architectures that support spatial and temporal pattern recognition, similar to the processing functions in biological neural circuits. These devices develop architectures that allow neuromorphic systems to perform hierarchical processing, enhancing their ability to handle tasks like sensory data analysis and decision-making in real-time, further mimicking brain-like adaptability [23].

In conclusion, the mechanisms of synaptic plasticity provide the foundation for building neuromorphic systems capable of adaptive learning and memory. By incorporating short- and long-term plasticity, as well as heterosynaptic interactions, neuromorphic engineering achieves a level of complexity and adaptability akin to biological systems. These mechanisms are essential for advancing neuromorphic applications, particularly in fields requiring high adaptability and real-time processing.

2.2. Methods for Mimicking Brain Networks in Neuromorphic Engineering

Replicating the adaptability and connectivity of biological neural networks within artificial systems is central to neuromorphic engineering. Biological networks achieve this adaptability through synaptic plasticity, enabling connections between neurons (synapses) to strengthen, weaken, form, or dissolve based on interactions and experiences. This capacity for continual adaptation supports essential cognitive processes such as learning, memory, and decision-making [24]. Achieving similar plasticity in artificial systems is

fundamental to creating neuromorphic systems that can operate with real-time reconfigurability and efficiency [25].

Various methods have been developed to emulate these adaptable properties in neuromorphic networks. Memristive devices are among the most widely explored, known for their ability to emulate both short- and long-term synaptic changes via resistive switching. Through ionic movement within the memristor material, these devices can simulate the formation and modification of conductive pathways, mirroring synaptic plasticity at a hardware level [21]. Additionally, nanowire networks provide self-organized conductive pathways that reconfigure based on applied electrical fields, simulating neural adaptation processes. While these methods allow some degree of reconfiguration, many conventional techniques struggle with selective, reversible control over synaptic pathways, which limits the potential for fully dynamic neuromorphic systems [26].

Photocatalytic methods offer a promising alternative due to their ability to control the growth and dissolution of conductive nanostructures using light. By utilizing photocatalytic growth of gold nanostructures on TiO_2 substrates, this approach enables on-demand creation of conductive connections under UV exposure, while selective dissolution of these structures facilitates adaptive pruning. This growth-pruning cycle directly emulates biological synaptic plasticity, establishing pathways that can be selectively created or removed, thereby creating a dynamically reconfigurable network [27]. Such an approach closely mirrors the functionality and connectivity of biological neural networks, supporting adaptive learning processes within artificial systems [7].

The following sections will introduce current techniques for mimicking neural networks and examine how photocatalysis uniquely enables the development of adaptive, bio-inspired systems capable of real-time reconfiguration.

2.2.1. Overview of Current Techniques

Replicating the adaptive qualities of biological neural networks within artificial systems is central to neuromorphic engineering, where synaptic plasticity enables learning and reconfigurable connectivity. Various methods have

been developed to emulate this plasticity in neuromorphic networks, with each method offering a unique mechanism to achieve dynamic, responsive behavior.

Memristive devices are among the most extensively studied components for neuromorphic systems due to their inherent ability to emulate synaptic behavior by adjusting resistance based on previous electrical inputs. This resistive switching mimics the process of “learning” by encoding past interactions in the device’s conductance state. The dynamic modulation of resistance in memristive devices enables both short-term and long-term plasticity, which are essential for adaptive neuromorphic networks [28]. By providing energy-efficient and scalable solutions, memristors are integral to the design of compact, brain-inspired systems.

Nanowire networks represent another promising approach due to their self-organizing properties, where microscale conductive pathways emerge and reconfigure in response to external stimuli. These networks consist of interconnected nanowires that form, strengthen, or dissolve connections depending on applied electrical fields, thereby mimicking the flexible connectivity of biological neural networks. The capacity for self-organization and collective switching allows nanowire networks to demonstrate adaptive responses similar to synaptic plasticity, although precise control over individual synaptic pathways within these networks remains a challenge [29].

Electrolyte gating is another method that has gained attention for its ability to mimic synaptic behavior via ionic transport. In electrolyte-gated devices, ions in an electrolyte solution are directed toward specific pathways under an applied voltage, modifying conductivity in a manner similar to biological synapses. This ionic modulation enables low-energy operation and tunable, reversible connections, making it suitable for applications where adaptability and low power consumption are critical. However, maintaining long-term stability in electrolyte-gated systems is an ongoing area of research for neuromorphic applications [30].

Each of these techniques, i.e., memristive devices, nanowire networks, and electrolyte gating, plays a critical role in advancing neuromorphic engineering by providing mechanisms for reconfigurable, adaptive connectivity.

Yet, challenges remain in achieving precise, repeatable control over individual connections, which is necessary for fully dynamic, brain-inspired computing systems. As these methods continue to evolve, they serve as the foundation for innovative hybrid approaches that push the boundaries of adaptability in neuromorphic systems.

2.2.2. Advantages of Photocatalysis for Adaptive Networks

Photocatalysis offers a unique approach in neuromorphic engineering for creating adaptive networks, leveraging light-driven chemical reactions to control the growth and dissolution of conductive pathways. This method stands out due to its precise, reversible control over network connectivity, making it an ideal solution for emulating synaptic plasticity and adaptability in artificial neural networks. By enabling both the formation and selective removal of conductive paths, photocatalysis provides an analogue to biological processes of synaptic strengthening and pruning, allowing for real-time reconfigurability [27]. Figure 2 illustrates photocatalytic growth process of gold structures on a TiO_2 substrate under UV light.

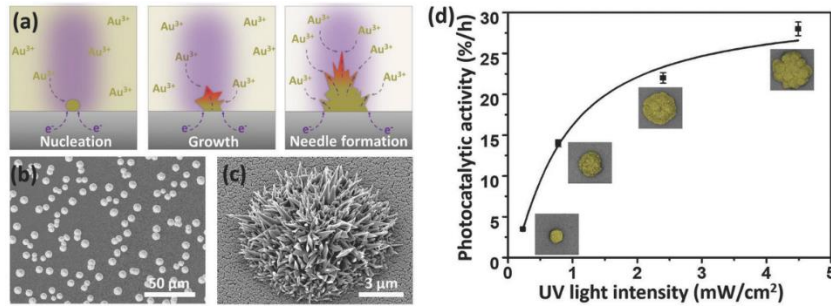


Figure 2. Photocatalytic growth process of gold structures on a TiO_2 substrate under UV light. (a) A schematic illustration showing the stages of nucleation, growth, and needle formation as Au^{3+} ions are reduced to gold by photogenerated electrons. (b) SEM image displaying the initial nucleation sites on the TiO_2 substrate. (c) SEM image highlighting the mature, needle-like gold nanostructures after growth. (d) Graph showing the relationship between UV light intensity and photocatalytic activity, demonstrating how higher intensities lead to increased growth rates. This figure is reproduced with permission from [27]. Copyright 2018 John Wiley and Sons.

One of the primary advantages of photocatalytic methods is spatial precision in connection growth. Conductive pathways can be initiated and extended along predefined patterns on a TiO_2 substrate by controlling exposure to UV light. This targeted growth process emulates the synaptic connectivity observed in biological neural networks, where connections form dynamically in response to environmental stimuli. For instance, recent studies demonstrated that localized UV irradiation on TiO_2 induces gold nanoparticle deposition along desired paths, providing a controllable and reproducible way to structure neuromorphic networks [7].

Another significant advantage of photocatalysis is the ability to control connection dissolution, which mimics synaptic pruning in biological systems. Using specific chemical agents, such as KI, grown gold structures can be selectively dissolved, allowing for the removal of connections no longer needed. This dual capability of growth and dissolution in a single system supports adaptive networks capable of reconfiguration based on functional requirements or changes in input, much like neural networks in the brain that continuously reorganize to optimize processing efficiency [7].

Photocatalysis also operates with relatively low energy requirements, as the primary drivers are light and simple chemical agents, making it energy-efficient compared to electrical or heat-based processes for altering conductivity. This low-energy operation aligns with the efficiency seen in biological processes and is essential for scalable neuromorphic systems intended for real-world applications [25]. Additionally, the use of light as an external stimulus provides a non-invasive way to control network connectivity, reducing wear on the device and potentially increasing its longevity [31].

In summary, photocatalysis offers several distinct advantages for creating adaptive networks in neuromorphic systems, including precise control over growth, reversible pruning capabilities, low energy demands, and non-invasive operability. These qualities make photocatalytic methods particularly promising for developing flexible and scalable neuromorphic architectures capable of real-time adaptability.

2.3. Photocatalysis as a Method for Dynamic Network Formation

Photocatalysis has emerged as a promising approach in neuromorphic engineering due to its capacity to enable dynamic, adaptable network formation using light-driven chemical reactions. This method offers an innovative way to control the growth and dissolution of conductive pathways, allowing for real-time reconfiguration of network connectivity. In neuromorphic systems, where adaptability and self-organization are crucial, photocatalysis provides a controlled mechanism for emulating synaptic plasticity, i.e., the ability to form, strengthen, or prune connections based on stimuli, similar to processes in biological networks [32].

The core of photocatalytic network formation lies in the selective deposition of conductive materials, such as gold, on a semiconductor substrate like TiO_2 . When exposed to UV light, TiO_2 generates electron-hole pairs, which facilitate the reduction of metal ions (e.g., Au^{3+}) in solution, depositing them as conductive metal on the substrate surface. This photo-induced process enables the precise formation of conductive paths that can act as “synapses” in neuromorphic networks, responding dynamically to external light stimuli. Through careful control of light intensity, exposure time, and chemical environment, photocatalysis allows for customizable and reversible network configurations, addressing the need for flexible, reconfigurable systems in neuromorphic computing [27].

One of the distinctive advantages of photocatalysis in dynamic network formation is its ability to support sequential growth and pruning cycles. The conductive pathways formed on TiO_2 can be selectively dissolved using chemical agents, such as KI, which facilitates the removal of connections, emulating the synaptic pruning seen in biological networks. This cyclic growth and pruning capability enable adaptive connectivity within the network, reflecting changes in input and environmental conditions, which is crucial for tasks like learning and memory [7].

The non-invasive, low-energy operation of photocatalysis also aligns well with the goals of neuromorphic engineering. Light-based control over the network reduces the physical wear that may result from electrical or mechanical control methods, potentially increasing the system's durability. Furthermore, the energy requirements for photocatalysis are relatively low, making it a suitable approach for scalable neuromorphic systems intended for real-time adaptability and efficiency in artificial intelligence applications [31].

In the following sections, we will describe the specific mechanisms underlying the photocatalytic process and examine how this approach is applied within neuromorphic systems to achieve dynamic, adaptive network formation.

2.3.1. Photocatalytic Process and Mechanisms

The photocatalytic process leverages light-driven chemical reactions to create and modify conductive pathways on semiconductor surfaces, a method well-suited for dynamic network formation in neuromorphic systems. TiO_2 is commonly used as a substrate for these reactions due to its photocatalytic properties, stability, and non-toxicity. Under UV light exposure, TiO_2 generates electron-hole pairs; electrons in the conduction band and holes in the valence band can participate in reduction-oxidation (redox) reactions. These reactions enable the deposition of conductive materials, such as gold, onto the TiO_2 surface, forming customizable pathways that act as synaptic connections in neuromorphic networks [25].

The formation of conductive pathways through photocatalysis begins with the photogeneration of electron-hole pairs on the TiO_2 surface when exposed to UV light. These electrons can reduce metal ions, such as Au^{3+} ions in solution, leading to the deposition of metallic gold on the substrate. The photocatalytic reduction of metal ions is influenced by several parameters, including UV light intensity, exposure duration, and the concentration of metal ions. Studies have demonstrated that higher light intensities and longer exposure times can increase deposition rates and alter the morphology of the gold structures, allowing for precise control over the shape and distribution of the conductive pathways [10].

Nucleation and growth dynamics play a critical role in the photocatalytic process, affecting the connectivity and stability of the deposited structures. Initial nucleation sites form as Au^{3+} ions are reduced, and subsequent growth of these nucleation sites can be modulated by adjusting the photocatalytic conditions. This growth process can produce different morphologies, including spherical, needle-like, or branched structures, depending on the photocatalytic environment. For instance, gold nanostructures grown under controlled UV light intensities and ion concentrations have shown needle-like formations, which are suitable for forming interconnected networks that mimic synaptic connectivity in biological systems [7].

Another essential aspect of the photocatalytic mechanism is the ability to dissolve these structures selectively, which is analogous to synaptic pruning in biological neural networks. By introducing a chemical agent like KI, which can dissolve the deposited gold, selective pruning of connections becomes possible. This dissolution process allows for reversible and adaptive changes in network connectivity, supporting a cyclic process of growth and pruning that enhances the network's ability to adapt to new stimuli or conditions [33].

Photocatalytic processes are also energy-efficient and non-invasive, primarily driven by UV light without the need for high temperatures or electric fields, which aligns well with the goals of neuromorphic engineering. This low-energy, light-driven method reduces wear and potential damage to the device, thus improving durability and making it scalable for real-world applications. Furthermore, the precision in photogenerated pathways enables the creation of adaptable, high-density networks, which are essential for neuromorphic systems aiming to emulate complex neural behaviors [31].

2.3.2. Applications of Photocatalysis in Neuromorphic Systems

Photocatalysis is emerging as a powerful method in neuromorphic systems, providing a means to establish and modify adaptive networks in a manner analogous to biological neural systems. This approach leverages light to initiate chemical reactions that can dynamically alter conductive pathways, enabling neuromorphic networks to reconfigure in response to environmental inputs.

This capability for real-time adaptability supports applications in artificial intelligence, where systems require continual learning and evolution [34].

One significant application of photocatalysis in neuromorphic systems is in the formation of highly customizable conductive pathways. Using UV light on photocatalytic materials like TiO_2 , researchers can generate electron-hole pairs that facilitate the growth of metallic nanoparticles along desired paths. This process mimics synaptic strengthening in biological systems and provides spatial control over connectivity, an essential factor in creating neuromorphic networks that can reconfigure dynamically as learning progresses [35].

In addition to connection formation, photocatalytic methods allow for selective pruning of these conductive pathways, analogous to synaptic pruning in the brain. This selective dissolution process is achievable through specific chemical agents that break down previously formed connections. The ability to remove unnecessary or redundant pathways on-demand enables the system to optimize its structure over time, enhancing both efficiency and adaptability [36].

Photocatalysis is particularly advantageous because it is a non-invasive and low-energy process. Using light rather than electrical currents minimizes wear on the system, increasing its durability. This quality is especially valuable in applications requiring long-term stability, such as sensory systems in robotics, where minimal intervention is preferred for sustained operation [37].

Finally, photocatalytic processes are energy-efficient, aligning with the requirements of scalable neuromorphic systems. Unlike other methods that consume considerable power and generate heat, photocatalysis requires only light and basic chemical agents, making it a highly efficient choice for low-power neuromorphic devices intended for applications such as wearable technologies and environmental sensing [38].

2.4. Components of the Photocatalytic System

The construction of adaptive neuromorphic systems using photocatalysis requires a combination of specific components, each playing a distinct role in enabling responsive, reconfigurable behavior. Central to this process are the

selection of a photocatalytic substrate, usually TiO_2 , a gold precursor solution that provides metal ions for the creation of conductive pathways, a UV light source to initiate the photocatalytic reactions, and controlled environmental conditions that influence reaction efficiency and stability. These components together enable the creation of dynamic networks that mirror the synaptic plasticity found in biological neural networks, offering a pathway to real-time reconfiguration in neuromorphic devices [39].

Photocatalytic substrates need to support efficient photo-induced electron-hole pair generation, with TiO_2 being one of the most commonly used materials due to its high stability, availability, and strong oxidative potential under UV light. When illuminated, TiO_2 generates electron-hole pairs that drive reduction-oxidation reactions, which are essential for the deposition and modulation of conductive pathways on its surface [40]. This ability to facilitate controlled nanoparticle deposition aligns with the synaptic connectivity found in neuromorphic architectures, where connectivity can be spatially managed to emulate biological neural networks [41].

The gold precursor solution, typically consisting of gold ions (Au^{3+}), is introduced to interact with the photogenerated charges on the TiO_2 surface, promoting the reduction of Au^{3+} ions to metallic gold. This reduction forms conductive gold nanoparticles selectively along illuminated regions, enabling the formation of precisely patterned conductive pathways. These pathways are crucial for emulating the adaptable synaptic links within artificial neural networks, allowing for growth and dissolution in response to stimuli [42].

The UV light source is integral to initiating the photocatalytic process by providing the energy required for electron excitation within TiO_2 . Key parameters such as wavelength, light intensity, and exposure duration—must be carefully controlled to regulate the rate of electron-hole generation and, consequently, the growth and dissolution of conductive pathways [43]. Optimizing these illumination conditions allows the system to achieve efficient, low-power reconfiguration, essential for neuromorphic applications.

Finally, environmental factors, including temperature, humidity, and surrounding gas composition, have a significant impact on photocatalytic activity

and device stability. Elevated temperatures and controlled humidity levels can enhance reaction kinetics, while certain gases, such as oxygen, influence the longevity and stability of the photocatalytic process. Proper control over these conditions ensures reliable and reproducible neuromorphic functionality.

2.4.1. Titanium Dioxide (TiO₂) as the Photocatalytic Substrate

Titanium dioxide (TiO₂) has emerged as the substrate of choice in photocatalytic applications, and its use in neuromorphic systems is well-founded due to a unique set of chemical and physical properties that align closely with the demands of dynamic, adaptive network formation. The robustness of TiO₂ as a substrate in photocatalytic processes stems from its chemical stability, high oxidation potential, and the efficient generation of electron-hole pairs under UV illumination. These characteristics are particularly beneficial in neuromorphic engineering, where the goal is to emulate synaptic behaviors like strengthening, weakening, and pruning of connections in a highly controlled, reversible manner [44].

Under UV illumination, TiO₂ absorbs photons with energy greater than or equal to its bandgap (~3.2 eV for anatase TiO₂), which excites electrons from the valence band to the conduction band, leaving behind holes in the valence band. This electron-hole pair generation is the catalyst for redox reactions on the surface of TiO₂, which can induce deposition or removal of materials like metal nanoparticles in a spatially controlled manner. The photogenerated electrons reduce metal ions in the surrounding solution to form conductive nanoparticles, creating pathways that can mimic the synaptic connections between neurons in a biological brain. This substrate, therefore, allows for patterned, customizable connectivity in neuromorphic systems, responding dynamically to UV exposure [45].

In practical terms, TiO₂ serves as a stable base on which metal nanoparticles, often gold, are deposited to form conductive paths. The deposition is achieved by illuminating TiO₂ with UV light in the presence of a metal precursor solution, allowing electrons to drive the reduction of metal ions at specific locations. This process is analogous to synaptic strengthening and provides a

means for forming new connections within the artificial network. Through careful control of UV illumination patterns, researchers can specify where conductive paths form, introducing a high level of spatial control that is vital for adaptive neuromorphic architectures [46]. TiO_2 's photoactivity thus provides the substrate with an innate programmability, facilitating configurations that can change over time, akin to learning in biological systems.

Beyond facilitating the formation of conductive paths, TiO_2 is renowned for its durability, maintaining functional integrity over extended periods of UV exposure without degrading, a crucial property for systems designed for long-term neuromorphic operations. The resistance of TiO_2 to photocorrosion ensures that the substrate can sustain numerous cycles of network reconfiguration without significant wear, making it suitable for applications like environmental monitoring or wearable electronics, where consistent performance over long periods is necessary [47]. Additionally, the wide bandgap of TiO_2 limits its activation to UV light, which allows precise on/off control over its photocatalytic activity, reducing unintended activation under visible light. This selectivity enhances the energy efficiency of TiO_2 -based neuromorphic systems, contributing to the low-power requirements essential for portable and wearable neuromorphic applications [48].

In summary, TiO_2 's role as a photocatalytic substrate is foundational in the creation of neuromorphic systems that aim to emulate the brain's adaptability. Its stability, controllable electron-hole pair generation, and selective reactivity under UV light collectively make TiO_2 an ideal substrate for systems requiring real-time adaptability and reconfiguration with low power consumption.

2.4.2. Gold Precursor Solution

The gold precursor solution, primarily chloroauric acid (HAuCl_4), is fundamental in the photocatalytic growth of gold nanoparticles on TiO_2 substrates, supporting the development of neuromorphic systems through the creation of adaptive, conductive pathways. HAuCl_4 offers significant advantages due to its stability in aqueous solution and its well-defined reduction pathway, which

enables precise control over the morphology and distribution of gold nanoparticles. This level of control is essential for constructing neuromorphic networks that emulate biological synaptic behavior, as it allows the formation of consistent, reliable conductive paths that can adjust and reconfigure based on external stimuli, mimicking the adaptive nature of neural connections in the brain [49] active precursor ions, such as Ag^+ and Pt^{4+} , have been explored in photocatalytic applications, yet HAuCl_4 remains preferred in neuromorphic designs due to the chemical stability and superior conductivity of gold. Silver ions can lead to less stable structures, as they are prone to oxidation and dissolution, which can reduce the long-term reliability of neuromorphic pathways. Platinum ions, while conductive, often require harsher reduction conditions and higher energy inputs, making them less practical for low-energy systems. Gold precursors thus offer a unique combination of stability, efficiency, and ease of reduction, facilitating the formation of durable, conductive networks that are critical for neuromorphic functionality [50].

The concentration of HAuCl_4 and the pH of the solution play crucial roles in determining the morphology, density, and growth rate of gold nanostructures. High precursor concentrations can produce denser nanoparticle layers, increasing conductivity but risking agglomeration if not carefully controlled. Lower concentrations offer finer control over particle size, ideal for neuromorphic systems that require precision in network formation. The pH of the solution is another factor; acidic conditions accelerate reduction by providing an abundance of protons, which can speed up nanoparticle formation. However, too low a pH can destabilize the TiO_2 substrate and cause uneven growth. Typically, a pH range of 2-4 is found to balance growth rate with particle stability, maintaining the uniformity required for high-performance neuromorphic systems [51].

Additives, such as isopropanol, serve as hole scavengers, enhancing the efficiency of photocatalytic reactions by stabilizing photogenerated holes on TiO_2 . This stabilization prevents rapid electron-hole recombination, allowing for a more efficient reduction of Au^{3+} to Au, and in turn, facilitating the consistent growth of nanoparticles. Stabilizers, such as citrate ions, can further

control nanoparticle shape, which may influence the conductive properties of the networks formed. This level of control is instrumental in creating neuromorphic pathways that can respond dynamically to electrical inputs, supporting a range of synaptic behaviors critical to neural network simulation [52].

Other parameters, such as UV illumination intensity, and the surface properties of the TiO_2 substrate, also significantly affect gold nanoparticle formation. Elevated temperatures enhance the reduction rate of HAuCl_4 , leading to faster nanoparticle growth, although they can cause irregularities in particle shape if not precisely regulated. Intense or prolonged UV illumination can accelerate electron-hole generation, thereby boosting reduction rates, but it may also increase agglomeration risks. The TiO_2 substrate's surface roughness and morphology impact the nucleation and growth of gold particles; a rougher surface provides more nucleation sites, leading to denser networks, which may enhance connectivity but reduce the uniformity crucial for neuromorphic applications [27].

2.4.3. UV Light Source and Illumination Conditions

The choice of UV light source and precise control over illumination conditions are pivotal in photocatalytic applications, particularly when using TiO_2 substrates for controlled gold nanoparticle growth. The intensity, wavelength, duration, and angle of UV illumination significantly affect the photocatalytic processes, influencing the morphology, size, and distribution of gold nanostructures. These parameters are essential in applications that require high precision, such as neuromorphic system development, where structured, predictable pathways of nanoparticles are required to simulate synaptic behavior. UV wavelength selection plays a primary role, as the energy provided must be sufficient to excite the TiO_2 substrate, typically requiring UV light in the 300-400 nm range. This excitation leads to electron-hole pair formation in TiO_2 , essential for the reduction of HAuCl_4 and subsequent deposition of gold nanoparticles. Studies have shown that shorter UV wavelengths (e.g., 300-350 nm) offer more energetic excitation, leading to more rapid electron-hole generation and, consequently, faster nucleation and growth of gold nanoparticles [53], excessive

energy can sometimes lead to agglomeration or uneven deposition, which must be managed to maintain uniformity in particle growth.

Light intensity, commonly measured in mW/cm^2 , directly influences the rate of electron-hole pair production in the TiO_2 substrate. High-intensity UV illumination increases the density of available charge carriers, facilitating faster reduction rates and denser particle deposition. However, if the intensity is too high, it can cause rapid growth that lacks fine control, resulting in larger, less defined nanoparticles. For applications requiring high-resolution neuromorphic patterns, moderate UV intensity is often preferable to allow for controlled, gradual deposition [54].

The UV exposure is another critical factor. Prolonged UV exposure can lead to larger particle sizes due to continued growth, which may enhance conductivity but reduce the spatial resolution necessary for neuromorphic applications. Shorter exposure times, on the other hand, allow for the formation of smaller, more precisely defined particles, which are better suited for creating complex networks. Experiments demonstrate that exposure times of 5-15 minutes achieve a balance between sufficient deposition and controlled particle size [55].

The angle of illumination also impacts nanoparticle formation, especially in systems where 3D structural control is desired. Direct illumination perpendicularly onto the substrate ensures uniform growth across the surface, while angled illumination can be used to create anisotropic growth patterns, essential for forming asymmetrical structures that mimic synaptic pathways. Studies indicate that slight angling of the light source can promote directional growth, beneficial in creating neuromorphic networks with directional conductivity.

2.4.4. Environmental and External Parameters

The process environment, including ambient temperature and humidity, influences the photocatalytic reaction rate and particle morphology. Controlled environments with stable temperature and low humidity are often preferred to reduce unwanted variability in growth patterns, as higher temperatures can accelerate nanoparticle growth and humidity can affect the stability of TiO_2 's

surface states. Maintaining ambient conditions ensures reproducibility and consistency across experiments, critical for scalable neuromorphic systems [56].

The reaction temperature is one of the most impactful parameters on photocatalytic activity, influencing growth kinetics and morphology of nanostructures. Increased temperatures can enhance the kinetic energy of particles, leading to accelerated electron-hole pair formation on the TiO_2 surface under UV illumination, thereby speeding up the reduction of gold ions to form nanostructures. Studies have shown that higher temperatures often produce larger or more complex gold nanostructures, which may be beneficial for conductivity but can compromise spatial resolution. Typically, temperatures between 25°C and 50°C are optimal for achieving a balance between growth rate and structural stability in neuromorphic networks [57].

The ambient humidity and atmospheric composition, particularly oxygen levels, play significant roles in the photocatalytic growth process on TiO_2 substrates. High humidity enhances the adsorption of water molecules on the TiO_2 surface, providing a source of protons that aid in the reduction process, which is essential for controlled nanoparticle formation. However, excessive moisture can increase diffusion rates on the substrate surface, potentially leading to agglomeration of nanoparticles, which could compromise the spatial resolution required in neuromorphic applications. An oxygen-rich atmosphere, while promoting recombination of electron-hole pairs, tends to slow down the reduction process, thereby allowing for controlled particle growth and reducing the risk of over-deposition. Thus, an environment with controlled low humidity and moderate oxygen levels is generally ideal for maintaining a balance between growth rate and particle stability, optimizing the performance of photocatalytic processes in neuromorphic device applications.

The local pH around the substrate surface can significantly influence the deposition process by affecting the availability of protons, which in turn accelerates the reduction of gold ions. However, when the pH is too low, it can destabilize the TiO_2 surface, resulting in uneven growth patterns. A balanced pH, typically around 3-4, supports stable nanoparticle formation while avoiding substrate degradation. Additionally, the concentration of ions in the

surrounding environment, such as Cl^- ions from the gold precursor, plays a crucial role in growth kinetics. Higher ionic concentrations promote faster particle nucleation, which can be advantageous for growth speed but may compromise uniformity. Achieving the right balance between pH and ion concentration is essential for ensuring reliable formation of synapse-like connections on the TiO_2 surface, which are critical for neuromorphic applications [58].

Applying external electric or magnetic fields during the photocatalytic growth process can refine the alignment and orientation of gold nanostructures, enhancing their applicability in neuromorphic systems. Electric fields influence ion migration, promoting the directional growth of nanostructures that mimic neural pathways, which is especially beneficial for creating aligned pathways with enhanced connectivity precision [59]. This controlled, directional growth is valuable for neuromorphic applications, where precise pathway alignment improves network functionality. Although magnetic fields are used less frequently, they can also impact particle distribution and aggregation, depending on the properties of the ions in the solution. These external fields provide an additional layer of control over structural orientation and spatial arrangement, which is crucial for constructing complex, hierarchical connectivity in neuromorphic networks.

Stabilizing agents in the surrounding medium play a crucial role in ensuring the stability and uniformity of nanoparticles during the growth process. Additives like isopropanol or ethylene glycol act as hole scavengers, which help in stabilizing electron-hole pairs generated on the TiO_2 surface, thereby controlling the growth rate of nanoparticles. These agents not only moderate the growth process but also prevent nanoparticle agglomeration by maintaining adequate spacing between particles. This spacing is critical for achieving the precise connectivity required in neuromorphic devices, where uniform particle distribution directly impacts device performance. Optimizing the concentration of stabilizing agents is essential, as too much can excessively slow down growth, while too little may compromise particle stability and lead to aggregation, undermining the desired uniformity in the network structure [60].

2.5. Photocatalytic Deposition and Control of Gold Nanostructures

Photocatalytic deposition of gold nanostructures on substrates like TiO_2 represents a critical method for fabricating conductive pathways in neuromorphic systems. The gold nanoparticle formation process leverages photocatalytic properties to drive reduction reactions at specific sites, enabling highly localized growth. This method is particularly beneficial for neuromorphic applications due to its ability to form controlled, reconfigurable networks that mimic biological synaptic connections. By adjusting experimental conditions such as light intensity, precursor concentration, and reaction time, it is possible to achieve precise control over the morphology and connectivity of gold nanostructures, which is essential for constructing adaptive neuromorphic networks [8].

The photocatalytic deposition approach is highly tunable, allowing for real-time adjustments to control the growth rate and structural properties of gold nanostructures. By modulating factors such as light wavelength and temperature, researchers can influence the rate of electron-hole pair generation on the TiO_2 surface, which directly impacts the nucleation and growth kinetics of gold particles. This tunability is essential for creating structured, high-fidelity networks that can be dynamically altered, an advantage over more static approaches like electrochemical deposition [61].

In addition to direct control over deposition rates, photocatalytic methods also facilitate patterned growth, a technique that is especially useful in creating spatially organized neural networks. By combining photocatalytic deposition with lithographic patterning, it is possible to establish predefined pathways for gold nanoparticle growth, enhancing the precision and functionality of neuromorphic systems. This patterning capability is advantageous in applications that require high connectivity and minimal crosstalk between pathways, such as in memory devices or complex computing architectures [62].

Moreover, the use of gold as the primary nanoparticle material is particularly advantageous for neuromorphic devices due to its excellent conductivity and resistance to oxidation, ensuring long-term stability. Gold nanoparticles offer high tunability in size and shape, factors which can be adjusted to optimize electronic properties like conductivity and plasmonic effects, which are crucial for effective signal transmission in neuromorphic architectures. The stability of gold nanostructures under environmental conditions also adds to the robustness of the photocatalytic approach, making it suitable for both laboratory-scale experiments and potential industrial applications [63].

Primary advantage of photocatalytic deposition is its energy efficiency compared to conventional heating or current-driven processes, which often require significant energy input. Photocatalytic growth, driven by light and simple chemical agents, aligns with the low-energy demands necessary for scalable neuromorphic systems. As such, this method stands out as a promising pathway for the development of adaptive, energy-efficient devices for next-generation computing [64].

2.5.1. Mechanism of Gold Nanoparticle Formation

Upon UV illumination, the TiO_2 substrate absorbs photons, resulting in the excitation of electrons from the valence band to the conduction band, leaving holes in the valence band. These electron-hole pairs serve as reactive sites where gold precursor ions, such as AuCl_4^- , are reduced to elemental gold (Au^0) by the excited electrons. The holes in the TiO_2 oxidize scavenger molecules in the surrounding solution, which maintains charge neutrality and allows for continuous gold deposition [47].

In the initial stages, gold ions adsorb onto the TiO_2 surface, where they are reduced and begin to nucleate as small clusters. The concentration of gold ions, UV intensity, and the presence of stabilizing agents all influence the size and shape of the forming particles. With controlled deposition, it is possible to produce nanoparticles with tunable sizes, which can influence electronic properties such as conductivity and plasmonic resonance. This tunability is essential for tailoring the interconnectivity of neuromorphic networks, where the size of

nanoparticles impacts signal transmission efficiency and overall network dynamics [44].

A key aspect of this process is the growth mechanism, which can proceed through either layer-by-layer or island growth, depending on the conditions. Lower precursor concentrations and shorter illumination times promote island growth, resulting in isolated, well-defined nanoparticles, while higher concentrations and longer illumination yield larger, continuous structures. For neuromorphic applications, where synaptic behavior relies on discrete, spatially separated connections, maintaining island growth is often preferred. Controlling these conditions allows for fine-tuning of network characteristics, such as connectivity density, which is pivotal for creating adaptive, reconfigurable neuromorphic systems [64].

Furthermore, additives such as isopropanol can act as hole scavengers, improving the reduction efficiency of gold ions and preventing agglomeration by promoting a uniform distribution of nanoparticles. This effect is especially beneficial in neuromorphic applications, where uniform particle spacing and controlled distribution contribute to precise emulation of synaptic networks [44]. Such additives enable the formation of consistent pathways with minimal crosstalk, which is essential for high-performance neuromorphic architectures.

2.5.2. Patterned Growth Using Lithography

In advanced neuromorphic engineering, achieving precise spatial control over conductive pathways is essential to emulate the complex connectivity of biological synaptic networks. Patterned growth through lithographic techniques allows for the selective deposition of gold nanoparticles on TiO_2 substrates in designated regions, enabling the spatial organization necessary for complex neural architectures. This method facilitates the precise placement of conductive pathways, minimizing crosstalk between network connections and enhancing device functionality, an aspect critical for the high fidelity required in neuromorphic applications [65].

Photocatalytic lithography combines photocatalysis with photomask-based patterning, achieving localized growth of gold nanoparticles. In this

method, a photomask is applied over the TiO_2 substrate, selectively exposing regions to UV light. This targeted illumination activates the photocatalytic properties of TiO_2 in specific areas, promoting the reduction of gold ions exclusively in the patterned regions, thus facilitating precise nanoparticle growth. This technique is particularly effective for creating high-resolution, structured pathways essential for neuromorphic computing applications, where connectivity precision is paramount [66].

Experimental parameters such as UV exposure time, mask design, and precursor concentration are critical in defining the resolution and uniformity of the patterned deposition. Shorter UV exposure times result in finer patterns with smaller nanoparticles, while well-designed masks allow for various structural configurations, from linear pathways to complex network-like patterns. These configurations can be tailored to improve connectivity and emulate synaptic structures in artificial neural networks, thereby advancing neuromorphic device performance [67].

A significant advantage of lithography-assisted photocatalytic growth is its compatibility with scalable and reproducible manufacturing processes. Unlike other methods that involve high-temperature or complex procedures, photocatalytic lithography operates under mild conditions, making it suitable for integration with flexible substrates and scalable production techniques. This adaptability supports the broader goal of developing neuromorphic systems that are both cost-effective and efficient for practical applications in computing and memory storage [68].

2.6. Role of Indium Tin Oxide (ITO) in Directing Gold Growth

Indium Tin Oxide (ITO) is commonly utilized as a transparent conducting layer in photocatalytic systems due to its excellent electrical conductivity and optical transparency. In the context of photocatalytic gold deposition, the ITO layer serves multiple functions. It not only enhances electron transport efficiency but also creates an interface that influences the growth patterns of gold nanoparticles on TiO_2 . This property is particularly relevant in neuromorphic

systems, where conductive pathways must be formed with high precision and stability to mimic biological synaptic functions [69].

The thickness of the ITO layer is also a critical parameter that affects gold deposition patterns. Thicker ITO layers provide a higher density of conduction pathways but may also introduce resistance to electron flow at larger thicknesses, which can influence the morphology and distribution of gold nanoparticles. Optimizing the thickness of the ITO layer is therefore essential to achieving a balance between conductivity and patterning precision. Research indicates that ITO layers within a specific thickness range (typically 20-100 nm) are optimal for maintaining efficient charge transfer while supporting stable gold nanoparticle growth [70]. The ITO thickness affects not only the overall deposition pattern but also the uniformity and stability of gold pathways in neuromorphic applications, where reliability and repeatability are crucial.

In addition, ITO's role extends beyond its conductive properties. The interaction between ITO and TiO_2 surfaces also impacts the adhesion and stability of deposited gold particles, making it crucial in applications where durability and longevity of conductive pathways are required. This factor is particularly relevant for neuromorphic devices intended for real-world environments, as robust and stable connections are necessary to ensure device performance over extended periods.

2.6.1. Formation of Schottky Barrier at TiO_2 -ITO Interface

The formation of a Schottky barrier at the TiO_2 -ITO interface plays a important role in directing gold nanoparticle growth by influencing charge transfer dynamics and enhancing photocatalytic activity. The Schottky barrier is a potential energy barrier formed when a semiconductor (TiO_2) comes in contact with a conductor or a conductive oxide (ITO). This barrier is essential in neuromorphic systems, as it regulates electron flow between the TiO_2 and ITO layers, effectively separating photogenerated electron-hole pairs and preventing rapid recombination [9]. By reducing recombination rates, the Schottky barrier enables a more sustained and controlled reduction process for gold ions on the

TiO₂ surface, facilitating localized and directed nanoparticle growth crucial for creating defined conductive pathways.

The Schottky barrier also serves to enhance the photogenerated charge separation by acting as an electron sink, where electrons from the TiO₂ semiconductor can transfer to the ITO layer. This electron transfer mechanism is particularly beneficial under UV illumination, as it increases the concentration of holes on the TiO₂ surface, which in turn accelerates the reduction of gold ions and promotes uniform nanoparticle nucleation. The presence of ITO not only stabilizes the charges generated in TiO₂ but also allows for precise control over where gold nanoparticles form, which is essential for structured connectivity in neuromorphic applications that mimic biological synapses [71].

Additionally, the physical properties of the ITO layer, such as thickness and transparency, further influence the formation and efficacy of the Schottky barrier. Optimal thicknesses of ITO facilitate efficient electron transfer without compromising transparency, ensuring that enough light reaches the TiO₂ layer for photocatalysis. Excessively thin ITO layers may lead to insufficient electron transfer capabilities, reducing the stability of the Schottky barrier, while overly thick layers can impede light penetration, thus decreasing photocatalytic efficiency. Achieving an appropriate balance in ITO thickness is therefore crucial, as it affects the Schottky barrier's effectiveness and, subsequently, the growth patterns of gold nanoparticles on the TiO₂ substrate [72].

In summary, the formation of a Schottky barrier at the TiO₂-ITO interface is a key factor in controlling gold nanoparticle growth, impacting both the localization and stability of particle formation. This controlled deposition process, facilitated by the Schottky barrier, is integral to the development of neuromorphic architectures that rely on precise, reconfigurable networks for optimized signal transmission and processing.

2.6.2. Heterojunctions in ITO-TiO₂ Interfaces: Theoretical Insights and Applications

The interface between ITO and TiO₂ forms a heterojunction that plays a critical role in influencing the photocatalytic and electronic properties of the

material system [73]. A heterojunction is created when two dissimilar semiconductors are brought into contact, leading to the alignment of their energy bands and the establishment of a built-in electric field. This phenomenon facilitates efficient charge carrier separation, which is crucial for enhancing photocatalytic activity [74].

The ITO-TiO₂ system forms a Type-II heterojunction due to the higher work function of ITO compared to TiO₂. This band alignment facilitates the transfer of photogenerated electrons from the conduction band of TiO₂ to ITO, while holes remain confined in the TiO₂ valence band. This efficient charge separation reduces recombination losses, significantly enhancing the photocatalytic efficiency of TiO₂. Additionally, the conductive properties of ITO as a sublayer improve electron collection and transport, further augmenting the system's performance in applications such as photocatalysis and neuromorphic systems [73].

The heterojunction interface in the ITO-TiO₂ system significantly influences key parameters, including the creation of a built-in electric field that facilitates the separation of photogenerated electron-hole pairs, enhanced carrier mobility through the conductivity of ITO for faster charge transfer, and improved optoelectronic properties as the ITO layer affects light absorption and transmission in the TiO₂ layer, crucial for photocatalytic and photoelectronic applications [75]. These properties make the ITO-TiO₂ heterojunction particularly suitable for advanced applications such as neuromorphic engineering. In this study, the heterojunction enables controlled photocatalytic growth of gold nanostructures along the edges of TiO₂ patterns under UV illumination, mimicking axonal connections in biological neural networks. The ITO layer ensures efficient electron transfer, localizing gold deposition at the interface and forming conductive pathways critical for adaptive neuromorphic systems [76].

The theoretical insights into the heterojunction dynamics provide a foundation for understanding its role in enhancing the material's performance. By optimizing parameters such as the thickness of the ITO layer and the quality of the interface, the heterojunction can be tailored for specific applications, ranging from renewable energy to bio-inspired computing [77].

2.6.3. Influence of ITO Layer Thickness on Growth Patterns

The thickness of the ITO layer plays a significant role in directing the growth patterns of gold nanostructures on TiO_2 substrates. ITO thickness affects both the electric field distribution at the interface and the photocatalytic efficiency of TiO_2 , thereby influencing the deposition and morphology of gold nanoparticles. A well-calibrated ITO layer enables controlled electron transfer and more uniform gold growth, essential for achieving the precise structural arrangement required in neuromorphic applications [70].

In thin ITO layers (less than 10 nm), the electron mobility is generally limited, leading to reduced photocatalytic efficiency. Such layers are less effective at facilitating the charge separation required for efficient gold ion reduction, resulting in sparse or uneven nanoparticle distribution. Thicker ITO layers, however, tend to enhance electron mobility and reduce recombination rates, creating a favorable environment for uniform nanoparticle growth. Studies have shown that an ITO thickness between 10 and 50 nm provides an optimal balance, allowing for sufficient electron transfer while maintaining the transparency needed for UV light penetration [78].

Moreover, increasing the ITO thickness beyond a certain point may hinder UV light transmission, reducing the photocatalytic activity of the underlying TiO_2 . As the ITO layer grows thicker, it begins to act as a partial barrier to UV light, attenuating the energy needed to excite electron-hole pairs in TiO_2 and thus slowing down the nanoparticle growth process. For neuromorphic applications, where consistent and controlled patterning is necessary, maintaining an ITO thickness within an optimal range is crucial. This balance supports the development of conductive pathways with high spatial precision, essential for high-functionality neural network emulation [79].

2.7. Controlled Pruning of Grown Nanostructures for Neuromorphic Systems

The controlled pruning of nanostructures is pivotal in neuromorphic engineering, enabling dynamic reconfiguration within artificial synaptic networks to mimic the adaptive plasticity seen in biological brains. In this context,

pruning refers to the selective removal or refinement of grown nanostructures, enhancing connectivity precision within the network. This controlled process allows for an optimized, adaptive response to changing stimuli or functional requirements, ensuring that only essential pathways remain active while redundant or inefficient connections are eliminated. Such pruning is fundamental in reducing signal interference and enhancing processing efficiency, ultimately leading to improved neuromorphic device performance [80].

Gold nanostructures, grown on substrates like TiO_2 via photocatalytic methods, form conductive pathways necessary for signal transmission in neuromorphic systems. However, as network complexity increases, excessive connectivity may lead to unintended crosstalk and reduced efficiency. Selective pruning helps maintain connectivity precision, supporting network adaptability by reorganizing pathways in response to new input, a mechanism reminiscent of synaptic plasticity in natural neural systems. This selective connectivity adjustment is integral to achieving neuromorphic networks that can functionally reorganize in real-time [81].

Various techniques in neuromorphic engineering replicate biological pruning through controlled physical and chemical means. These include methods like localized laser ablation, chemical dissolution, and voltage-induced disconnection, which selectively reduce or reshape conductive pathways within the network. Such approaches afford high precision over connectivity density and morphology, a necessity for emulating the neurobiological mechanisms of learning and memory adaptation in artificial systems. By modulating the connectivity, these techniques enable networks to undergo controlled "learning" and "forgetting" processes, a defining feature of intelligent neuromorphic devices [82].

Subsequent sections examine targeted pruning techniques, such as the refinement of axonal-like structures to enhance network efficiency, various engineering approaches to emulate biological pruning, and chemical dissolution using agents like KI. KI enables selective gold structure removal by dissolving specific regions within the network, thereby enhancing spatial resolution and adaptability. Such pruning strategies are instrumental in creating neuromorphic

systems capable of real-time adaptability, an essential attribute for advanced computing architectures designed to operate efficiently under dynamic conditions [83].

2.7.1. Pruning of Axonal Structures in Neuromorphic Systems

The selective pruning of axonal structures in neuromorphic systems is a key mechanism to emulate the efficiency and adaptability of biological neural networks. Axonal pruning allows for the targeted reduction of connections within a network, refining signal pathways to enhance computational efficiency and adaptability. This process is modeled after biological synaptic plasticity, where redundant or weak axonal connections are removed to optimize learning and memory functions. By implementing controlled pruning in neuromorphic architectures, engineers can maintain high processing accuracy while reducing energy demands, crucial for developing neuromorphic devices capable of real-time adaptation and efficient information processing [84].

In neuromorphic systems, axonal-like connections often consist of gold or other conductive nanostructures grown on semiconductor substrates like TiO_2 . The deliberate removal of these structures helps manage connectivity density, which is essential in avoiding excessive crosstalk and improving signal integrity within complex circuits. This targeted pruning not only aids in enhancing processing efficiency but also increases the system's robustness to noise, a common challenge in densely connected networks. Pruning techniques can be tailored to control specific network parameters such as connection strength and distribution, providing a high degree of flexibility in circuit design and operation [84].

Pruning methods in neuromorphic engineering range from physical techniques, such as laser ablation, to chemical methods involving selective dissolution agents like KI. For instance, laser ablation offers high precision in eliminating specific axonal structures, allowing for selective connectivity adjustments that mirror neurobiological processes of axonal trimming and synaptic reconfiguration. Similarly, KI-based chemical dissolution facilitates the targeted removal of gold pathways, preserving the desired connectivity while

eliminating superfluous routes. Such techniques are invaluable in neuromorphic systems where high fidelity and reconfigurability are required to adapt to changing functional demands and environmental stimuli [83].

Additionally, voltage-induced pruning provides another promising avenue by applying localized electric fields to weaken or disconnect certain pathways selectively. This approach simulates natural processes in the brain, where synaptic strength adjusts in response to electrical signaling. By selectively adjusting voltages, neuromorphic systems can dynamically adapt their network configurations, achieving on-demand reconfiguration similar to brain-like learning and forgetting. Voltage-based pruning, along with chemical and physical methods, presents a comprehensive toolkit for creating neuromorphic systems that are resilient, adaptable, and capable of performing complex tasks with high efficiency [80].

2.7.2. Techniques for Mimicking Pruning in Neuromorphic Engineering

In neuromorphic engineering, mimicking the biological process of pruning is essential for creating adaptable and efficient artificial neural networks. Various techniques have been developed to emulate pruning, each contributing to the reduction or reconfiguration of connections within a neuromorphic network. These techniques are designed to simulate the selective elimination of synaptic connections observed in biological systems, where the brain prunes unnecessary or underused connections to enhance functionality and reduce energy consumption. By incorporating pruning mechanisms, neuromorphic systems can dynamically optimize connectivity, enhancing processing speed and accuracy while lowering overall power requirements [84].

Laser ablation is one of the most precise physical methods for pruning in neuromorphic systems, enabling the targeted removal of individual nanostructures or clusters. By using focused laser beams, engineers can achieve sub-micron resolution in disconnection, which is essential for applications requiring intricate network reconfigurations. Laser ablation also allows for real-time pruning adjustments, an advantageous feature for neuromorphic devices needing adaptability in response to changing tasks or input signals. This technique's

precision and adaptability make it highly effective for creating complex networks that can adjust their connectivity patterns on demand [83].

Chemical dissolution techniques, such as the use of KI, offer an alternative approach to selective pruning. KI acts as a reducing agent, dissolving gold nanostructures on substrates like TiO_2 in a controlled manner. By applying KI solutions to specific areas, it is possible to selectively prune connections without affecting the overall network structure. This selective dissolution not only facilitates precise pruning but also maintains the structural integrity of surrounding connections, making it ideal for applications in neuromorphic systems that require high connectivity and minimal interference between pathways [27].

Voltage-induced pruning provides another method for emulating biological pruning processes by selectively applying localized electric fields to weaken or disconnect specific connections. This approach simulates neuroplasticity, wherein synaptic connections are strengthened or weakened in response to activity levels. Voltage-based pruning allows for the real-time adjustment of connectivity patterns in response to environmental stimuli or changing computational demands. This method is especially valuable in neuromorphic systems designed for continuous learning and reconfiguration, as it enables adaptive responses that mirror the dynamic nature of biological neural networks [24].

Together, these pruning techniques offer a robust toolkit for designing neuromorphic systems capable of real-time adaptability and energy-efficient operation. By integrating laser ablation, chemical dissolution, and voltage-based disconnection methods, engineers can create networks that not only learn and remember but also “forget” redundant connections, optimizing functionality in a manner reminiscent of the human brain’s efficiency and flexibility [29].

2.7.3. Chemical Dissolution for Pruning Using Potassium Iodide (KI)

In the context of neuromorphic systems, chemical dissolution using KI offers a precise, controllable method for pruning gold nanostructures grown on TiO_2 substrates. This approach involves selective application of KI as a reducing agent, allowing for the targeted dissolution of specific connections within a neuromorphic network. By introducing KI into the system, engineers can

achieve localized removal of gold structures without disrupting the surrounding network, thus enabling the fine-tuning of connectivity essential for adaptive learning and memory processes in artificial synaptic networks [10].

The mechanism by which KI induces selective dissolution is based on its ability to act as a reducing agent in the presence of gold nanoparticles. When KI is applied to gold-coated TiO₂ substrates, it facilitates the reduction of gold ions, effectively dissolving the metallic structures. This process is particularly beneficial for neuromorphic systems, as it enables precise pruning of overgrown or redundant pathways that could otherwise interfere with network efficiency and increase energy consumption. The KI dissolution method, therefore, plays a critical role in maintaining a streamlined network configuration, optimizing both connectivity and signal fidelity [69].

Experimental parameters such as the concentration of KI, the application area, and the duration of exposure can all be finely controlled to determine the extent and specificity of dissolution. Higher concentrations of KI result in faster dissolution rates, allowing for rapid reconfiguration of network patterns. However, for applications requiring gradual adjustment, lower concentrations and controlled exposure times are preferred. This adjustability offers flexibility in network design, making KI-based dissolution an invaluable tool for creating dynamic, adaptive neuromorphic systems that can continuously modify their structure in response to new inputs or changing functional requirements [58].

In comparison to other pruning techniques, KI-based chemical dissolution is relatively simple to implement and does not require high temperatures or complex equipment, making it a scalable solution for both laboratory and industrial applications. This technique's compatibility with low-cost and ambient-condition processing further supports its potential for integration into large-scale neuromorphic device production, where scalability and cost-effectiveness are critical. Overall, KI-driven chemical dissolution is a practical and efficient method for emulating synaptic pruning in artificial networks, enhancing both the adaptability and robustness of neuromorphic systems [41].

2.7.4. Parameters Affecting the KI Dissolution Process

Chemical pruning using KI provides a precise and adaptable approach for controlling the connectivity of neuromorphic networks by selectively removing gold nanostructures grown on TiO_2 substrates. This method leverages the selective dissolution properties of KI, allowing targeted pruning of conductive pathways within a neuromorphic network. The introduction of KI facilitates the dissolution of gold structures through its ability to act as a reducing agent, which is especially useful for refining network patterns to minimize crosstalk and optimize synaptic-like connectivity in artificial neural networks [23].

The selective action of KI is attributed to its redox potential, which, when applied to gold-deposited TiO_2 substrates, reduces gold ions and dissolves existing nanostructures. This selective dissolution helps manage network density, retaining essential pathways while eliminating redundant connections[85]. For neuromorphic systems that aim to mimic the adaptive plasticity of biological synapses, KI-assisted dissolution provides a controllable method for structural reorganization, maintaining the balance between connectivity and signal clarity essential for optimized performance [14].

Adjustable parameters in the KI dissolution process, such as concentration, exposure duration, and application method, enable precise control over pruning outcomes. Higher concentrations of KI accelerate dissolution, beneficial for rapid reconfiguration, while lower concentrations provide gradual adjustments for sensitive network modifications. The flexibility of KI concentration and application timing makes it an efficient method for tuning network structures in response to evolving functional requirements or environmental stimuli, akin to synaptic plasticity in biological systems [47].

Compared to physical pruning techniques, KI-based chemical pruning is cost-effective and operates under mild conditions, making it feasible for scalable applications. The simplicity of the KI dissolution process, requiring neither complex equipment nor extreme conditions, supports its integration into scalable neuromorphic device fabrication, making it suitable for both experimental and potential commercial applications. This method offers a pathway to create

adaptive and resilient networks that can self-optimize through selective pruning, providing a foundation for robust neuromorphic computing platforms [29].

2.8. Sequential Growth and Pruning Cycles for Adaptive

Neuromorphic Networks

Sequential growth and pruning cycles are critical for constructing neuromorphic networks that can adapt to changing conditions, similar to synaptic plasticity observed in biological neural networks. This dynamic approach, combining growth phases with targeted pruning, allows the network to restructure and refine its pathways over time, enhancing the adaptability and functionality required for complex computations. By alternating between photocatalytic growth of gold nanostructures and selective dissolution through agents like KI, these systems can emulate the natural processes of strengthening and weakening connections, which are foundational for learning and memory in biological systems [26].

The process begins with a growth phase, where UV-activated photocatalysis induces the formation of conductive gold pathways on TiO_2 substrates. These initial structures establish foundational connections, forming conductive routes that facilitate signal transmission within the network. Following this phase, a controlled pruning stage using KI is introduced, selectively dissolving redundant or inefficient pathways. This cycle of growth and pruning enables the neuromorphic network to optimize its structure, maintaining only the most efficient and necessary pathways for current processing needs [69].

Sequential cycles also allow for continuous structural adaptation in response to environmental stimuli or shifting functional demands. This adaptability is essential for neuromorphic applications, where system requirements evolve over time. Repeated cycles of growth and pruning ensure that the network remains flexible, providing a balance between stability and reconfigurability. Each cycle reinforces pathways that are frequently utilized while diminishing those that are underused, which supports an adaptive architecture that can self-organize in response to diverse inputs and operational demands [24].

These growth-pruning cycles establish a feedback mechanism that improves network performance over time, similar to the biological processes of synaptic plasticity and memory consolidation. This adaptive functionality is particularly relevant for applications such as machine learning and data processing, where dynamic reconfiguration enables efficient handling of complex tasks and evolving data inputs. The ongoing restructuring offered by these sequential cycles holds potential for creating neuromorphic networks with lifelike learning capabilities and long-term functional stability [84].

2.8.1. Integration of Growth and Pruning for Dynamic Networks

The integration of growth and pruning cycles is essential for constructing neuromorphic networks that demonstrate dynamic, adaptive behaviors similar to biological neural systems. This integrated approach balances the expansion and refinement of network pathways, enabling the system to respond flexibly to varying functional requirements. By coupling photocatalytic growth with selective pruning through chemical dissolution, such as KI, the network can undergo continuous reconfiguration. This adaptability supports applications where real-time changes in connectivity and network structure enhance performance, such as adaptive computing and real-time learning systems [86].

During the growth phase, UV-activated photocatalysis induces the deposition of gold nanoparticles on TiO_2 substrates, creating conductive pathways necessary for signal transmission. These growth pathways form the foundational structure of the network, which can be expanded to increase connectivity or intensified to enhance signal strength. Following growth, a targeted pruning phase uses agents like KI to selectively dissolve unnecessary or redundant pathways, refining the network's connectivity. This balance between creation and removal of pathways is essential for sustaining efficient information processing and resource optimization within the network [27].

The dynamic nature of these integrated growth and pruning cycles enables the network to adapt to shifts in operational demands, a feature that is increasingly vital in neuromorphic engineering. This process mimics synaptic plasticity in biological systems, where synaptic strengths are continuously

modified in response to learning and memory requirements. Through controlled growth and selective pruning, neuromorphic networks can dynamically evolve, allowing for an efficient distribution of resources and maximizing performance in changing environments [87].

Repeated growth and pruning cycles allow the network to "learn" by strengthening frequently used pathways and weakening or removing those that are seldom utilized, much like Hebbian learning principles in neuroscience. This self-organizing capability is particularly advantageous for developing networks that require minimal external intervention for reconfiguration, making them suitable for autonomous systems. The combination of adaptive growth with selective pruning enhances the network's ability to perform complex, context-dependent computations, opening new avenues for implementing advanced learning algorithms within neuromorphic hardware [88].

2.8.2. Balancing Photocatalytic Growth with KI Dissolution

Balancing photocatalytic growth with KI-induced dissolution is crucial for creating neuromorphic networks that can dynamically adjust their connectivity in response to operational demands. Photocatalytic growth, facilitated by UV light on TiO_2 substrates, provides a mechanism for controlled deposition of gold nanoparticles, forming conductive pathways essential for neuromorphic signaling. However, as network complexity increases, excess or redundant pathways may arise, requiring selective pruning to maintain efficient connectivity. The addition of KI as a dissolution agent enables targeted removal of specific pathways, ensuring that the network remains optimized for signal transmission without unnecessary interference [14].

The process of balancing growth with dissolution involves carefully controlling experimental parameters such as light intensity, KI concentration, and exposure duration. High UV intensities accelerate the photocatalytic reduction of gold ions, leading to rapid nanoparticle growth, but can also cause agglomeration and reduced spatial resolution. By introducing KI at controlled concentrations, it is possible to selectively dissolve overgrown structures, restoring the precision needed for high-performance neuromorphic applications. The

interplay between these two processes allows for real-time adjustments to network structure, crucial for adaptive behaviors in neuromorphic computing [42].

The advantage of integrating photocatalytic growth with KI dissolution lies in its ability to mimic biological mechanisms of synaptic strengthening and weakening. Just as biological neurons reinforce essential connections while pruning less-used pathways, neuromorphic networks benefit from this dual mechanism by adapting their connectivity patterns based on usage and function. This capability is essential for applications requiring a high degree of plasticity, such as artificial intelligence systems that benefit from real-time learning and forgetting cycles. In this way, balancing growth and dissolution not only supports the physical structure of the network but also enhances its functional adaptability [24].

In applications where high-resolution pathways are essential, such as pattern recognition and memory storage, fine-tuning the balance between gold nanoparticle growth and KI-induced dissolution ensures optimal performance. The resulting network can maintain structural flexibility while avoiding issues related to signal interference or excess connectivity. This careful balance allows for the creation of scalable, reconfigurable systems capable of handling complex information processing tasks with minimal external intervention, a key requirement for next-generation neuromorphic devices [13].

2.8.3. Simulating Adaptive Neural Processes through Sequential Cycles

Simulating adaptive neural processes in neuromorphic networks requires integrating sequential cycles of growth and pruning, emulating the natural process of synaptic plasticity. In biological systems, synaptic connections are constantly remodeled based on neural activity, allowing the brain to adapt to new information and experiences. Translating this adaptability into neuromorphic systems involves developing mechanisms that facilitate both the formation and selective removal of conductive pathways. Sequential cycles of photocatalytic growth and KI dissolution have shown promise in mimicking this process, allowing networks to dynamically reorganize in response to varying stimuli and functional demands [18].

Sequential growth-pruning cycles begin with controlled photocatalytic deposition of gold nanoparticles on substrates like TiO_2 , forming conductive pathways that establish initial network connectivity. As the system operates, certain pathways may become overgrown or less critical, potentially creating interference and reducing efficiency. Introducing targeted pruning via KI dissolution addresses these issues, dissolving specific gold structures to refine connectivity. By repeating this cycle, the network achieves a balance between structural stability and functional adaptability, supporting complex information processing while maintaining optimal performance [25].

These cycles enable the neuromorphic network to undergo continuous self-optimization, adjusting its connectivity patterns based on use and environmental input. Just as neurons in the brain strengthen or weaken connections through repeated experiences, neuromorphic systems utilizing sequential growth and pruning can adapt to operational demands, reinforcing frequently used pathways and dissolving those that are redundant. This adaptability is vital for applications such as machine learning and real-time data analysis, where rapid responsiveness and the ability to reorganize based on new data inputs are crucial [19].

Sequential cycles not only support adaptability but also enhance the longevity of neuromorphic devices by preventing overgrowth and ensuring that only necessary connections persist. This approach aligns with the goal of creating low-maintenance, long-lasting systems capable of emulating biological intelligence through hardware-based plasticity. By simulating these adaptive neural processes, neuromorphic devices can achieve more realistic cognitive functions, offering new possibilities for advanced computing and artificial intelligence that closely resemble human learning and memory retention [12].

2.9. Flowchart of Lithography Process

The following flowchart illustrates the steps involved in the lithography process using the AZ 5214E photoresist. This photoresist is an image reversal resist, specifically utilized to create negative patterns on substrates. The

detailed methodology and experimental conditions for this process are thoroughly discussed in my published paper, which serves as a reference for replicating the experiments accurately.

Nr.	process step	Process parameters
1	Substrate cleaning	3 min acetone (grade 9) 2 min isopropanol (grade 9) Wash with DI Dry with N ₂ gas
2	Dehydrate	2 min 120 °C on hotplate 2 min for cooling
3	Oxygen treatment	HDMS 100
4	Spin coating	3 ml AZ5214 Spin-coat parameters: 30 sec, 4000 rpm Desired thickness: 1.4 µm
5	Soft bake	50 sec @ 110 °C
6	Exposure	32 mj, 1.3 sec
7	Second bake	2 min @ 120 °C
8	Flood exposure	300 mj, 13.1 sec
9	Developing	AZ726, 1 min
10	Hard bake	1 min @ 120 °C

Chapter 3

3. Publications in Peer-Reviewed Journals

This chapter presents an overview of the three research papers that constitute the core contributions of this thesis. These publications collectively investigate the photocatalytic growth and chemical dissolution of gold structures on titanium dioxide substrates as foundational processes for neuromorphic systems. Each paper addresses distinct aspects of this topic, ranging from understanding the mechanisms of growth and dissolution to the development of experimental methodologies and techniques for creating adaptive and reconfigurable networks. Together, these studies lay the groundwork for advancing the design and functionality of neuromorphic architectures, providing valuable insights into the parameters and processes that govern these systems.

The first paper explores the role of ITO-TiO₂ heterojunctions in directing photocatalytic gold growth, emphasizing their potential for enhancing neuromorphic connectivity. By systematically investigating the impact of the ITO layer beneath patterned TiO₂ substrates, the study highlights how heterojunctions facilitate electron transport and concentrate photocatalytic activity along the edges of defined patterns. These findings underscore the significance of material layering and microstructural optimization in achieving precise and controlled gold deposition, paving the way for advanced methods in neuromorphic network fabrication.

The second paper builds on the findings of the first study by systematically investigating the influence of ITO layer thickness and UV light exposure on photocatalytic gold growth. This research provides an in-depth analysis of

how variations in these parameters affect the morphology of gold structures and introduces innovative methods to achieve more uniform patterned growth. The study emphasizes the critical role of template design in controlling the spatial organization of conductive pathways, offering valuable insights for the precise fabrication of neuromorphic networks.

The third paper explores the integration of sequential growth and pruning cycles as a novel strategy to emulate neural adaptability. By combining photocatalytic deposition with controlled chemical dissolution using KI, this research demonstrates a method for iteratively refining gold structures. This approach transitions from static network fabrication to dynamic, reconfigurable architectures, effectively mimicking the synaptic plasticity observed in biological systems. The findings underscore the potential of this dual-process methodology to advance adaptive neuromorphic networks.

Together, these publications collectively contribute to the overarching goal of advancing scalable and energy-efficient neuromorphic systems. Through innovative material engineering and experimental methodologies, they establish a foundation for adaptive and reconfigurable network architectures. The subsequent sections provide a detailed exploration of the findings, emphasizing their significance in the broader context of neuromorphic engineering and dynamic system design.

3.1. Photocatalytic edge growth of conductive gold lines on microstructured TiO₂-ITO substrates

3.1.1. Introduction

F. Abshari, S. Veziroglu, B. Adejube, A. Vahl, and M. Gerken, "Photocatalytic Edge Growth of Conductive Gold Lines on Microstructured TiO₂-ITO Substrates," *Langmuir*, vol. 40, no. 36, pp. 19051–19059, Sep. 2024, doi: 10.1021/acs.langmuir.4c02106.

Copyright © 2024 by the authors. Published by American Chemical Society. This article is an open access article distributed under the terms and conditions of the Creative Commons Attribution (CC BY) license (<https://creativecommons.org/licenses/by/4.0/>).

Statement about the own contribution:

For this publication, I contributed by writing the manuscript, collecting data, analyzing the results, and performing SEM, AFM, and conductance measurements of the samples. Additionally, I participated in developing the research idea.

Conceptualization	Planning	Implementation	Manuscript Preparation
Medium	Medium	High	High

3.1.2. Abstract

In the first paper, titled "Photocatalytic Edge Growth of Conductive Gold Lines on Microstructured TiO₂-ITO Substrates," the research aimed to explore the directed growth of conductive pathways by harnessing photocatalytic properties. This study directly contributes to the thesis's overarching goal of creating adaptive and efficient networks for neuromorphic systems by presenting a mechanism to precisely control the spatial deposition of conductive materials. By introducing an innovative approach to growing gold structures along the edges of TiO₂-ITO microstructures, the research enhanced the precision and control of growth patterns. These advancements are pivotal for minimizing

crosstalk and maximizing connectivity in neuromorphic architectures, addressing critical challenges in the field.

The methodology employed a novel approach by integrating an ITO sub-layer beneath a titanium dioxide (TiO_2) thin film. This configuration facilitated the formation of a Schottky barrier, which effectively directed photogenerated electrons towards the edges of the patterned region. Using UV-stimulated photocatalytic reduction, gold deposition was precisely confined to the edges, while suppressing undesired surface growth. The experimental framework emphasized the critical interactions between material thickness, substrate design, and illumination conditions, providing a robust pathway for achieving dynamic and localized deposition. This approach underlines the potential for precise control in fabricating neuromorphic networks.

This paper directly contributes to the thesis objectives by presenting a technical method to tackle challenges in creating directional and controlled conductive networks, which are fundamental to neuromorphic engineering. The findings demonstrate the feasibility of achieving precise material deposition and lay the groundwork for applying these concepts to more intricate network architectures in future research endeavors.

3.1.3. Published Paper

Photocatalytic Edge Growth of Conductive Gold Lines On Microstructured TiO₂–ITO Substrates

Fatemeh Abshari,* Salih Veziroglu, Blessing Adejube, Alexander Vahl, and Martina Gerken



Cite This: *Langmuir* 2024, 40, 19051–19059



Read Online

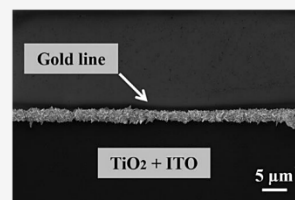
ACCESS |

Metrics & More

Article Recommendations

Supporting Information

ABSTRACT: Titanium dioxide is well-known for its excellent photocatalytic properties. UV-controlled photodeposition of gold on TiO₂ is achieved by photocatalytic reduction of precursor ions from a tetrachloroauric solution. During the growth process on the surface, clusters grow from nucleation centers and coalescence is observed for sufficiently long UV illumination times, resulting in gold structures with complex shapes. Here, we hypothesize and demonstrate that the growth process is altered by employing an ITO sublayer below the TiO₂ layer. Photocatalytic gold growth experiments on a microstructured thin film stack of 6 nm ITO and 70 nm TiO₂ lead to strongly localized gold growth along the edge of the patterned area. A conductive gold line with a height of 3.8 μm is achieved along the edge of the TiO₂-coated region, while gold growth on the surface of TiO₂ is effectively suppressed. For substrates coated only with ITO or TiO₂, no edge growth is observed. Furthermore, for an 845 nm thick TiO₂ layer, either with or without ITO sublayer, gold growth on the TiO₂ surface is dominant. Thus, for the effective steering of electrons to the edge, both the ITO sublayer and a sufficiently thin TiO₂ layer are necessary. This modified method of photocatalytic deposition—electrons photogeneration in a thin layer, collection in a dedicated conductive sublayer, and growth by reduction at a different position—opens opportunities for localized material deposition. We are in particular aiming at extending the toolbox of neuromorphic engineering by providing a technical implementation of stimulus-controlled dynamic formation of directional conductive interlinks.



■ INTRODUCTION

Neuromorphic engineering aims to develop efficient computing approaches inspired by biological neural networks.¹ Synaptic connections between individual neurons in a neural network are reconfigured dynamically. These connections develop over different time scales: Fast synaptic plasticity involves changes at the local level of synaptic connections between two neurons, whereas slow blooming and pruning take place globally throughout the neural network. Many studies have focused on mimicking the fast synaptic plasticity using memristive devices owing to their unique capability of in-memory computing.² Investigation of synaptic connections at a global scale in biological neural networks as well as development of efficient approaches to integrate them into future bioinspired systems remain ongoing areas of research.³ Recently, neuromorphic nanowire networks with memristive properties have been studied.^{4–6} These networks are self-organized, with the nanowires as one-dimensional (1D) conductive pathways. Collective switching properties arise from a complex network topology suitable for memristive architectures. In neural networks, the capacity to dynamically regulate stimuli and control the formation and dissolution of network connections is a crucial factor.⁷ Mimicking the global interactions of neuron assemblies was initially achieved by investigating global connectivity through electrolyte gating within a liquid medium.⁸ In this paper, our focus lies on the slow-growing formation of 1D long-range connections that are potentially suitable for the on-demand adaptability of a

network topology. For this purpose, we investigate the photocatalytic deposition of conductive gold lines from solution on UV-stimulated TiO₂.

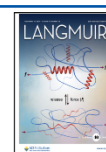
TiO₂ has been widely utilized as a semiconductor photocatalyst owing to its remarkable properties including excellent photocatalytic properties, simple and cost-effective processing, nontoxicity, and chemical inertness.^{9–12} Gold growth on the surface of TiO₂ thin films has been demonstrated by photoreduction of HAuCl₄ in the presence of UV light.^{13–15} Numerous studies have focused on investigating the factors that influence the morphology of the resulting gold structures. In addition to the crystal structure and morphology of the underlying TiO₂ thin film, the composition and pH of the precursor solution, illumination intensity, and duration play an important role in determining the morphology and coverage of the deposited gold structures.^{16–18} Our recent study¹⁸ revealed that UV illumination time and intensity significantly influence the growth and morphology of Au clusters on TiO₂ thin films. The growth process begins with the formation of stable Au nuclei on the TiO₂ surface. Extended UV exposure facilitates

Received: June 5, 2024

Revised: August 21, 2024

Accepted: August 21, 2024

Published: August 28, 2024



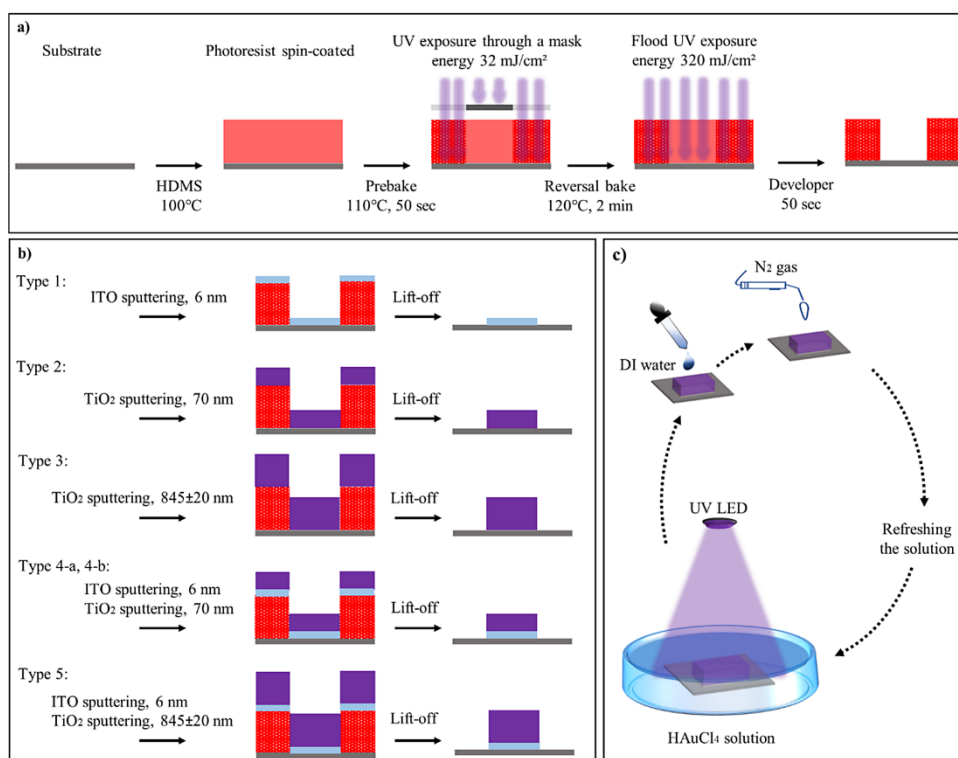


Figure 1. Schematic illustration of the substrate preparation process and the growth illumination setup. (a) Lithography process steps using AZ5214E photoresist on a Si wafer substrate with a 1 μm thermal oxide layer. (b) Illustration of the sputtering and lift-off steps, presenting resulting substrate patterns (type 1: ITO (6 nm), type 2: TiO_2 (70 nm), type 3: TiO_2 (845 nm), types 4-a and 4-b: ITO (6 nm) and TiO_2 (70 nm) and type 5: ITO (6 nm) and TiO_2 (845 nm)). (c) Schematic representation of the cyclic photocatalytic growth experiment. Each cycle begins with UV illumination, followed by substrate washing with deionized water, drying with N_2 gas, and refreshing the solution, leading to another round of illumination.

the reduction of additional Au^{3+} ions, resulting in a larger cluster formation. Higher UV intensity accelerates Au cluster nucleation and growth, leading to needle-like structures. This results in locally increased electric fields and electron densities at the sharp tips, promoting the preferential reduction of Au^{3+} ions in these regions. Here, we demonstrate that the UV illumination time affects the width and height of the gold lines. Longer UV illumination times lead to more photocatalytic reduction of HAuCl_4 on the TiO_2 –ITO substrate. Over time, we observe the growth of larger clusters and coalescence to a conductive gold line.

The photocatalytic deposition of gold nanoparticles on a TiO_2 thin film with a columnar morphology was demonstrated under ultraviolet (UV) light irradiation using a gold precursor solution.¹⁹ Lateral selectivity in the deposition of metallic structures has been achieved by selective illumination using shadow masks and by patterning the underlying TiO_2 thin film using lithography techniques.^{7,16,18} In a recent study, Au/ TiO_2 – C_3N_4 composites with plasmonic gold nanoparticles were developed, showing superior photocatalytic performance due to the high visible light absorption and prolonged lifetime of photoexcited charge carriers.²⁰ A similar work has demonstrated the coalescence of gold clusters under UV light, emphasizing photon energy-dependent pathways that influence photocatalytic behavior. These findings provide additional context for understanding the role of UV

illumination in the growth and morphological modification of gold particles.²¹

Here, we utilize photocatalysis to grow gold lines on TiO_2 thin films patterned by lithography. The addition of a thin layer of indium tin oxide (ITO) below TiO_2 is investigated. Owing to the higher work function of ITO compared to TiO_2 , a Schottky barrier is formed at the TiO_2 –ITO interface.^{22,23} We hypothesize that the transfer of photogenerated electrons from TiO_2 to ITO changes the photocatalytic growth process on the microstructured TiO_2 –ITO substrates. In this study, the gold growth is investigated experimentally with and without the ITO sublayer and two TiO_2 layer thicknesses.

EXPERIMENTAL SECTION

Substrate Preparation. UV photolithography was used to create microstructures on silicon wafers, as illustrated in Figure 1a. Five types of substrates, designated as types 1–5, were subsequently prepared by physical vapor deposition (PVD) of ITO and/or TiO_2 coatings. To obtain the type 1 substrate, a thin layer of ITO (6 nm) was deposited, whereas the type 2 substrate was created by deposition of a 70 nm thick TiO_2 layer. The type 4-a and type 4-b substrates were fabricated by depositing a 6 nm layer of ITO followed by a 70 nm layer of TiO_2 . Then a lift-off process was carried out to remove the remaining photoresist together with the ITO or TiO_2 layers on top of it. The fabrication processes of different substrate types, including sputtering and lift-off steps, are summarized in Figure 1b. To convert the TiO_2 thin films to the anatase phase, the substrates

underwent a heat treatment process. To achieve thicker TiO_2 with a different morphology, a second TiO_2 sputtering method was exploited for the type 3 and type 5 substrates (see [Supporting Information](#) for details).

Photocatalytic Gold Growth Experiment. In this section, the photocatalytic gold growth experiment is detailed. The photocatalytic reduction of precursor ions from a HAuCl_4 solution was achieved by utilizing UV-illuminated TiO_2 and ITO patterns. To prepare the precursor solution, 99.99% pure Gold(III) chloride powder (Sigma-Aldrich) was carefully mixed with deionized water in a ratio of 15 mg to 60 mL. The components were thoroughly blended to achieve a homogeneous solution. The substrate was positioned at the bottom of a glass beaker with a diameter of 5 cm, and 15 mL of the prepared solution was added subsequently. Above the beaker, a UV LED (Nichia) with a wavelength of 365 nm was positioned at a distance of ~ 7 cm to provide an intensity of ~ 3.7 mJ/cm² (measured using a Newport optical power meter). The illumination process on the type 1, 2, 3, 4-a, and 5 substrates was conducted in two steps: an initial 150 min of illumination, followed by refreshing the precursor solution and another 60 min of illumination. The type 4-b substrate underwent a three-step illumination, with each round lasting 150 min. After each illumination round, the substrate was thoroughly washed and dried. [Figure 1c](#) schematically illustrates the cyclic illumination of the substrates in the photocatalytic growth experiment, and [Table 1](#) summarizes the key parameters for each of the samples.

Table 1. Material Compositions and Illumination Times for Each Type of Substrate^a

Material composition	illumination time	
	150 min, 60 min	3 × 150 min
ITO	Type 1	
TiO_2	Type 2 and 3	
ITO/TiO_2	Type 4-a and 5	Type 4-b

^aType 4-b substrates were illuminated three times for 150 min. All other substrates were first illuminated for 150 min followed by a second 60 min illumination.

Sample Characterization after Gold Growth. After the gold growth, the morphology and chemical composition of the samples were examined using scanning electron microscopy (SEM, Supra55VP-Carl Zeiss) at an acceleration voltage of 3 kV (with a 3 mm working distance) and EDX (Oxford Instruments, Ultim Max 65). Additionally, atomic force microscopy analysis in tapping mode (cantilever description: spring constant 2 N/m and resonance frequency ~ 70 kHz) was carried out utilizing an atomic force microscope (Renishaw, MODEL alpha300 A) equipped with a Leica DM2500 microscope. Conductance measurements were performed using the Everbeing BD-6 modular probe station, equipped with micromanipulators for precise contacting, a PSM-1000 microscope, and a Motic Moticam 3+ CCD camera for high-quality image acquisition. A Keithley 2400 Sourcemeter, configured in a two-contact setup, facilitated accurate and reliable conductance measurements by recording the current response to voltage ramps.

RESULTS AND DISCUSSION

Morphological Characterization via SEM. For each substrate type 1–5, several samples were fabricated and analyzed. [Figure 2](#) shows representative SEM images of the different types of substrates after the photocatalytic gold growth process. SEM images of two different samples of each substrate type are included in [Figure S1](#). In the first row of [Figure 2](#), SEM images of type 1 substrates are shown. The SEM images are taken such that an edge between the uncoated wafer, i.e., the brighter region in the upper section of the image, and the ITO-coated wafer, i.e., the darker region in the lower section, is visible. The formation of randomly distributed

gold islands with dimensions less than 1 μm is observed on the ITO surface.

The type 2 substrates exhibit island growth of gold on the TiO_2 -coated regions, and some spherically grown structures are also observed. Larger spherical structures, with an average dimension of approximately 400 nm, and smaller spheres, averaging around 120 nm in size, are observed. Furthermore, some of the grown particles take on shapes that resemble triangles and polygons. One can observe instances of superposition in certain areas, wherein spherical particles are found on top of planar particles. The edge appears brighter in the SEM image, but does not show enhanced gold growth.

The type 3 substrates also show gold growth in the TiO_2 -coated region. The morphology of the grown particles reflects that of the type 2 substrate, featuring two main categories: spherical and polyhedral planar particles. Notably, the three-dimensional structure of spherical particles is more prominently visible on these substrates. The grown polyhedral planar particles exhibit triangular and polygonal forms, with instances of superposed stacks evident in SEM images. For none of the type 1 to 3 substrates, the photodeposited gold structures reach the percolation threshold within the illumination time of 210 min.

A very different growth situation is observed for the type 4-a and 4-b substrates with a thin TiO_2 –ITO layer and two different UV illumination times. On these substrates, gold growth is solely observed at the edge between the uncoated and the coated region. No considerable gold growth is observed on the surface of the TiO_2 –ITO thin film stack apart from the edge region. The morphology of the grown particles on the type 4 substrates differs significantly from the previous observations. Instead of spherical and planar formations, flower-shaped structures are formed at the edges. These structures consist of crossed plates of grown gold closely arranged to create a uniform line. For the type 4-b substrate with a total illumination time of 450 min, a continuous gold line is formed along the edge of the microstructured TiO_2 –ITO thin film stack.

SEM images of type 5 substrates with a thick TiO_2 layer on ITO reveal that particles are mostly grown on the surface. Three of the four investigated type 5 substrates show only little growth along the edge, whereas more gold growth along the edge is observed for one substrate (see [Figure S2](#)). The morphology of the particles on the TiO_2 surface resembles that of type 2 substrates. While planar particles are also observed, the distinguishing feature lies in the spherically grown particles. Nanostars are formed here, featuring a 3D structure with needle-like protrusions.

From the SEM images, the gold surface coverage for the different substrate types was estimated. For this purpose, two different methods were implemented: (1) manual counting and (2) automated image analysis. [Figure 3b](#) showcases the SEM image of a type 4 substrate overlaid with a grid for manual counting. The gold surface coverage was estimated within each section of the displayed grid, and the acquired values were integrated in the x -direction. This results in the surface coverage plot as a function of the y -position depicted in [Figure 3a](#). The edge between the uncoated and coated wafers is set to $y = 0$. The procedure is repeated for all substrate types, and more data are given in the [Supporting Information](#).

As previously observed, the type 4 substrates exhibit a distinct behavior compared to the other substrates with dominant gold growth along the edge and insignificant growth

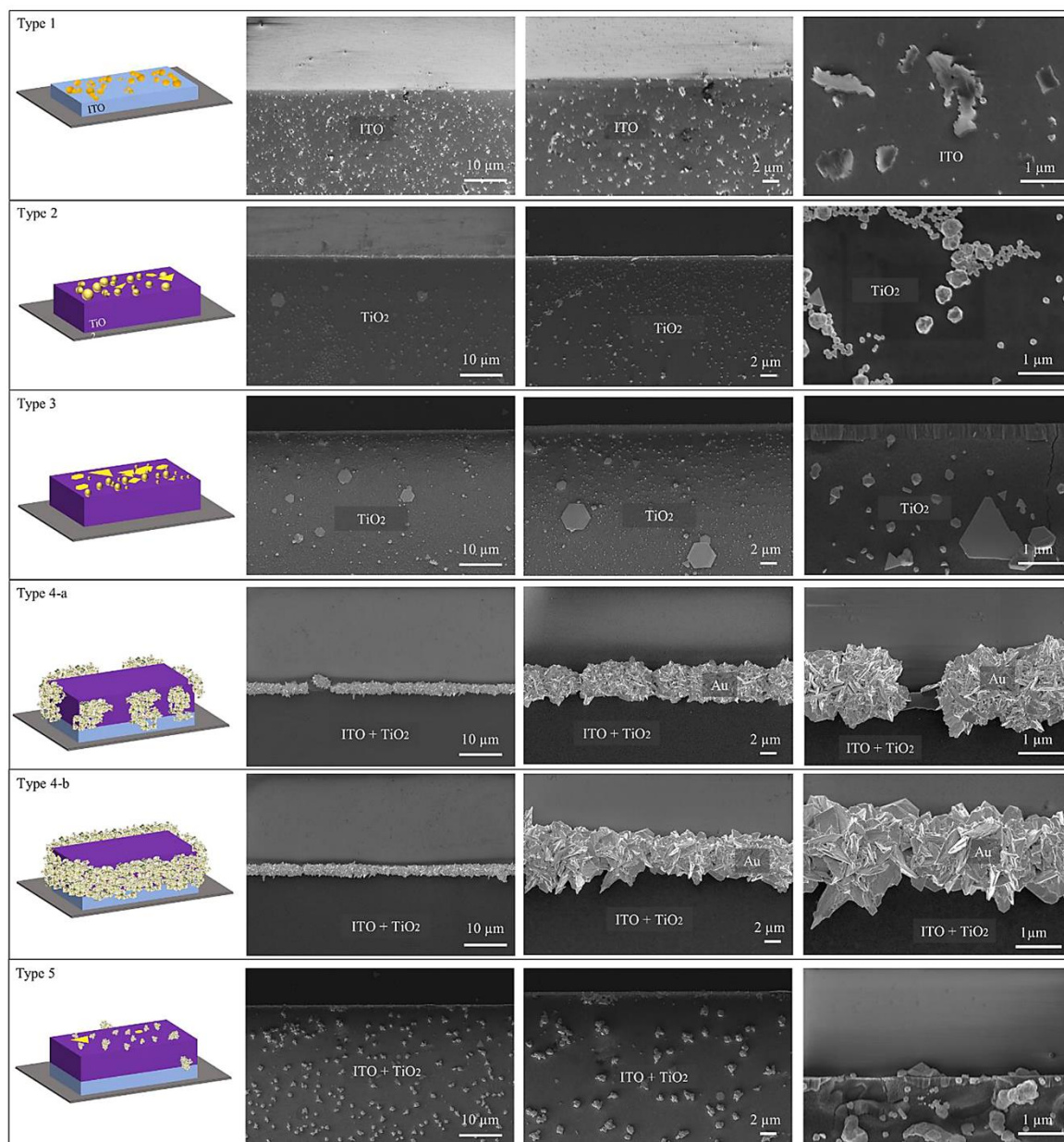


Figure 2. SEM images of the five different types of substrates (type 1–type 5), as listed in Table 1, following gold growth. In each of the SEM images, an edge between the uncoated wafer, i.e., the upper section of each image, and the coated wafer, i.e., the lower section, is visible. The 3D schemes on the left side visualize the structural details of each substrate.

on the TiO_2 -coated surfaces. For the other substrate types, however, significant gold growth is observed on the TiO_2 -coated surfaces. The gold coverage on the surface away from the edge, i.e., from $y = -20$ to $y = -10 \mu\text{m}$ in Figure 3c, is summarized in Table 2. It is highest for the type 3 and type 5 substrates with approximately 12 and 15% gold coverage on TiO_2 surface, respectively. The type 1 and type 2 substrates exhibit roughly 5% surface coverage, whereas the coverage

away from the edge in the type 4-a and 4-b substrates is almost negligible.

Morphological Characterization via AFM Analysis. In this section, we investigate the topography images obtained from atomic force microscopy and perform 3D visualization of the grown gold lines on type 4-a and 4-b substrates. Both substrates share a common structure, featuring the combination of ITO and TiO_2 patterns. The distinguishing factor lies in the variation of the illumination time during the photocatalytic

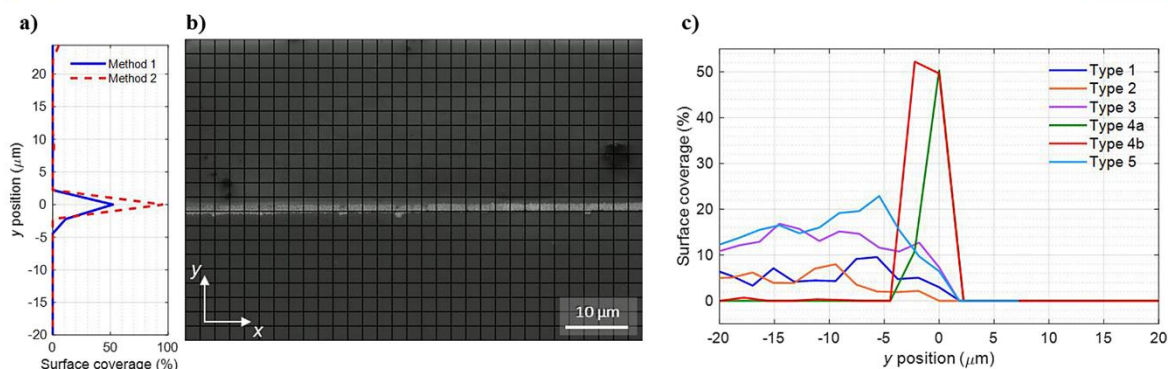


Figure 3. Evaluation of the gold surface coverage (see Figure S2 for details). (a) Averaged surface coverage per row for the SEM image in (b) is plotted. Method 1 uses manual estimation of surface coverage with an overlaid grid on the SEM image as seen in (b). Method 2 exploits an automated image evaluation. (c) Surface coverage results obtained by manual counting for all of the different substrate types. The edge is positioned at $y = 0$.

Table 2. Surface Coverage (%) of Gold on the TiO_2 -Coated Substrate Away From the Edge^a

substrates	type 1	type 2	type 3	type 4-a	type 4-b	type 5
surface coverage (%)	5.2	5.7	12	0	0.2	15

^aThe coverage is averaged for the section from $y = -20$ to $y = -10$ μm in Figure 3c.

growth process. The AFM analysis generates detailed topography images showcasing the surface features of the gold lines grown on the type 4-a (Figure 4a,b) and type 4-b (Figure 4d,e) substrates. Additionally, height profiles are extracted

along the red lines indicated in Figure 4a,d, depicting the approximate height of the grown lines on each of the two substrates. For type 4-a, a peak height of ~ 3.5 μm and a full width at half-maximum (fwhm) of ~ 4.9 μm are obtained for the grown gold line as depicted in Figure 4c. For the type 4-b substrate with a longer illumination time, a height of ~ 3.8 μm and a fwhm of ~ 4.7 μm are observed. The type 4-a substrate shows a higher spatial variability of the height along the grown line compared to the type 4-b substrate.

Characterization of Chemical Composition via EDX Analysis. Energy-dispersive X-ray spectroscopy (EDX) was carried out to investigate the elemental composition of the lines grown on type 4 substrates. In Figure 5a the EDX

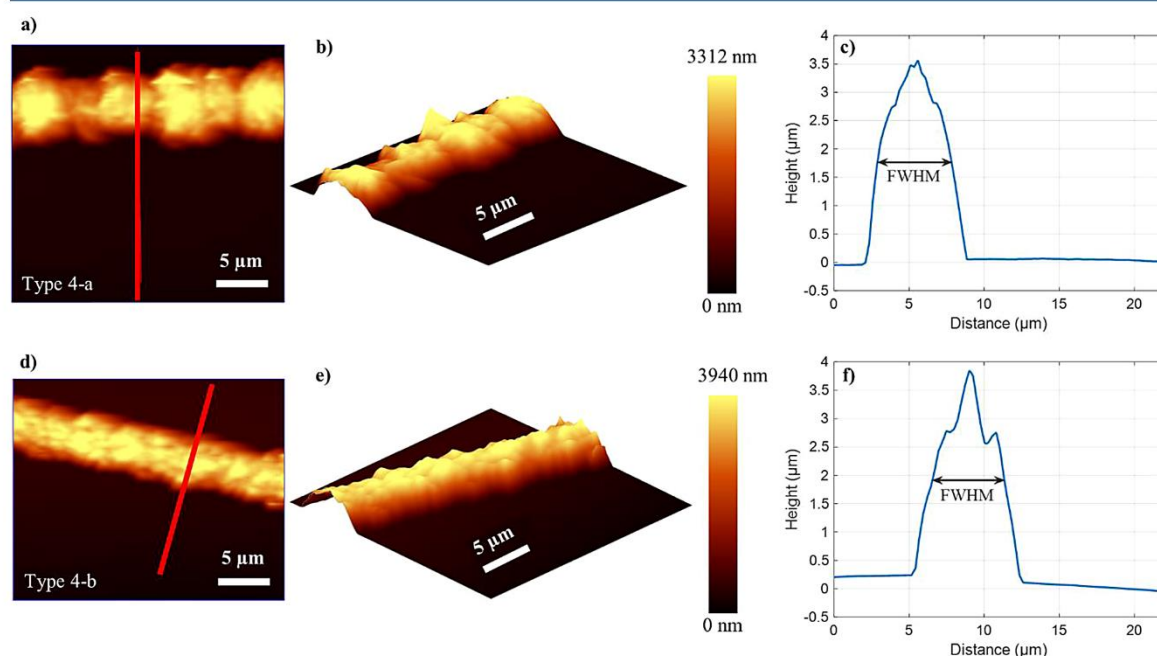


Figure 4. AFM images of the grown gold lines on the (a, b) type 4-a and (d, e) type 4-b substrates. (a, d) Top view topography images, (b, e) 3D visualizations, and (c, f) height profiles extracted along the red lines indicated in (a) and (d).

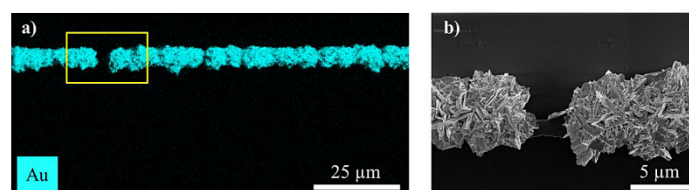


Figure 5. (a) EDX elemental map of a type 4-a substrate, showing the distribution of Au. (b) SEM image of the marked area in (a) with a gap in the grown Au line.

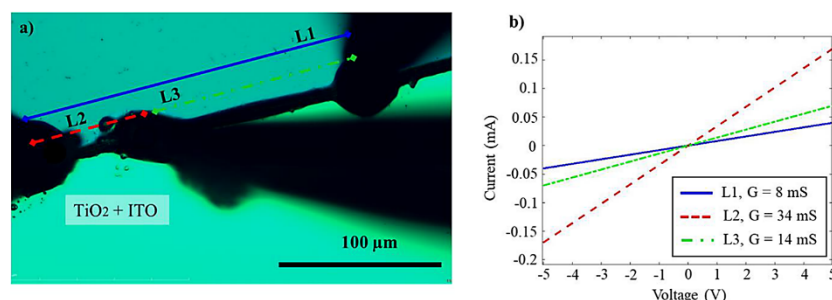


Figure 6. Conductance measurement of gold lines. (a) Optical microscopy image of the type 4-b substrate featuring gapless grown gold lines. Three needles of the hard contact probe station are precisely arranged to form three lines with distinct lengths: L1 (180 μm), L2 (60 μm), and L3 (120 μm) for conductance measurements. (b) Measured I–V diagrams for the three lines indicated in (a) with their corresponding conductance values: L1 (8 mS), L2 (34 mS), and L3 (14 mS).

elemental map highlights the distribution of gold (Au), providing clear evidence that the grown line is indeed composed of gold. Furthermore, the absence of gold signals in the areas away from the edge is noted, confirming that growth is concentrated at the edge for these samples. For a better understanding of the line's morphology, Figure 5b presents the SEM image of the marked region in Figure 5a, revealing a gap within the grown gold line. Additional EDX results are provided in Figure S3 for more detailed analysis.

Conductance Measurement. Here, the conductivity of the gold lines at the edges of the type 4-a and type 4-b substrates is investigated. This examination serves to analyze the electrical properties important for application in neuromorphic networks. A hard contact probe station device was employed for conductivity measurements. Due to the microscopic sizes of the photodeposited gold structures and the limited visibility under the microscope, only three probes were brought into contact with a photodeposited gold line at a given time. The application of a voltage ramp ranging from -5 to $+5$ V allowed for the recording of current between two probes, as illustrated in Figure 6. Given the narrow width of approximately $5\ \mu\text{m}$ of the gold lines, which closely matches the size of the measurement needle tips, obtaining accurate and reliable contacting imposed experimental challenges. Additionally, the delicate nature of the grown gold lines and their tendency to detachment from the substrate during measurements posed a recurring challenge, necessitating careful handling to preserve the sample integrity. Given the presence of gaps in the grown line of the type 4-a substrates, achieving a uniform and gap-free line also posed a challenge. However, we successfully identified a line with a length of $180\ \mu\text{m}$ and measured its conductance. To ensure a trustworthy comparison, the conductance of a line with an identical length of $180\ \mu\text{m}$ was measured in the type 4-b substrate. The conductances of the lines are 3 mS for the type 4-a substrate and 8 mS for the

type 4-b substrate, as determined from the slope of the I–V curves (see Figure S4). Reference conductance measurements on the surface of the TiO_2 lines without gold confirmed their nonconductive nature.

Additionally, conductance measurements were carried out at varying line lengths for the type 4-b substrate. Three needles of the hard contact probe station were arranged along a line as shown in part a, resulting in three distinct lines indicated as L1, L2, and L3. The I–V diagrams for each of the three lines are demonstrated in Figure 6b. Line L1, situated between the two outer needles with a length of $180\ \mu\text{m}$, demonstrated a conductance of 8 mS. For line L2, with a length of $60\ \mu\text{m}$, a conductance value of 34 mS was measured. Meanwhile, line L3, with a length of $120\ \mu\text{m}$, exhibited a conductance of 14 mS. The approximate values for the lengths are attributed to the substantial size difference between the needle tips and the line width. Analysis of the I–V diagram for these three lines reveals a noteworthy pattern: as the length increases, the conductance decreases, aligning with expectations.

In combination, the SEM, AFM, and EDX images reveal distinct gold growth patterns on the type 4 substrates compared to the other substrate types. While gold growth is observed on the TiO_2 –ITO-coated surface for the other substrate types, type 4 substrates show gold growth only along the edge between the coated and uncoated surface areas. Given that there is no edge growth for the reference substrates with a single ITO layer (type 1), a single $70\ \text{nm}$ TiO_2 layer (type 2), and a single $845\ \text{nm}$ TiO_2 layer, we conclude that the combination of the ITO and TiO_2 layers is essential for gold growth along the edges. On the other hand, the type 5 substrate, comprising a $6\ \text{nm}$ ITO layer and a thick TiO_2 layer, does not exhibit significantly enhanced edge growth or suppressed surface growth. Here, two effects need to be considered: the electron diffusion distance to the ITO interface

and the layer morphology. The illumination is conducted from the top. Considering the TiO_2 anatase refractive index as

$$n(\lambda = 365 \text{ nm}) = 3.0 - i0.0012 \quad (1)$$

The absorption coefficient is approximately 400 cm^{-1} at the peak wavelength of 365 nm.²⁴ Hence, even with the 845 nm thick TiO_2 layer, electron generation is expected to occur throughout the depth of the layer. Transfer-matrix simulations for normal-incidence illumination predict a UV-light intensity drop of approximately 10% within the 845 nm TiO_2 layer. The LED has a spectral half-width of about 9 nm and the absorption increases toward 350 nm. Thus, a larger fraction of the short-wavelength photons is absorbed (50% intensity drop within the 845 nm TiO_2 layer calculated for an excitation wavelength of 355 nm). Once gold growth starts, part of the light is reflected on the gold and the absorption is decreased in this area. Also, additional scattering effects are expected due to surface roughness and gold nanoparticles that are not included in the simulation.

The distribution of electrons within the TiO_2 layer is additionally influenced by thin-film interference effects. The wavelength of the UV excitation light in TiO_2 is approximately 122 nm (365 nm divided by the refractive index). Thin-film interference maxima are expected to have a spatial distance of 61 nm at normal incidence. For the 845 nm TiO_2 layer, approximately 14 maxima (and minima) in electron generation are expected to pass from top to bottom. The 70 nm TiO_2 layer just exceeds one period in the spatial interference pattern.

The photogenerated electrons diffuse in the TiO_2 layer. For the 845 nm thick TiO_2 layer, the carrier generation occurs at a greater average distance to the ITO interface. Only for electrons reaching the ITO layer, changes are expected in the gold growth. We estimate the diffusion length as the characteristic length as

$$x_c = \sqrt{4Dt_D} \quad (2)$$

where the exponent of the one-dimensional diffusion result²⁵ is equal to -1 . Due to the thin-film geometry and homogeneous illumination, one-dimensional diffusion is a good model. Once the islands of gold start growing, additional effects occur. For analyzing the onset of gold growth, the one-dimensional model is sufficient. Considering, e.g., an electron diffusion constant²⁶ $D = 1 \times 10^{-6} \text{ m}^2/\text{s}$ and a diffusion time of $t_D = 10 \text{ ns}$ before recombination, $x_c = 200 \text{ nm}$ is obtained.

The expected diffusion length of approximately 200 nm suggests that electrons generated in the 70 nm TiO_2 layer efficiently pass the Schottky barrier into the ITO. This estimation explains the quenched gold growth on the TiO_2 -coated surface of type 4 substrates. Photogenerated electrons are efficiently collected into the ITO layer and are thus not available for photocatalytic deposition of gold at the surface. Only part of the electrons generated in the 845 nm thick TiO_2 layer are expected to reach the ITO layer. This is in line with the observed gold growth on the surface of the type 5 substrates.

In addition to suppressing gold growth on the TiO_2 surface, the ITO sublayer also promotes electron transport to the edge and gold growth along the edge of the microstructured region. Gold growth along the edge starts from gold islands at the edge. The islands show coalescence as they grow, forming a conductive gold line along the edge. Just considering the discussion so far, more electrons are expected to reach the ITO layer for the type 5 substrates than for the type 4 substrates

due to the thicker TiO_2 layer. Thus, for the type 5 substrates, surface and edge growth are expected. Experimentally, only one of the four type 5 substrates exhibits significant edge growth. Therefore, another factor influences gold growth.

We attribute the additional effects to the different deposition methods for the thick 845 nm TiO_2 layer. Cracking of the layer is desired and induced in the fabrication to allow for the efficient transfer of carriers to the TiO_2 -solution interface. This different layer morphology reduces the diffusion time to the solution and fosters gold growth at the surface. As gold growth at the surface is dominant in the type 5 samples, the carrier transfer to the solution appears additionally enhanced, while the edge growth is suppressed. It needs to be noted that the different TiO_2 film morphologies will also have an effect on the optical properties and thus on the electron generation rate as a function of depth in the layer. For an enhanced edge growth, a TiO_2 layer deposition method generating homogeneous layers without cracks appears preferable. This reduces the electron recombination rate and enhances the transfer of electrons to ITO.

By using the proposed approach with an ITO sublayer, all photocatalytically deposited gold contributes to the formation of a conductive line. Compared to simply depositing gold on a line-shaped microstructured TiO_2 layer, this approach has the advantage that electrons are collected from a larger region, achieving faster coalescence of the conductive line. This effect is clearly observed by comparing the type 4-a and type 5 substrates. For both substrates, the same UV illumination time is used and the type 4-a substrates already have significantly longer conductive segments.

CONCLUSIONS

In summary, our study introduces an approach to grow gold lines along the edges of patterned TiO_2 -ITO substrates through the photocatalytic reduction of precursor ions from HAuCl_4 solution by UV-stimulated TiO_2 . We further investigated the impact of two different TiO_2 layer thicknesses—70 and 845 nm—on the gold growth properties. EDX analysis confirmed the composition of the grown line as gold. Comprehensive SEM and AFM analysis of the physical morphology shows a gold line approximately $7 \mu\text{m}$ wide and $4 \mu\text{m}$ high. The conductance is approximately 8 mS for a $180 \mu\text{m}$ long section.

Our main application focus is the on-demand formation of long-range connections in neuromorphic networks. Photodeposition of conductive gold lines along the edges of a photocatalytically active ITO/ TiO_2 thin film stack complements the toolbox of neuromorphic engineering by providing a technical implementation of stimulus-controlled dynamic formation of directional conductive interlinks. With this type of functionality, the grown gold lines show a certain resemblance to the role that axons take in signal transmission in neural networks. For neuromorphic computing, time scales on the order of minutes to hours are suitable to mimic the slow evolution of the topology of biological neuronal networks.

The proposed approach to photocatalytic deposition—photogeneration of electrons in a thin-film layer, collection in a dedicated conductive sublayer, and growth by reduction at a different position—opens opportunities for localized material deposition. It is also promising for other shapes of microstructures, and it will be interesting to investigate how far this effect of localized deposition extends to the nanoscale. While our main aim was to achieve uniform conductive gold lines, the

different types of TiO₂–ITO substrates investigated here are also of high interest for photocatalytic applications as well as for biosensing applications. Charge carriers are collected for localized enhancement of photocatalysis at the ITO/TiO₂ edges of type 4 substrates. On the other hand, a uniform photocatalytic performance is achieved across the surface of the type 5 substrates. This approach may be utilized for other types of photocatalytic reactions in microreactors. Also, the localized gold microstructures may be functionalized for biosensing allowing for localized sensing.

■ ASSOCIATED CONTENT

Supporting Information

The Supporting Information is available free of charge at <https://pubs.acs.org/doi/10.1021/acs.langmuir.4c02106>.

Details of the substrates preparation, SEM images of the different types of substrates and their corresponding gold surface coverage evaluation, I–V diagrams of gold lines grown on the two type 4 substrates, and band diagram of the Schottky barrier formed at the TiO₂–ITO interface (PDF)

■ AUTHOR INFORMATION

Corresponding Author

Fatemeh Abshari – Chair for Integrated Systems and Photonics, Department of Electrical and Information Engineering, Faculty of Engineering, Kiel University, D-24143 Kiel, Germany; orcid.org/0009-0001-3067-3252; Email: fa@tf.uni-kiel.de

Authors

Salih Veziroglu – Chair for Multicomponent Materials, Department of Materials Science, Faculty of Engineering, Kiel University, D-24143 Kiel, Germany; Kiel Nano, Surface and Interface Science KiNSIS, Kiel University, D-24118 Kiel, Germany; orcid.org/0000-0002-1310-6651

Blessing Adejube – Chair for Multicomponent Materials, Department of Materials Science, Faculty of Engineering, Kiel University, D-24143 Kiel, Germany

Alexander Vahl – Chair for Multicomponent Materials, Department of Materials Science, Faculty of Engineering, Kiel University, D-24143 Kiel, Germany; Kiel Nano, Surface and Interface Science KiNSIS, Kiel University, D-24118 Kiel, Germany; Leibniz Institute for Plasma Science and Technology, 17489 Greifswald, Germany

Martina Gerken – Chair for Integrated Systems and Photonics, Department of Electrical and Information Engineering, Faculty of Engineering, Kiel University, D-24143 Kiel, Germany; Kiel Nano, Surface and Interface Science KiNSIS, Kiel University, D-24118 Kiel, Germany

Complete contact information is available at: <https://pubs.acs.org/10.1021/acs.langmuir.4c02106>

Author Contributions

The manuscript was written through contributions of all authors. All authors have given approval to the final version of the manuscript.

Notes

The authors declare no competing financial interest.

■ ACKNOWLEDGMENTS

This work is supported by the Deutsche Forschungsgemeinschaft (DFG, German Research Foundation) – Project-ID 434434223 – SFB 1461. The Alexander von Humboldt Foundation supported two research stays of Martina Gerken at University College Dublin. Martina Gerken thanks John Sheridan and Ra'ed A. Malallah for fruitful discussions on photochemical processes at UCD.

■ REFERENCES

- (1) Kendall, J. D.; Kumar, S. The Building Blocks of a Brain-Inspired Computer. *Appl. Phys. Rev.* **2020**, 7 (1), No. 011305.
- (2) Strukov, D. B.; Snider, G. S.; Stewart, D. R.; Williams, R. S. The Missing Memristor Found. *Nature* **2008**, 453 (7191), 80–83.
- (3) Wright, C. D. Precise Computing with Imprecise Devices. *Nat. Electron.* **2018**, 1 (4), 212–213.
- (4) Sangwan, V. K.; Hersam, M. C. Neuromorphic Nanoelectronic Materials. *Nat. Nanotechnol.* **2020**, 15 (7), 517–528.
- (5) Zhu, X.; Lee, S. H.; Lu, W. D. Nanoionic Resistive-Switching Devices. *Adv. Electron. Mater.* **2019**, 5 (9), No. 1900184.
- (6) Tang, J.; Yuan, F.; Shen, X.; Wang, Z.; Rao, M.; He, Y.; Sun, Y.; Li, X.; Zhang, W.; Li, Y.; Gao, B.; Qian, H.; Bi, G.; Song, S.; Yang, J. J.; Wu, H. Bridging Biological and Artificial Neural Networks with Emerging Neuromorphic Devices: Fundamentals, Progress, and Challenges. *Adv. Mater.* **2019**, 31 (49), No. 1902761.
- (7) Veziroglu, S.; Paulsen, M.; Schardt, J.; Adejube, B.; Aktas, C.; Vahl, A.; Gerken, M. Photocatalytic Deposition for Metal Line Formation. In *Bio-Inspired Information Pathways: From Neuroscience to Neurotronics*; Springer International Publishing, 2023; 241–263.
- (8) Gkoupidenis, P.; Koutsouras, D. A.; Malliaras, G. G. Neuromorphic Device Architectures with Global Connectivity through Electrolyte Gating. *Nat. Commun.* **2017**, 8 (1), 1–8.
- (9) Yu, Y.; He, T.; Guo, L.; Yang, Y.; Guo, L.; Tang, Y.; Cao, Y. Efficient Visible-Light Photocatalytic Degradation System Assisted by Conventional Pd Catalysis. *Sci. Rep.* **2015**, 5 (1), 1–6.
- (10) Safajou, H.; Khojasteh, H.; Salavati-Niasari, M.; Mortazavi-Derazkola, S. Enhanced Photocatalytic Degradation of Dyes over Graphene/Pd/TiO₂ Nanocomposites: TiO₂ Nanowires versus TiO₂ Nanoparticles. *J. Colloid Interface Sci.* **2017**, 498, 423–432.
- (11) Vahl, A.; Veziroglu, S.; Henkel, B.; Strunskus, T.; Polonskyi, O.; Aktas, O. C.; Faupel, F. Pathways to tailor photocatalytic performance of TiO₂ thin films deposited by reactive magnetron sputtering. *Materials* **2019**, 12 (17), 2840.
- (12) Kusmirek, E. A CeO₂ Semiconductor as a Photocatalytic and Photoelectrocatalytic Material for the Remediation of Pollutants in Industrial Wastewater: A Review. *Catalysts* **2020**, 10 (12), 1435.
- (13) Kedves, E. Z.; Pap, Z.; Hernadi, K.; Baia, L. Significance of the Surface and Bulk Features of Hierarchical TiO₂ in Their Photocatalytic Properties. *Ceram. Int.* **2021**, 47 (5), 7088–7100.
- (14) Binas, V.; Venieri, D.; Kotzias, D.; Kiriakidis, G. Modified TiO₂ Based Photocatalysts for Improved Air and Health Quality. *J. Materiomics* **2017**, 3 (1), 3–16.
- (15) Salomatina, E. V.; Fukina, D. G.; Koryagin, A. V.; Titaev, D. N.; Suleimanov, E. V.; Smirnova, L. A. Preparation and Photocatalytic Properties of Titanium Dioxide Modified with Gold or Silver Nanoparticles. *J. Environ. Chem. Eng.* **2021**, 9 (5), No. 106078.
- (16) Veziroglu, S.; Obermann, A. L.; Ullrich, M.; Hussain, M.; Kamp, M.; Kienle, L.; Leibner, T.; Rubahn, H. G.; Polonskyi, O.; Strunskus, T.; Fiutowski, J.; Es-Souni, M.; Adam, J.; Faupel, F.; Aktas, O. C. Photodeposition of Au Nanoclusters for Enhanced Photocatalytic Dye Degradation over TiO₂ Thin Film. *ACS Appl. Mater. Interfaces* **2020**, 12 (13), 14983–14992.
- (17) Guo, Y.; Siretanu, I.; Zhang, Y.; Mei, B.; Li, X.; Mugele, F.; Huang, H.; Mul, G. PH-Dependence in Facet-Selective Photodeposition of Metals and Metal Oxides on Semiconductor Particles. *J. Mater. Chem. A* **2018**, 6 (17), 7500–7508.
- (18) Veziroglu, S.; Ghorri, M. Z.; Kamp, M.; Kienle, L.; Rubahn, H. G.; Strunskus, T.; Fiutowski, J.; Adam, J.; Faupel, F.; Aktas, O. C.

Photocatalytic Growth of Hierarchical Au Needle Clusters on Highly Active TiO₂ Thin Film. *Adv. Mater. Interfaces* **2018**, *5* (15), No. 1800465.

(19) Mendoza-Diaz, M. I.; Cure, J.; Rouhani, M. D.; Tan, K.; Patnaik, S. G.; Pech, D.; Quevedo-Lopez, M.; Hungria, T.; Rossi, C.; Estève, A. On the UV-Visible Light Synergetic Mechanisms in Au/TiO₂Hybrid Model Nanostructures Achieving Photoreduction of Water. *J. Phys. Chem. C* **2020**, *124* (46), 25421–25430.

(20) Shi, Q.; Zhang, X.; Li, Z.; Raza, A.; Li, G. Plasmonic Au Nanoparticle of a Au/TiO₂-C₃N₄ Heterojunction Boosts up Photooxidation of Benzyl Alcohol Using LED Light. *ACS Appl. Mater. Interfaces* **2023**, *15* (25), 30161–30169.

(21) Zhang, J.; Wang, H. D.; Zhang, Y.; Li, Z.; Yang, D.; Zhang, D. H.; Tsukuda, T.; Li, G. A Revealing Insight into Gold Cluster Photocatalysts: Visible versus (Vacuum) Ultraviolet Light. *J. Phys. Chem. Lett.* **2023**, *14* (18), 4179–4184.

(22) Dai, W.; Wang, X.; Liu, P.; Xu, Y.; Li, G.; Fu, X. Effects of Electron Transfer between TiO₂ Films and Conducting Substrates on the Photocatalytic Oxidation of Organic Pollutants. *J. Phys. Chem. B* **2006**, *110* (27), 13470–13476.

(23) Irfan, F.; Tanveer, M. U.; Moiz, M. A.; Husain, S. W.; Ramzan, M. TiO₂ as an Effective Photocatalyst Mechanisms, Applications, and Dopants: A Review. *EPJ. B* **2022**, *95* (11), 1–13.

(24) Jolivet, A.; Labbé, C.; Frilay, C.; Debieu, O.; Marie, P.; Horcholle, B.; Lemarié, F.; Portier, X.; Grygiel, C.; Duprey, S.; Jadwisieniczak, W.; Ingram, D.; Upadhyay, M.; David, A.; Fouchet, A.; Lüders, U.; Cardin, J. Structural, Optical, and Electrical Properties of TiO₂ Thin Films Deposited by ALD: Impact of the Substrate, the Deposited Thickness and the Deposition Temperature. *Appl. Surf. Sci.* **2023**, *608*, No. 155214.

(25) Crank, J. *The mathematics of diffusion*, 2nd ed.; Oxford university press, 1975, 12.

(26) Schneider, J.; Matsuoka, M.; Takeuchi, M.; Zhang, J.; Horiuchi, Y.; Anpo, M.; Bahnemann, D. W. Understanding TiO₂ photocatalysis: Mechanisms and Materials. *Chem. Rev.* **2014**, *114* (19), 9919–9986.

Supporting Information

Photocatalytic edge growth of conductive gold lines on microstructured TiO₂-ITO substrates

Fatemeh Abshari^{a,}, Salih Veziroglu^{b,c}, Blessing Adejube^b, Alexander Vahl^{b,c,d}, Martina Gerken^{a,c}*

^aChair for Integrated Systems and Photonics, Department of Electrical and Information Engineering, Faculty of Engineering, Kiel University, Kaiserstr. 2, D-24143 Kiel, Germany

^bChair for Multicomponent Materials, Department of Materials Science, Faculty of Engineering, Kiel University, Kaiserstr. 2, D-24143 Kiel, Germany

^cKiel Nano, Surface and Interface Science KiNSIS, Kiel University, Christian-Albrechts-Platz 4, D-24118 Kiel, Germany

^dLeibniz Institute for Plasma Science and Technology, Felix-Hausdorff-Str. 2, 17489 Greifswald, Germany

*Email: fa@tf.uni-kiel.de

Table of Contents

Substrate preparation	S3
Figure S1: SEM images of the different types of substrates	S5
Figure S2: Gold surface coverage evaluation of the different types of substrates.....	S7
Figure S3. I-V diagram of a 180- μm long line on the type 4-a and type 4-b substrates.....	S8
Figure S4. Schottky barrier formation at the TiO_2 -ITO interface	S8
References	S9

Substrate preparation

As the first step to prepare the substrates, single-side polished 4-inch silicon wafers (111 orientation, Microchemicals GmbH) with a SiO₂ thermal oxide layer (1000 nm thick, wet thermal oxide) were diced into 10×10 mm pieces (Aurotech company, Wafer Dicing DAD3350 model). The resulting substrates were cleaned with acetone and isopropanol (both Sigma-Aldrich) in an ultrasonic bath (Martin Walter Ultraschalltechnik) at grade 9. They were then thoroughly dried using pure nitrogen gas.

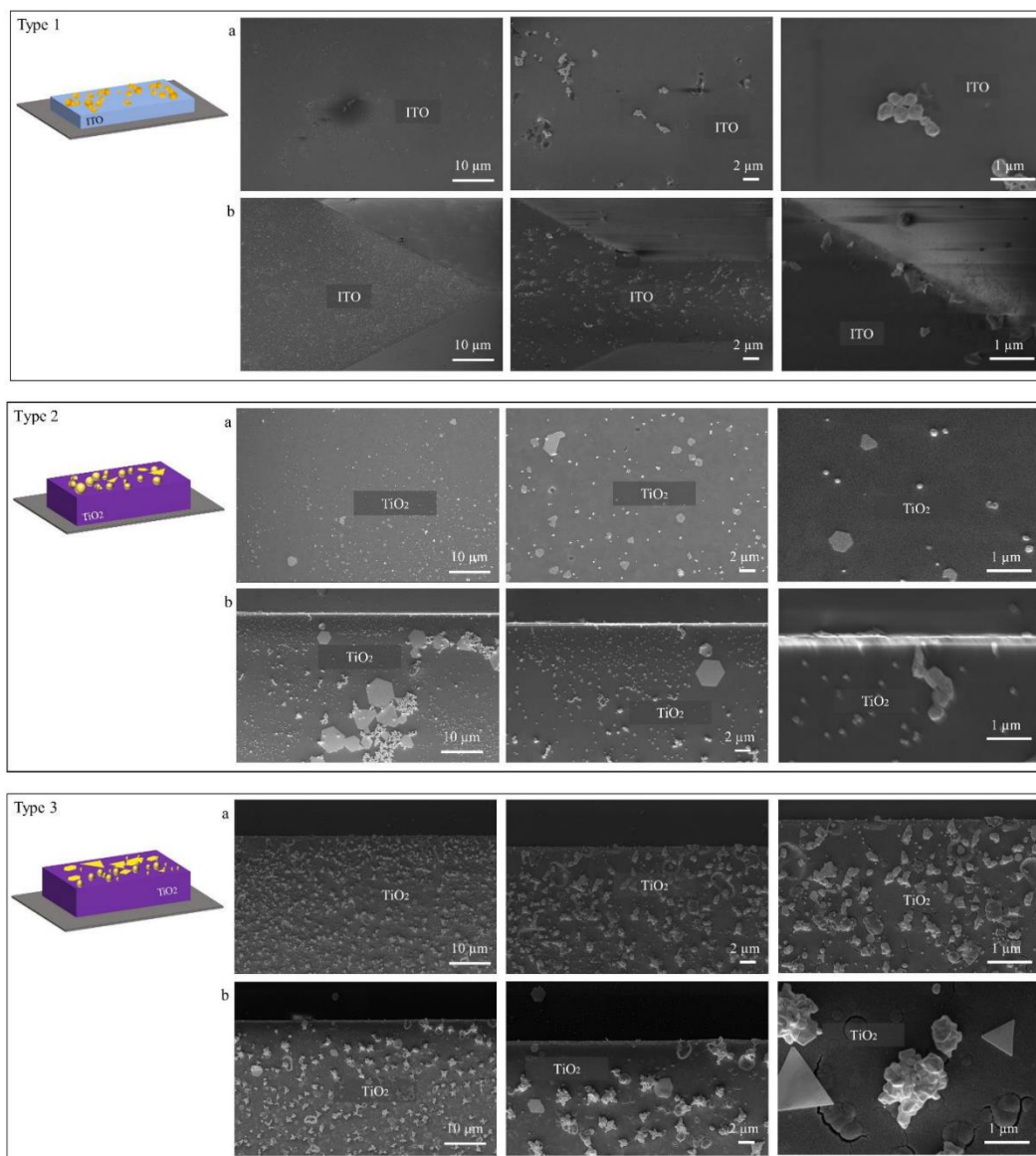
A 5-inch lithography mask including reflective chromium structures (Rose Fotomasken) with feature sizes down to 50 μm and different line shapes was used to create microstructures on the substrate via UV photolithography. To enhance adhesion, hexamethyldisilane (HDMS) was first applied to each silicon substrate at 100°C. Next, 200 μL of AZ5214E photoresist (Microchemicals GmbH) was spin coated at 3000 rpm for 30 seconds (ST22model, Robotechnik). The substrates were prebaked on a hot plate at 110°C for 50 seconds. Utilizing a mask aligner (SUSS MicroTec), they were exposed to UV light with an energy of 32 mJ/cm² through the designed lithography mask. A reversal bake was performed on a hot plate at 120°C for 2 minutes. Subsequently, a flood UV exposure with an energy of 320 mJ/cm² was conducted. The final step in the lithography process was to develop the non-exposed areas during the first illumination, using AZ726 developer (Microchemicals GmbH). Hence, the substrates were immersed in the developer for 50 seconds. To eliminate any remaining developer on the substrates, they were washed with deionized water and subsequently dried with a pure nitrogen gas gun. The schematic of the UV photolithography process is illustrated in Figure 1a.

To deposit the ITO coatings, a 3-inch In₂O₃/SnO₂ (90/10 wt%) target with a purity of 99.99% was used (Kurt J. Lesker). The deposition process was conducted by a sputtering machine with a

tooling factor of 191. Meanwhile, the TiO₂ coatings were deposited using a 3-inch TiO₂ target with a purity of 99.99% (Kurt J. Lesker) by a sputtering machine with a tooling factor of 28. The base pressure in the vacuum chamber was set at 3.6×10^{-7} Pa (3.6×10^{-9} mbar). This low base pressure was crucial for achieving high-quality film deposition and minimizing contamination. During the sputtering of TiO₂ layer, the pressure of the sputtering chamber was maintained at 2.1×10^{-3} mbar. The distance between the titanium target and the substrate during sputtering was approximately 10 cm. This distance was carefully controlled to ensure uniform film deposition across the substrate surface. For lift-off, the substrates were placed vertically in a beaker containing acetone, secured with a holder, and were subjected to ultrasonic agitation for 10 minutes. Subsequently, they were immersed in isopropanol for an additional 5 minutes. The substrates were thoroughly rinsed with deionized water and dried using nitrogen gas. To convert the TiO₂ thin films to anatase phase, the substrates underwent a heat treatment process. The four substrates were heated at 400°C in a muffle furnace for 90 minutes. Following this step, they were promptly cooled using a metal plate.

To achieve thicker TiO₂ with a different morphology, a second TiO₂ sputtering method was exploited for the type 3 and type 5 substrates. To build the type 5 substrate, a 6 nm ITO sublayer was coated by PVD prior to the deposition of an $845 \text{ nm} \pm 20 \text{ nm}$ TiO₂ layer using a sputtering system equipped with a DC planar magnetron source (Advanced Energy, MDX 500). Metallic titanium target (Ti-Goodfellow, 99.99%, 5 cm diameter) was used for sputtering, with argon (Ar) and oxygen (O₂) as process and reactive gases, respectively. The substrates were placed into the vacuum chamber and the base pressure was set to about 5×10^{-5} Pa using a turbo molecular pump (Pfeiffer Vacuum, HiPace 400) and a rotary pump (Agilent Technologies, SH-110). An Ar/O₂ gas mixture with a constant ratio of 250:10 sccm was supplied using a precise mass-flow-control system (MKS, Multi Gas Controller 647C) at a DC power of 120 W (BeamTech DC Pulse Power

Supply MPS1500P). The substrates were rotated at 30 rpm to ensure homogeneous film deposition. Following the 2-hour sputtering process, the prepared TiO₂ thin films underwent heat treatment in a muffle furnace at a temperature of 400°C for 90 minutes and then directly quenched in air.



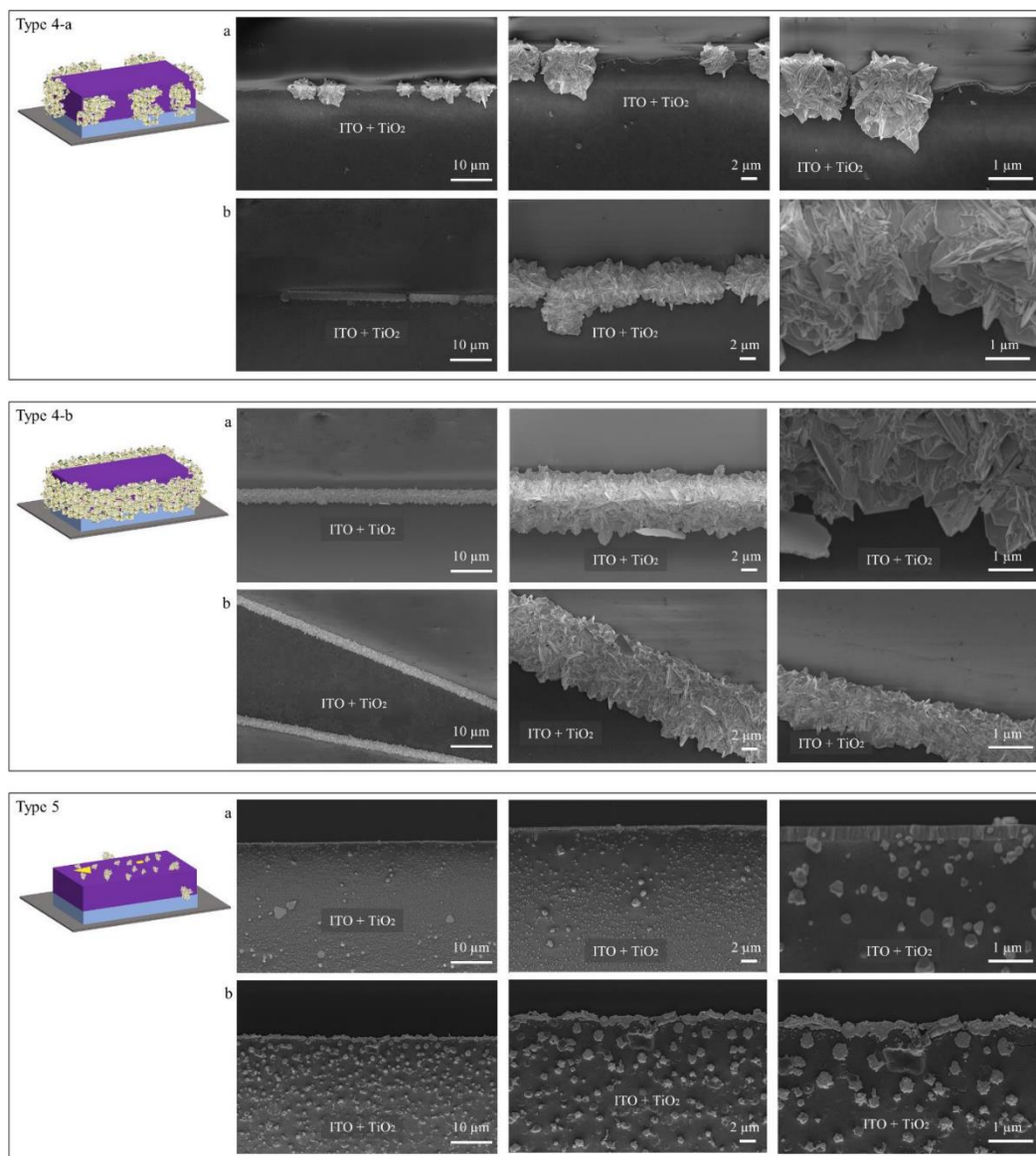


Figure S1. SEM images of the different types of substrates (type 1 – type 5). For each substrate type, two different samples (a and b) are demonstrated for comparison.

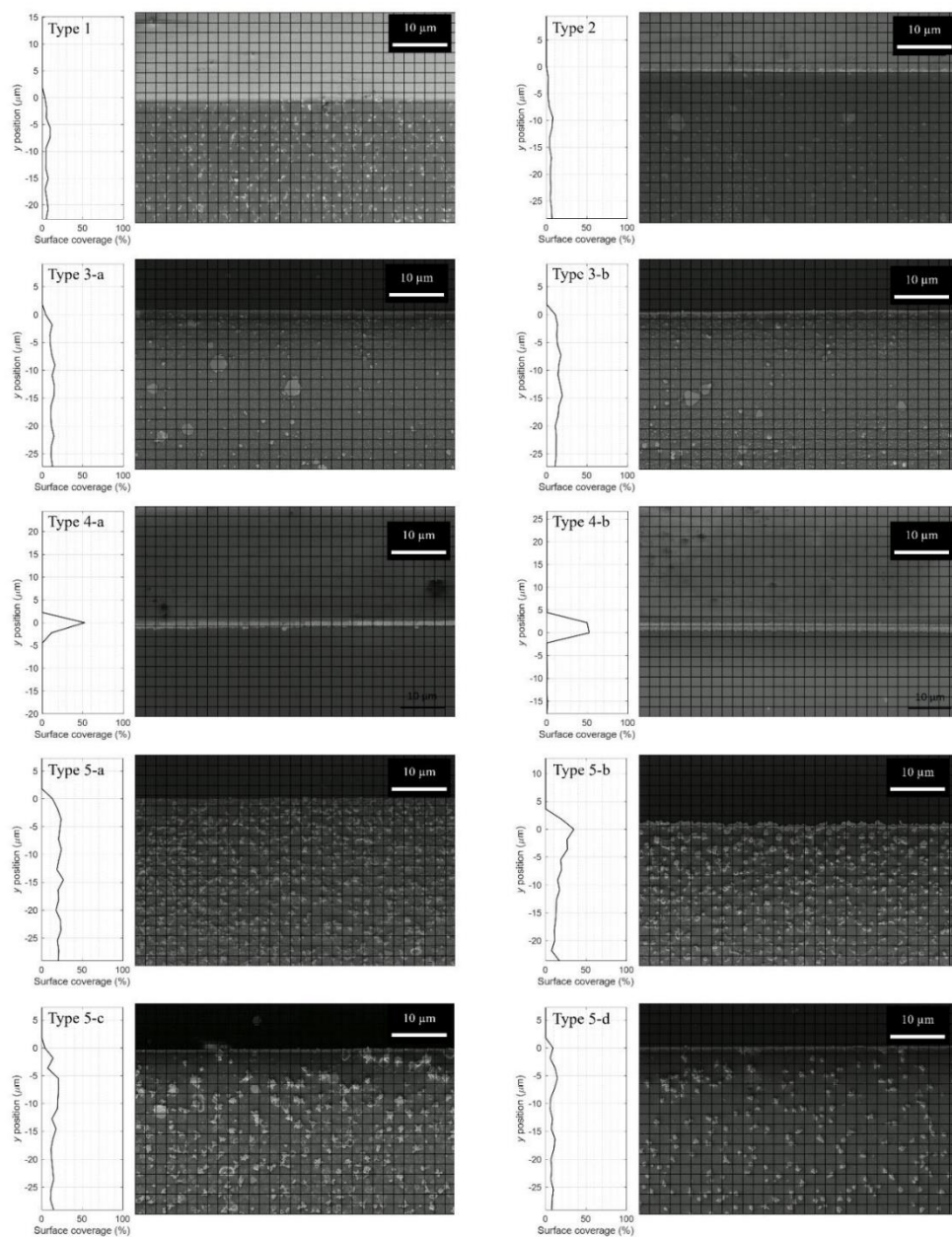


Figure S2. SEM images of the different types of substrates (type 1 – type 5) along with their corresponding gold surface coverage evaluation. Two samples of type 3 and four samples of type 5 substrates are studied and the results are shown for comparison.

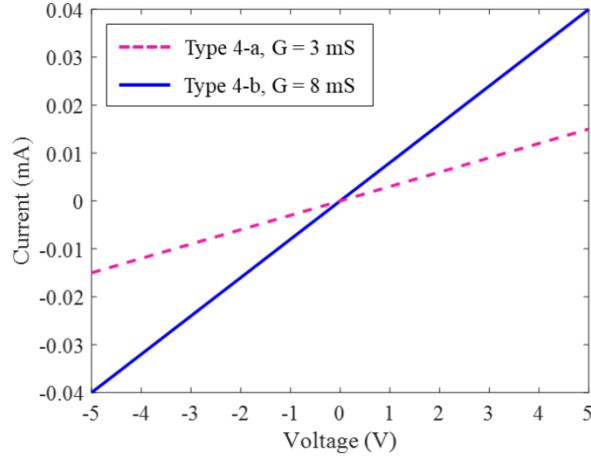


Figure S3. I-V diagram measured for a 180- μm long line on the type 4-a and type 4-b substrates with their corresponding conductance values: type 4-a (3 mS) and type 4-b (8 mS).

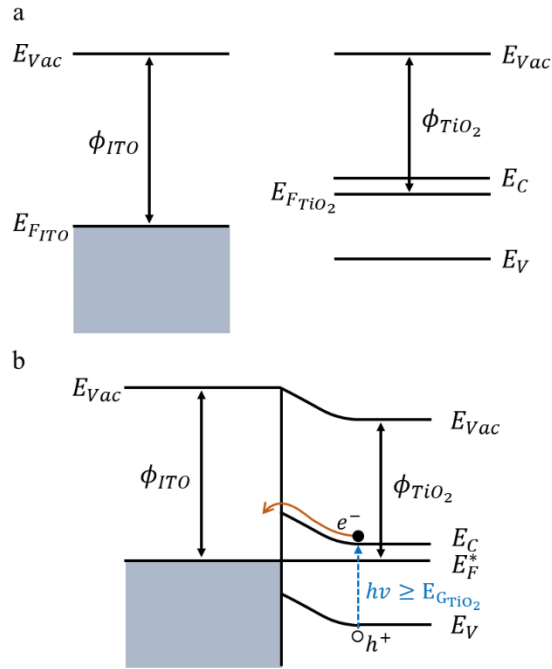


Figure S4. (a) Band diagrams of conductive ITO (left) and semiconductor TiO_2 (right). (b) Since ITO has a higher work function than TiO_2 , a Schottky barrier is formed at the TiO_2 -ITO interface

[S1]. When the sample is exposed to UV light ($h\nu \geq E_{\text{G}_{\text{TiO}_2}}$), electron-hole pairs are generated within the TiO_2 layer causing a shift in its Fermi level. To re-establish equilibrium, the photogenerated electrons flow across the junction from TiO_2 to ITO. This results in a continuous flow of photogenerated electrons from TiO_2 towards ITO.

References

[S1] Dai, W.; Wang, X.; Liu, P.; Xu, Y.; Li, G.; Fu, X. Effects of Electron Transfer between TiO_2 Films and Conducting Substrates on the Photocatalytic Oxidation of Organic Pollutants. *J. Phys. Chem. B* **2006**, 110(27), 13470-13476.

3.2. ITO-TiO₂ Heterojunctions on Glass Substrates for Photocatalytic Gold Growth along Pattern Edges

3.2.1. Introduction

F. Abshari, M. Paulsen, S. Veziroglu, A. Vahl, and M. Gerken, "ITO-TiO₂ Heterojunctions on Glass Substrates for Photocatalytic Gold Growth Along Pattern Edges," *Catalysts*, vol. 14, no. 12, p. 940, Dec. 2024, doi: 10.3390/catal14120940.

Copyright © 2024 by the authors. Published by MDPI, Basel, Switzerland. This article is an open access article distributed under the terms and conditions of the Creative Commons Attribution (CC BY) license (<https://creativecommons.org/licenses/by/4.0/>).

Statement about the own contribution:

For this publication, I collected the data, wrote the manuscript, conducted the data analysis, prepared the samples, and performed the SEM and conductance measurements. Additionally, I contributed to developing the research idea.

Conceptualization	Planning	Implementation	Manuscript Preparation
Medium	High	High	High

3.2.2. Abstract

The second paper, titled "ITO-TiO₂ Heterojunctions on Glass Substrates for Photocatalytic Gold Growth along Pattern Edges," explores the relationship between ITO layer thickness and photocatalytic gold deposition on TiO₂ substrates. The study aimed to investigate how different ITO configurations influence gold nanostructure growth, particularly along pattern edges, to establish highly conductive and spatially resolved pathways. This research aligns closely with the thesis' overarching goal of advancing adaptive and reconfigurable neuromorphic systems through precise photocatalytic techniques that emulate neural connectivity.




This study contributes to the broader thesis objectives by offering a comprehensive understanding of how ITO-TiO₂ heterojunctions can be engineered to optimize photocatalytic performance. By examining the interplay between material properties and photocatalytic activity, the research addresses the critical challenge of achieving uniform and controlled gold growth, a foundational requirement for designing neuromorphic networks. The findings underscore the role of ITO layer thickness in shaping gold nanoparticle formation, directly supporting the thesis's focus on developing bio-inspired electronic systems with enhanced adaptability and precision.

The methodology involved the fabrication of six distinct glass substrates, each with varying ITO layer thicknesses combined with a uniform TiO₂ layer, to systematically investigate the influence of ITO configurations on gold deposition. Photocatalytic experiments utilized UV illumination to activate the TiO₂ substrate, facilitating gold ion reduction and the formation of nanoparticles. Scanning electron microscopy (SEM) was employed to characterize the resulting gold structures, evaluating their morphology, uniformity, and conductivity. The study revealed that a 6-nm ITO layer beneath a 70-nm TiO₂ film provided optimal conditions for uniform gold line formation with enhanced edge-specific growth, highlighting the potential of this configuration for neuromorphic applications requiring precise and reliable connectivity.

3.2.3. Published Paper

Article

ITO-TiO₂ Heterojunctions on Glass Substrates for Photocatalytic Gold Growth Along Pattern Edges

Fatemeh Abshari ^{1,*} , Moritz Paulsen ¹, Salih Veziroglu ^{2,3} , Alexander Vahl ^{2,3,4} and Martina Gerken ^{1,3,*} 

¹ Chair for Integrated Systems and Photonics, Department of Electrical and Information Engineering, Faculty of Engineering, Kiel University, Kaiserstr. 2, 24143 Kiel, Germany; mopa@tf.uni-kiel.de

² Chair for Multicomponent Materials, Department of Materials Science, Faculty of Engineering, Kiel University, Kaiserstr. 2, 24143 Kiel, Germany; sve@tf.uni-kiel.de (S.V.); alva@tf.uni-kiel.de (A.V.)

³ Kiel Nano, Surface and Interface Science KiNSIS, Kiel University, Christian-Albrechts-Platz 4, 24118 Kiel, Germany

⁴ Leibniz Institute for Plasma Science and Technology, Felix-Hausdorff-Str. 2, 17489 Greifswald, Germany

* Correspondence: fa@tf.uni-kiel.de (F.A.); mge@tf.uni-kiel.de (M.G.); Tel.: +49-43188-06255 (F.A.); +49-43188-06250 (M.G.)

Abstract: This study investigates the effects of varying indium tin oxide (ITO) layer thicknesses and the patterning of the ITO layer on the growth of metallic gold (Au) nano- and microstructures on titanium dioxide (TiO₂) templates. The ITO-TiO₂ heterojunction serves to collect photogenerated electrons in the ITO sublayer, facilitating their transport to the pattern edges and concentrating photocatalytic activity at these edges. Six template types were fabricated on glass substrates, with systematic variations in ITO thickness (0, 3, 6, 10, and 30 nm) and different ITO patterning methods (either continuous or patterned with the TiO₂ layer). Photocatalytic gold growth was carried out on each of the substrates, and morphological analysis was conducted using scanning electron microscopy (SEM). Results showed that a 6 nm ITO layer beneath a 70 nm TiO₂ layer yielded the most uniform gold lines, characterized by 3D flower-shaped structures and enhanced edge growth. Conductance measurements indicated a value of 23 mS, suggesting potential applications in bio-inspired electronics. These findings provide insights into optimizing gold structure growth for advanced neuromorphic devices.

Keywords: photocatalytic deposition; heterojunction; titanium dioxide; indium tin oxide; gold; microstructure; glass substrate; neuromorphic engineering; ITO-TiO₂ heterojunction



Citation: Abshari, F.; Paulsen, M.; Veziroglu, S.; Vahl, A.; Gerken, M. ITO-TiO₂ Heterojunctions on Glass Substrates for Photocatalytic Gold Growth Along Pattern Edges. *Catalysts* **2024**, *14*, 940. <https://doi.org/10.3390/catal14120940>

Academic Editor: Raphaël Schneider

Received: 17 November 2024

Revised: 12 December 2024

Accepted: 16 December 2024

Published: 19 December 2024



Copyright: © 2024 by the authors. Licensee MDPI, Basel, Switzerland. This article is an open access article distributed under the terms and conditions of the Creative Commons Attribution (CC BY) license (<https://creativecommons.org/licenses/by/4.0/>).

1. Introduction

Neuromorphic engineering is dedicated to designing advanced computing systems that are inspired by the structure and function of biological neural networks, aiming for greater efficiency and innovation [1]. In neural networks, synaptic connections between neurons are continuously and dynamically reconfigured. These connections evolve across various time scales: rapid synaptic plasticity causes local changes at synaptic junctions between two neurons, while slower processes such as synaptic blooming and pruning occur more broadly across the entire neural network. Numerous studies have concentrated on replicating rapid synaptic plasticity using memristive devices due to their distinctive ability to mimic key synaptic behaviors. Memristive devices have demonstrated properties such as spike-timing-dependent plasticity (STDP), long-term potentiation (LTP), and long-term depression (LTD), which are essential mechanisms underlying synaptic plasticity in biological systems. These characteristics make memristive devices particularly promising for use as electronic synapses, enabling the emulation of dynamic brain-like processes [2,3]. Research continues to explore synaptic connections on a global scale in biological neural networks as well as to develop new methods for integrating these mechanisms into future bio-inspired systems [4]. Neuromorphic nanowire networks exhibiting

memristive properties have become a subject of study [5–8]. These networks are inherently self-organized, with nanowires forming one-dimensional (1D) conductive pathways. The complex topology of these networks leads to collective switching behaviors, making them well-suited for memristive architectures. In neural networks, the ability to dynamically adjust stimuli and manage the formation and dissolution of connections is essential [9]. Initially, replicating the global interactions of neuron assemblies was accomplished by exploring global connectivity via electrolyte gating in a liquid medium [10]. In this paper, we concentrate on the slow development of one-dimensional long-range connections, which may enable flexible adaptation of network topology. To achieve this, we examine the photocatalytic deposition of gold lines utilizing heterojunctions of UV-activated TiO_2 and ITO.

To achieve this, TiO_2 , a highly effective photocatalyst, was chosen for its excellent properties in photocatalytic processes [11]. The combination of TiO_2 with an ITO layer forms a heterojunction that can enhance electron collection and transport, which is crucial for efficient growth processes [12]. This heterojunction, under UV illumination, facilitates the photocatalytic deposition of gold nanoparticles, enabling the creation of gold lines on the TiO_2 surface. The ability to control and modify the growth of these lines opens up potential applications in bio-inspired electronics, such as neural interfaces and devices for bioelectronics [13].

TiO_2 is extensively used as a semiconductor photocatalyst due to its exceptional photocatalytic efficiency, straightforward and economical processing, non-toxicity, and chemical stability [14–17]. The growth of gold on TiO_2 thin films has been achieved through the photoreduction of HAuCl_4 under UV light [18–20]. A range of studies has examined the factors affecting the morphology of the resulting gold structures. The morphology and coverage of the deposited gold structures are significantly influenced by several factors, including the crystal structure and morphology of the underlying TiO_2 thin film, the composition and pH of the precursor solution, and the intensity and duration of illumination [21–23].

Under UV light, TiO_2 generates electron-hole pairs, with electrons moving to the conduction band. These electrons reduce Au^{3+} ions from HAuCl_4 to form neutral gold atoms, which aggregate into conductive gold deposits on the TiO_2 surface. The holes oxidize surrounding molecules, completing the photocatalytic process [24]. A recent study developed $\text{Au/TiO}_2\text{--C}_3\text{N}_4$ composites incorporating plasmonic gold particles, which demonstrated enhanced photocatalytic efficiency due to increased visible light absorption and extended lifetimes of the photoexcited charge carriers [25]. A related study highlighted the coalescence of gold clusters under UV light, focusing on photon energy-driven mechanisms that affect photocatalytic activity. These results offer further insight into how UV illumination contributes to the growth and morphological changes of gold particles.

Previous research has investigated TiO_2 -ITO heterojunctions on glass substrates and demonstrated rectifying behavior at the semiconductor–semiconductor heterojunction [11,26]. To accurately describe the interface between TiO_2 and ITO, we refer to it as a heterojunction, as both TiO_2 and ITO are semiconductors. An ITO- TiO_2 heterojunction is expected to form at this semiconductor–semiconductor interface, which influences the photocatalytic growth of gold particles. This terminology aligns with the focus of the special issue on heterojunctions and enhances the precision of our description [27]. ITO was found to serve as an acceptor for electrons photogenerated in TiO_2 [11,26]. Recently, we suggested the idea of collecting photogenerated electrons with an ITO sublayer for transport to pattern edges and concentration of photocatalytic activity to these edges [13]. In that study, we utilized a 6-nm ITO sublayer beneath a 70-nm TiO_2 on a silicon substrate and demonstrated successful photocatalytic growth of gold lines along pattern edges.

Here, we present a systematic study of the influence of ITO thickness in the ITO- TiO_2 heterojunction on photocatalytic gold growth, as depicted schematically in Figure 1. This work builds upon previous studies, but with a key distinction: while the earlier research utilized silicon wafers with thermal oxide as substrates, this study investigates the effect of

glass substrates. The transparency of the glass substrates introduces new considerations for gold growth, particularly in terms of UV illumination and the ability to observe and monitor the process. We aim to investigate the influence of varying ITO thicknesses while maintaining uniformity in other parameters, such as UV intensity and the gold solution. By controlling these variables, we can better understand the impact of ITO thickness on gold nanoparticle growth. Six distinct template types were prepared with varying ITO thicknesses, and growth experiments were conducted under identical conditions. Relevant data for each template type can be found in Table 1, and the substrate preparation details are provided in Section 4. For each template type, two substrates were prepared and analyzed.

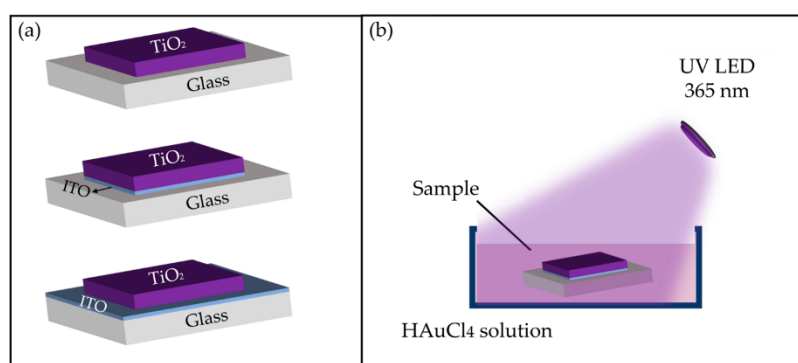


Figure 1. Schematic illustrations of template structures and the illumination setup. (a) Three types of TiO₂ patterns on glass substrates: the top shows a TiO₂ pattern on glass, the middle shows a TiO₂ pattern with a thin ITO layer beneath TiO₂ on glass, and the bottom shows a TiO₂ pattern with a thin ITO layer covering the entire glass substrate. (b) Schematic of the illumination setup, showing the template placed in a beaker with HAuCl₄ solution under UV LED illumination (365 nm).

Table 1. Different template types and their corresponding ITO and TiO₂ thicknesses.

Template Type	ITO Thickness	ITO Extend	TiO ₂ Thickness
Type 1/TiO ₂ -70_ITO-0	0 nm	none	70 nm
Type 2/TiO ₂ -70_ITO-3	3 nm	under TiO ₂	70 nm
Type 3/TiO ₂ -70_ITO-6	6 nm	under TiO ₂	70 nm
Type 4/TiO ₂ -70_ITO-10	10 nm	under TiO ₂	70 nm
Type 5/TiO ₂ -70_ITO-30	30 nm	under TiO ₂	70 nm
Type 6/TiO ₂ -70_ITO-6-unstr.	6 nm	substrate coated completely	70 nm

2. Results

2.1. Morphological Characterization via SEM

In this section, the morphology of the gold particles grown for ITO-TiO₂ heterojunctions with different ITO layer thicknesses is characterized using scanning electron microscopy (SEM). The SEM measurements were conducted using a Supra55VP instrument from Carl Zeiss, operated at an acceleration voltage of 3 kV and a working distance of 3 mm. This method provides high-resolution imaging to examine the size, shape, and spatial distribution of the particles across the substrates.

Each sample type is analyzed individually, highlighting the variation in nanoparticle growth across the different template structures. For each type of template, two samples were prepared, and the corresponding SEM images are presented as (a) and (b). The analysis aims to capture the effects of different ITO layer thicknesses and configurations on particle growth, providing a comparative study of the samples.

2.1.1. SEM Analysis of Type 1/TiO₂-70_ITO-0: TiO₂ Patterns

As anticipated and previously reported in studies on photocatalytic growth on TiO₂ [28], two distinct types of gold particles were observed on the surface of the TiO₂ patterns. The first type consisted of 2D stacked structures, exhibiting various geometrical shapes such as rectangles, hexagons, and polygons. Interestingly, several of these 2D stacks appeared incomplete, as highlighted by a red square in Figure 2, where a partially formed stack is clearly visible.

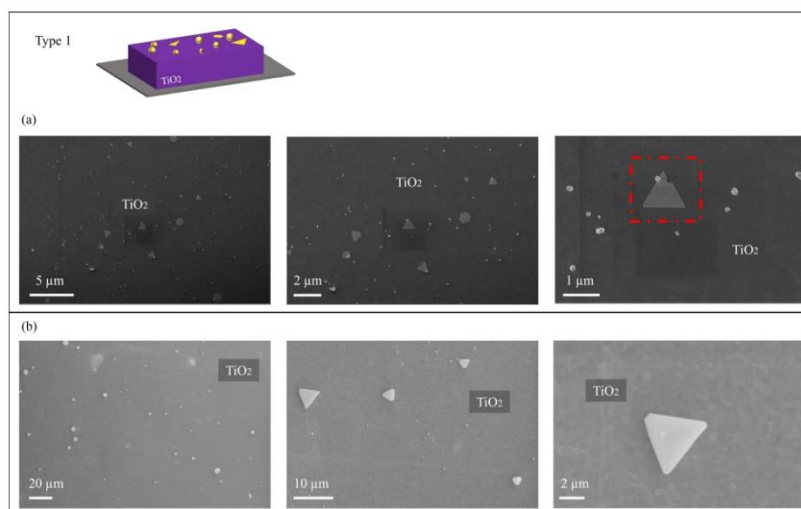


Figure 2. SEM images of Type 1/TiO₂-70_ITO-0 template showing two types of grown gold particles on the surface of TiO₂: (a) Sample 1, and (b) Sample 2, highlighting the presence of 2D stacks and smaller spherical particles. A partially formed 2D stack is indicated by a red square in (a).

The second type of particles observed were spherical, smaller in size compared to the 2D stacks. Notably, no particle growth was detected along the edges of the TiO₂ patterns. The overall quantity of particles on the TiO₂ surface was relatively low. The spherical particles were largely isolated, with only a few instances where they were found clustered together. In addition, in some areas, spherical particles were seen growing on top of the 2D stacks, further illustrating the variability in particle formation across the surface.

2.1.2. SEM Analysis of Type 2/TiO₂-70_ITO-3: TiO₂ Patterns with 3 nm ITO Layer

The morphology of the gold particles grown on the Type 2 template, consisting of TiO₂ patterns with a 3 nm ITO layer, closely resembles that observed in the Type 1/TiO₂-70_ITO-0 samples. Two distinct morphologies are present: spherical particles and 2D stacks, predominantly hexagonal in shape shown in Figure 3. Additionally, several incompletely formed stacks can be observed, similar to those seen in Type 1/TiO₂-70_ITO-0. However, a notable increase in the quantity of gold particles is evident, particularly with the spherical morphology.

All observed particles are grown on the surface of the TiO₂ patterns, with no significant particle growth along the edges of the patterns. While some spherical particles are also found atop the 2D stacks, the overall distribution remains dispersed, with the particles still largely separated from one another, as seen in earlier samples. This indicates that despite the increased particle count, significant aggregation or clustering has not occurred.

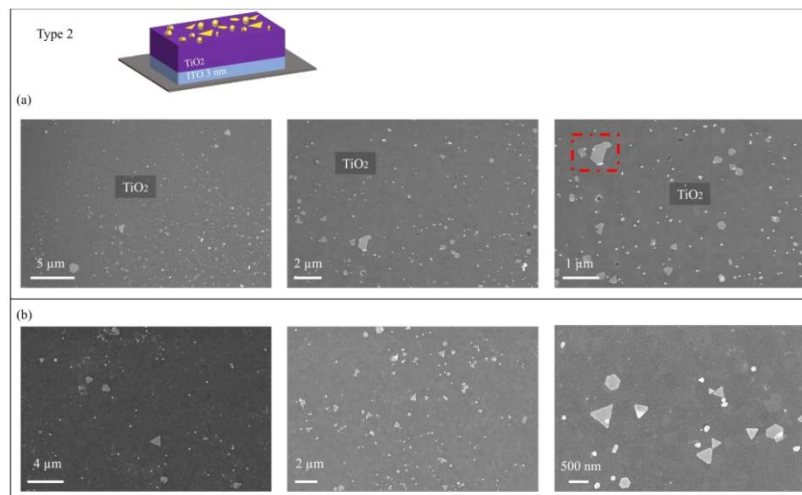


Figure 3. SEM images of Type 2/TiO₂-70_ITO-3 template showing the morphology of grown gold particles on the surface of TiO₂: (a) Sample 1 and (b) Sample 2 depicting the distribution of 2D stacks and smaller spherical particles. A partially formed 2D stack is indicated by a red square in (a).

2.1.3. SEM Analysis of Type 3/TiO₂-70_ITO-6: TiO₂ Patterns with 6 nm ITO Layer

In the Type 3 template, which includes a 6 nm ITO layer beneath the TiO₂ patterns, a third morphological shape of gold particles was observed (see Figure 4), adding to the previously identified spherical and 2D stack formation.

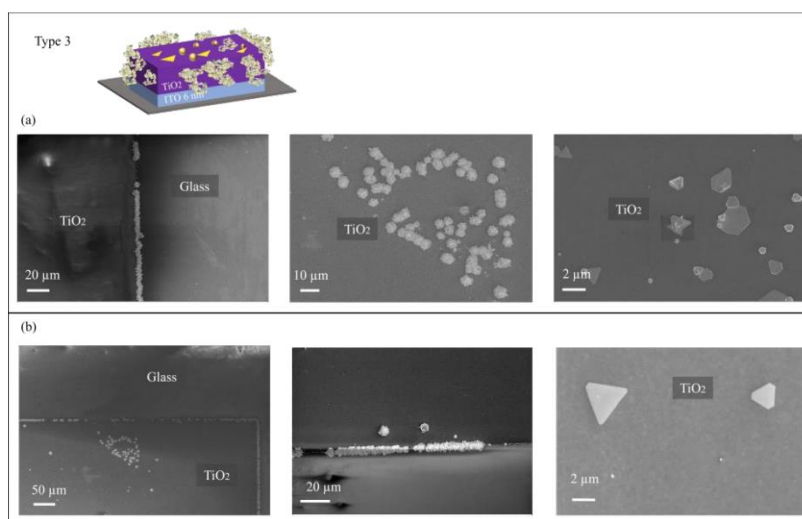


Figure 4. SEM images of Type 3/TiO₂-70_ITO-6 template after gold growth: (a) Sample 1 and (b) Sample 2, highlighting the emergence of 3D flower-like structures along the edges of the TiO₂ patterns, alongside isolated spherical particles and limited 2D stacks.

While spherical gold particles were still present on the surface of the TiO₂, their quantity was notably low, with only isolated instances observed across the substrate. These spherical particles were small in number and remained separated, showing no significant clustering or attachment.

2D stacks, primarily hexagonal in shape, were also detected, and in several instances, they were seen growing on top of each other, forming stacked structures. Despite the

growth of these 2D stacks in layered formations, their overall quantity on the surface of the TiO_2 remained limited. Additionally, no significant growth of either the spherical particles or 2D stacks was observed along the edges of the TiO_2 patterns; both morphologies were restricted to the surface of the patterns.

The most distinctive feature of this template was the emergence of a new, third morphology, a 3D flower-like structure. These particles, resembling hedgehog shapes with needle-like branches, were found growing predominantly along the edges of the TiO_2 patterns. In some regions, these flower-shaped particles aligned next to each other, forming a near-continuous line along the pattern's edge, though there were occasional gaps between them. This suggests a strong preference for edge growth, which was more uniform compared to the surface. The SEM images of the Type 3 template, which features a 6 nm ITO layer beneath the TiO_2 patterns, reveal the presence of two distinct morphologies of gold particles: 2D stacks and 3D flower-like structures. The 2D stacks, primarily hexagonal in shape, are observed in small quantities, while the 3D flower-like particles, which exhibit needle-like structures, are more prominent, particularly along the edges of the TiO_2 patterns. These flower-like structures show some degree of alignment along the edge, although they do not form a continuous line.

2.1.4. SEM Analysis of Type 3/ TiO_2 -70_ITO-6: TiO_2 Patterns with Manual Scratches

In this section, the results of the SEM analysis for the template with manual scratches on the TiO_2 surface are presented. The SEM images (Figure 5) clearly show the growth of gold particles on the surface of TiO_2 , with nucleation occurring predominantly in the manually created scratches. These scratches, which vary in width, serve as localized sites for the gold particle formation. The SEM images indicate that the gold particles were successfully nucleated both in the thinner and wider scratched areas. The density of the gold particles appears higher in the narrower scratches, suggesting that smaller features might enhance the nucleation and growth of gold nanoparticles. In contrast, wider scratches exhibit a more scattered distribution of gold particles, albeit still concentrated in the scratched regions. This observation highlights the importance of the surface features in controlling the localization of gold growth. It appears that only very limited gold growth appears on intact TiO_2 surface areas while scratches or edges in the ITO- TiO_2 promote and concentrate the gold growth. The nucleation sites in the scratches demonstrate a clear relationship between the surface morphology and gold particle deposition.

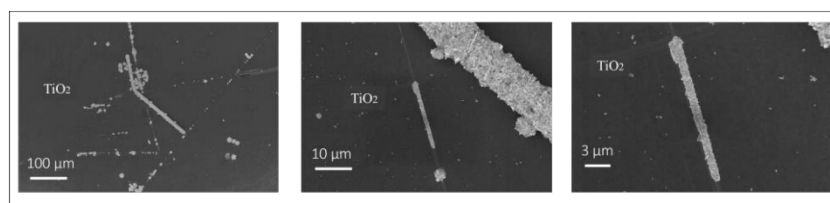


Figure 5. SEM images of the TiO_2 surface with manual scratches of varying widths, showing the growth of gold particles on the TiO_2 surface. The nucleation of gold occurs primarily within the scratches.

2.1.5. SEM Analysis of Type 4/ TiO_2 -70_ITO-10: TiO_2 Patterns with 10 nm ITO Layer

The SEM analysis of templates featuring a 10 nm ITO layer beneath the TiO_2 patterns revealed two distinct morphologies of gold particles (see Figure 6). First, 2D stacks of gold particles were observed, characterized by hexagonal and rectangular shapes. However, these stacks were relatively sparse, indicating limited formation across the substrate.

In addition to the 2D stacks, 3D flower-shaped particles were identified on the surface of TiO_2 . These flower-shaped particles exhibited a more prominent presence compared to the 2D stacks, but their distribution was uneven. The individual flower structures displayed visible gaps between them, suggesting that they did not aggregate closely. Notably, these 3D

flower-shaped particles did not form a continuous line along the edge of the TiO_2 patterns. Instead, they appeared scattered across the surface, lacking a cohesive arrangement. The SEM analysis revealed three distinct morphologies of gold particles: spherical particles, 2D stacks, and flower-shaped particles. While both 2D stacks and flower-shaped particles were present, the flower-shaped particles exhibited more prominent growth, particularly along the edges of the TiO_2 patterns. However, the distribution of these flower-shaped particles was uneven, with noticeable gaps between them, highlighting the variability in growth behavior across the substrate.

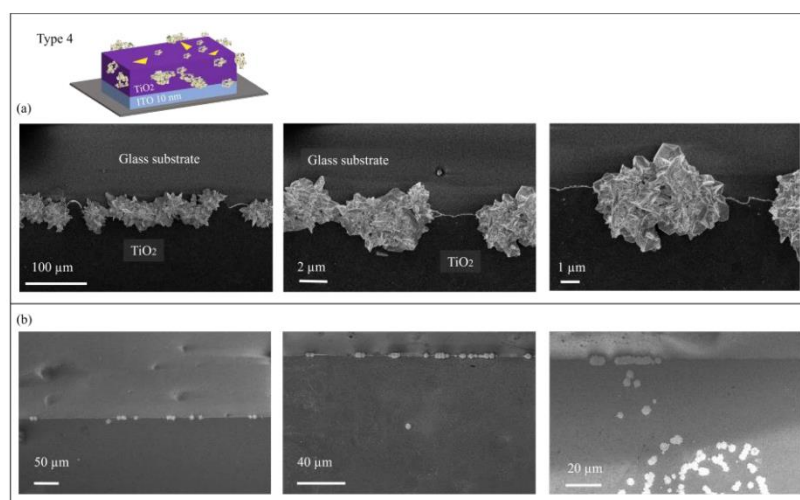


Figure 6. SEM images of Type 4/ TiO_2 -70_ITO-10 template after gold growth: (a) Sample 1 and (b) Sample 2, showing distinct morphologies of gold particles including sparse 2D stacks and unevenly distributed 3D flower-shaped particles on the TiO_2 surface, with visible gaps indicating limited aggregation.

2.1.6. SEM Analysis of Type 5/ TiO_2 -70_ITO-30: TiO_2 Patterns with 30 nm ITO Layer

On the templates featuring a 30 nm ITO layer beneath the TiO_2 , three distinct morphological shapes of gold particles were observed. The first morphology consisted of spherical gold particles, which displayed a notable increase in quantity and coverage across the surface of the TiO_2 . This enhanced density suggests a more efficient growth process under the specific conditions provided by the ITO layer.

The second morphology observed was that of 2D stacks, which are presented in both hexagonal and rectangular shapes. These stacks exhibited a high quantity and substantial surface coverage; however, it was noted that the spherical particles did not grow in close proximity to one another, maintaining noticeable separations. Furthermore, while the 2D stacks demonstrated good structural integrity, their sizes appeared to be smaller than those observed in previous sample types, indicating a potential size reduction in the growth process.

The third morphology consisted of flower-shaped gold particles. These particles were prominently observed on the surface of the TiO_2 in Figure 7, exhibiting intricate branching structures that seemed to suggest an interaction between clusters. However, despite this potential for interaction, the flower-shaped particles were still observed to grow separately. These larger gold structures were unable to form a continuous line along the edge of the pattern, resulting in only a few short, uniform segments along the edge. This indicates that while there was some level of organization, the overall alignment and connectivity of the particles require further optimization.

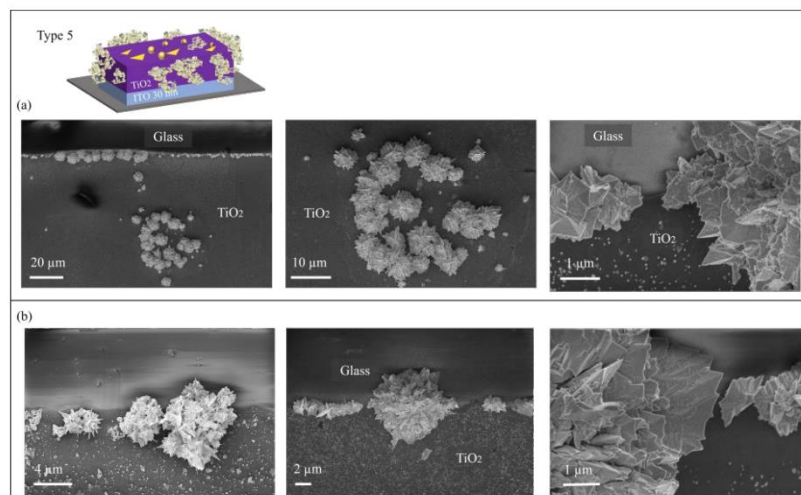


Figure 7. SEM images of Type 5/TiO₂-70_ITO-30 template after gold growth: (a) Sample 1 and (b) Sample 2, illustrating three distinct morphologies of gold particles, including spherical particles, 2D stacks with varied shapes, and hedgehog-like flower structures on the TiO₂ surface, with varying distribution and density.

2.1.7. SEM Analysis of Type 6/TiO₂-70_ITO-6-unstr.: TiO₂ Patterns with 6 nm ITO Layer Across the Entire Substrate

In this analysis in Figure 8, the templates with a 6 nm ITO layer extending across the entire substrate exhibit morphological characteristics that are somewhat similar to those observed in Type 3, differing primarily in the placement of the ITO layer. Unlike Type 3, where the ITO was localized beneath the TiO₂ patterns, Type 6 features ITO uniformly distributed across the substrate.

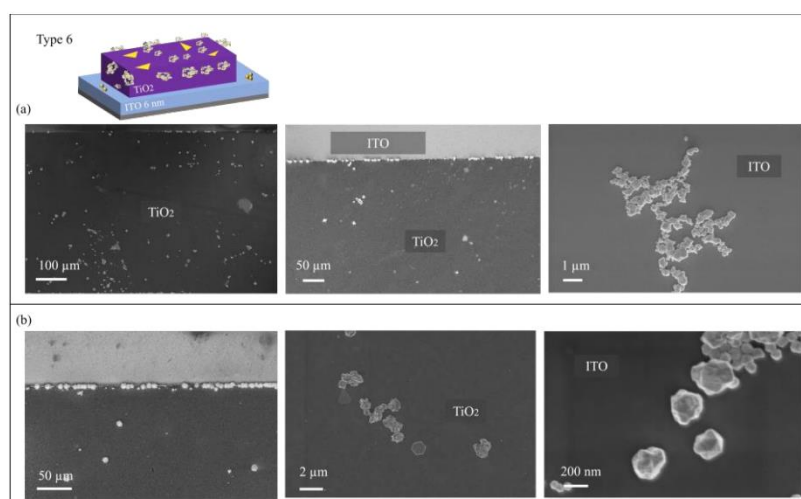


Figure 8. SEM images of Type 6/TiO₂-70_ITO-6-unstr. template after gold growth: (a) Sample 1 and (b) Sample 2, illustrating primarily 2D stacks in low quantities, 3D flower-shaped particles on the TiO₂ surface, and spherical particles on the ITO layer, with attempts at cluster interaction but no formation of a continuous line along the edges.

The shapes of the grown particles reveal a lack of spherical particles. Instead, primarily 2D stacks were observed in triangular forms, though these structures appeared in very low

quantities. Additionally, 3D flower-shaped particles were identified on the surface of the TiO_2 ; however, these structures seemed to be incompletely formed. Notably, while the 3D flower shapes exhibited closer proximity to one another than in previous types, they still failed to form a uniform line along the edge of the TiO_2 patterns.

Furthermore, SEM analysis of the ITO surface revealed the presence of spherical particles formed on the 6 nm ITO layer. These spherical particles appeared to be attached to one another, with an average dimension of approximately 200 nm.

2.2. Conductance Measurement of Gold Lines on TiO_2 Patterns

As observed in the SEM analysis, uniform gold lines were clearly visible on the edge of the TiO_2 patterns in both Type 3 TiO_2 -70_ITO-6 and Type 6/ TiO_2 -70_ITO-6-unstr. templates. The gold line on the Type 3 template measured approximately 75 μm in length, while the line on Type 6 was estimated to be around 20 μm . However, further conductance analysis revealed differences in their electrical properties.

Conductance measurements were performed using a hard-contact probe station, specifically the Everbeing BD-6 modular probe station, equipped with precision micromanipulators, a PSM-1000 microscope, and a Motic Moticam 3+ CCD camera for high-resolution image capture. The Keithley 2400 Sourcemeter, configured in a two-probe setup, applied a voltage ramp from -5 V to $+5\text{ V}$, allowing for current measurements between the two probes.

On the Type 6/ TiO_2 -70_ITO-6-unstr. templates, it was not possible to measure a uniform conductance along the suspected 30 μm line. Although an area resembling a continuous line was identified, it failed to demonstrate measurable conductivity. Conversely, on Type 3/ TiO_2 -70_ITO-6 templates, the approximately 75 μm gold line demonstrated clear conductive properties. The I-V curve, fitted with a linear regression, showed a conductance value of 23 mS.

3. Discussion

The electron transfer process plays a fundamental role in the formation of gold wires during photocatalytic growth on TiO_2 surfaces. UV light generates electron-hole pairs in the TiO_2 material, and the excited electrons migrate to the surface, where they interact with gold ions (Au^{3+}) from the gold chloride solution. This interaction promotes the reduction and nucleation of gold nanoparticles. The presence of an ITO- TiO_2 heterojunction layer significantly influences this electron transfer process [11,26]. Photogenerated electrons are collected in the ITO sublayer, facilitating their transport to the pattern edges and concentrating photocatalytic activity at these edges. A thicker ITO layer increases the availability of free electrons, improving conductivity and enhancing electron mobility. This, in turn, facilitates the nucleation of gold particles, particularly along the edges of the TiO_2 patterns. The thickness and positioning of the ITO layer—whether beneath the TiO_2 or across the entire substrate—are crucial factors in controlling the uniformity and quality of the gold line. By optimizing the ITO layer, the distribution and morphology of the gold nanoparticles can be better regulated, ensuring more uniform and controlled growth of gold lines along the TiO_2 edges [12].

As observed in the SEM analysis, with 3 nm ITO, the growth of gold particles was moderately increased compared to templates without ITO, but the growth was not highly focused. With a 6 nm ITO layer, the growth of gold particles became more localized along the edges, resulting in a more uniform gold line [22]. However, when the ITO thickness was increased to 10 nm and 30 nm, although the ITO conductivity was higher, the gold growth became more dispersed. This suggests that due to the higher conductivity in the ITO, electrons are more effectively transferred to existing gold nucleation sites instead of uniform nucleation along the structure edge. Therefore, an intermediate conductivity of the ITO layer appears optimal for the growth of conductive gold lines with uniform thickness.

In this section, the results of the morphological analysis obtained through scanning electron microscopy (SEM) are discussed in more detail, comparing and analyzing the

different template types. When comparing Templates Type 1/TiO₂-70_ITO-0 and Type 2/TiO₂-70_ITO-3, it was observed that the presence of ITO significantly enhanced the growth and coverage of gold particles on the surface of TiO₂. While specific quantification of coverage was not performed, the observed increase in the distribution and density of gold particles suggests a significant enhancement. In this context, “coverage” refers to the fraction of the TiO₂ surface covered by gold particles, rather than the number of particles per unit area. However, no notable changes in the morphology of the grown particles were detected; both templates exhibited two-dimensional (2D) stacks alongside smaller spherical particles. Furthermore, the 3 nm ITO layer did not promote focused growth along the edges of the patterns. In contrast, Template Type 3/TiO₂-70_ITO-6 revealed a new 3D flower-like morphology, indicating more concentrated growth at the edges, resulting in a more localized and uniform distribution. To better understand the distribution of different nanoparticle types, a systematic investigation was conducted, categorizing the observed gold particles into three categories: spherical particles, 2D stacks and flower-shaped particles. A comparison of the relative occurrence of each category across different template types is provided in Table 1. The average length of the growth along the edges measured approximately 75 μm , which is considered acceptable for further research in neuromorphic engineering [29].

As the thickness of the ITO increased in Template Type 4/TiO₂-70_ITO-10, the small spherical particles were no longer observed, which was initially unexpected. Instead, larger 3D flower-shaped particles with sharper needle-like formations were present. However, these particles did not cluster as closely together as observed in Template Type 3/TiO₂-70_ITO-6, which hindered the formation of a uniform line along the edges or the surface of TiO₂. Interestingly, while spherical particles were absent in Type 4/TiO₂-70_ITO-10, they were observed again in Template Type 5/TiO₂-70_ITO-30, suggesting a different growth dynamic at the 30 nm ITO thickness. Upon further inspection of the SEM images of Type 5/TiO₂-70_ITO-30, it appears that the small spherical particles were indeed absent in these samples as well, aligning with the overall trend of larger, more irregular gold structures dominating the surface. This discrepancy highlights the complexity of the growth process and suggests that the ITO thickness and its interaction with TiO₂ significantly affect the nanoparticle morphology, with less uniform clustering at higher ITO thicknesses.

To further investigate the effects of increased ITO thickness, Template Type 5/TiO₂-70_ITO-30 was examined. In the SEM images, an increased number of smaller spherical particles were observed on the surface compared to Template Type 2/TiO₂-70_ITO-3. However, the size of the 2D stacks decreased. A higher quantity of 3D flower-shaped particles was noted both on the surface and edges of TiO₂. Yet, similar to Template Type 4/TiO₂-70_ITO-10, these particles failed to grow in close proximity, preventing the formation of a continuous line.

Consequently, it was determined that Template Type 3/TiO₂-70_ITO-6 exhibited the optimal parameters for achieving a uniform gold line along the edges. This raises the question of whether the ITO layer should be exclusively positioned beneath the TiO₂ or if a TiO₂ pattern on a 6 nm ITO substrate, such as on soda-lime glass, would yield better results. Thus, Template Type 6/TiO₂-70_ITO-6-unstr. was fabricated for further analysis. SEM images of this template revealed a similar lack of spherical particles as seen in Template Type 3/TiO₂-70_ITO-6. Additionally, the quantity of 2D stacks was reduced, further highlighting a focus on the 3D flower-shaped particles. However, the interactions between gold clusters along the edges were less pronounced, and the maximum length of the gold line achieved was approximately 20 μm , which is notably shorter than that of Template Type 3/TiO₂-70_ITO-6.

In this study, we anticipated that the heterojunction between the ITO and TiO₂ would primarily promote growth along the edges, with minimal growth observed on the TiO₂ surface. However, to investigate this further, we manually created scratches of varying widths on the TiO₂ surface and observed the gold nanoparticle growth. As expected, a higher concentration of gold particles was observed within the scratches, with nucleation

occurring more readily in the narrower lines. Interestingly, we also noticed an unexpected increase in gold growth across the surface of TiO_2 in Template Type 3, even though the original hypothesis suggested that the growth would be confined to the edges. The variation in gold growth on the TiO_2 surface with different ITO thicknesses suggests that this phenomenon could be attributed to either defects in the ITO layer or accidental imperfections in the scratching process. These observations highlight the complex nature of the growth mechanism, where factors such as the ITO layer's integrity and surface modifications may influence the overall nanoparticle distribution.

Across all template types, no growth of particles on the glass substrate was observed. In Template Type 6/ TiO_2 -70_ITO-6-unstr., despite the presence of ITO covering the entire substrate, only a few small spherical particles were identified, which is not ideal for achieving a uniform and continuous gold line along the edges. The low density and small size of these particles hinder the formation of a more consistent and well-defined structure. Thus, from the physical morphology characterization, it can be concluded that Template Type 3/ TiO_2 -70_ITO-6 possesses the most favorable parameters for achieving a uniform line and localized growth along the edges.

The ITO- TiO_2 heterojunction plays a crucial role in controlling the growth of gold particles by facilitating the collection and transport of photogenerated electrons under UV illumination. The ITO layer, acting as a conductive substrate, enhances electron transfer from the TiO_2 layer to the gold precursor solution, promoting the reduction of gold ions. This electron transfer is key in enabling uniform and localized growth of gold lines, particularly at the edges of TiO_2 patterns. By adjusting the thickness of the ITO layer, we can control the rate and uniformity of gold deposition, which is essential for achieving the desired gold line structures for bio-inspired electronics applications.

In our experiments, the ITO- TiO_2 heterojunction significantly influenced the morphology of the gold nanoparticles. The interaction between the ITO layer and TiO_2 not only facilitated the photocatalytic reduction of gold ions but also played a critical role in shaping the size, density, and distribution of the resulting gold structures. The presence of the ITO layer beneath TiO_2 enhanced electron mobility, which in turn increased the local gold nanoparticle growth at the edges of the TiO_2 patterns. This heterojunction setup enabled better control over the deposition process, contributing to the formation of more uniform and localized gold lines, particularly in Template Type 3/ TiO_2 -70_ITO-6, compared to other configurations.

Looking ahead, the use of ITO- TiO_2 heterojunctions presents several promising possibilities for future applications in bioelectronics and neuromorphic engineering. By optimizing the ITO layer thickness and TiO_2 patterning, we can further enhance the precision of gold growth, making it possible to create more complex, conductive networks that emulate the properties of biological neural networks. These networks could be integrated into neural interfaces, prosthetics, or other bio-inspired systems, where controlled, localized growth is essential for improving signal transmission and reducing resistance. Furthermore, the ability to tune the heterojunction for specific applications could lead to more efficient, flexible, and scalable designs in the development of next-generation bioelectronics.

As highlighted in the introduction, one of the primary objectives of this study is to replicate the growth patterns of gold lines to emulate the formation of axons in neurons. This biomimetic approach seeks to harness the conductive properties of gold to facilitate effective signal transmission, which is a crucial function of axons in neural communication.

In the context of neuronal signaling, axons are specialized structures that conduct electrical impulses away from the neuron's cell body. For the gold structures to effectively mimic this function, they must demonstrate sufficient electrical conductivity. The conductance measurement obtained from the current-voltage (I-V) diagram revealed a value of 23 mS.

This level of conductance indicates that the gold lines possess adequate conductivity to potentially facilitate the transfer of electrical signals, similar to how axons transmit impulses between neurons. High conductance values are essential for minimizing resistance

losses in signal propagation, which can lead to more efficient communication within neural networks. The conductivity of the gold lines opens opportunities for bio-inspired electronics, potentially advancing the development of neural interfaces, prosthetics, and other devices that integrate with biological systems.

In this series of experiments, we focused specifically on photocatalytic gold growth while varying the ITO conditions. It is crucial to acknowledge that other parameters significantly influence the quality and uniformity of the grown lines on the various substrate types we prepared. For example, the introduction of additives in gold chloride such as isopropanol or acetone, as well as the inclusion of surfactants, can notably enhance the growth rate of gold particles. This adjustment may lead to the formation of longer gold lines, particularly in Template Types 4 and 5, which feature increased ITO thickness.

Additionally, the intensity and wavelength of the UV LED utilized during the illumination process play a pivotal role in determining the characteristics of the gold lines. Higher-intensity UV light can promote more effective photocatalytic activity, potentially resulting in more consistent and uniform gold growth.

This study thoroughly examined ITO-TiO₂ heterojunctions with varying ITO thicknesses for fixed other photocatalytic gold growth parameters. Future research should explore these additional factors to further understand their impact on the morphology and conductivity of gold lines, ultimately aiming to refine the fabrication process for improved performance in bioelectronic applications. By utilizing transparent glass substrates, we open new opportunities for in-situ monitoring with optical transmission measurements as well as illumination options from the glass substrate side.

4. Materials and Methods

4.1. Substrate Preparation

The preparation of substrates begins with soda-lime glass, which is diced into 10 mm × 10 mm pieces using a Wafer Dicing model DAD3350 from Aurotech. The diced substrates are then subjected to a thorough cleaning process in an ultrasonic bath (Martin Walter Ultraschalltechnik AG, Straubenhardt, Germany) using acetone and isopropanol (Sigma-Aldrich, St. Louis, MO, USA). Following cleaning, the substrates are completely dried with pure nitrogen gas to eliminate any residual solvents.

In this study, six types of templates are prepared to explore the effects of varying ITO layer thicknesses beneath TiO₂. The first template, designated as Type 1/TiO₂-70_ITO-0, is designed as a reference and consists solely of a patterned layer of TiO₂ without any underlying ITO. The subsequent types—Type 2/TiO₂-70_ITO-3 through Type 5/TiO₂-70_ITO-30—feature TiO₂ patterns with varying ITO thicknesses: 3 nm, 6 nm, 10 nm, and 30 nm, respectively. Type 6/TiO₂-70_ITO-6-unstr. differs by having a uniform ITO layer of 6 nm sputtered across the entire surface of the substrate, onto which the TiO₂ pattern is applied.

The lithography process, utilized for all types, commences with the application of hexamethyldisiloxane (HMDS) to enhance photoresist adhesion, followed by the spin-coating of 600 µL of AZ5214E photoresist (Microchemicals GmbH, Ulm, Germany) at 3000 rpm for 30 s. The substrates are prebaked on a hot plate at 110 °C for 50 s before being exposed to UV light through a 5-inch mask featuring reflective chromium structures with line patterns as small as 50 µm (provided by Rose Fotomasken, Bergisch Gladbach, Germany). The exposure is carried out using a SUSS MicroTec mask aligner, delivering an energy dose of 32 mJ/cm². A reversal bake is performed at 120 °C for 2 min, followed by flood UV exposure with an energy dose of 320 mJ/cm². The unexposed areas are subsequently developed using AZ726 developer (Microchemicals GmbH, Ulm, Germany) for one minute, rinsed with deionized water, and dried using nitrogen gas. In Figure 9a the schematic of the lithography steps is illustrated.

For Type 1/TiO₂-70_ITO-0, after lithography, a 70 nm-thick layer of TiO₂ is deposited through sputtering using a 3-inch TiO₂ target (purity 99.99%, Kurt J. Lesker Company GmbH, Dresden, Germany). The lift-off process involves immersing the substrates in

acetone for 10 min while being subjected to ultrasonic agitation, followed by a 5-min immersion in isopropanol. Finally, the substrates are rinsed with deionized water and dried with nitrogen gas.

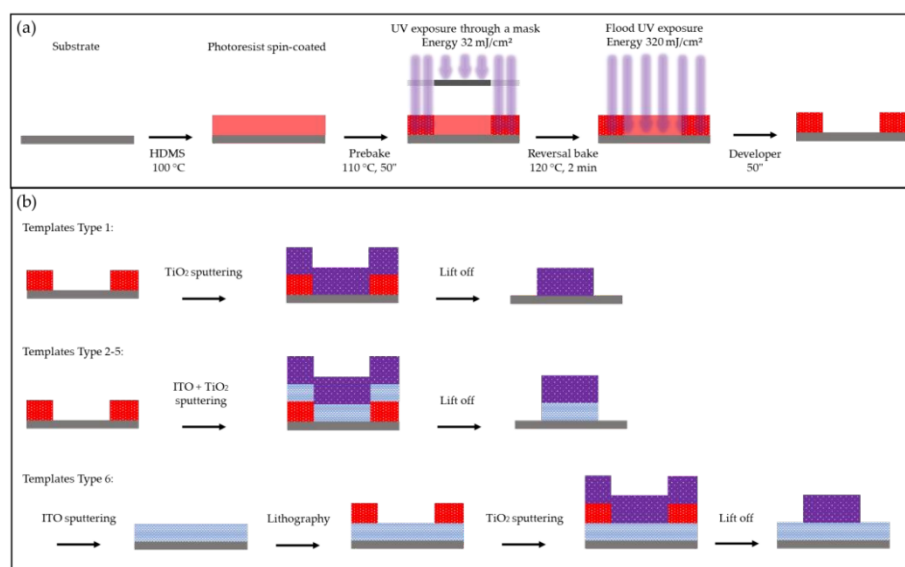


Figure 9. Schematic illustration of the substrate preparation process. (a) Lithography process steps utilizing AZ5214E photoresist on soda-lime glass substrates. (b) Schematic representation of the deposition processes for ITO and TiO₂ across different template types (Type 1/TiO₂-70_ITO-0: TiO₂ only, Type 2: TiO₂ with 3 nm ITO, Type 3: TiO₂ with 6 nm ITO, Type 4: TiO₂ with 10 nm ITO, Type 5: TiO₂ with 30 nm ITO, and Type 6: uniform 6 nm ITO layer with TiO₂).

For Types 2 through 5, the fabrication process is similar to that of Type 1/TiO₂-70_ITO-0, beginning with lithography as described above. Afterward, ITO is deposited using physical vapor deposition (PVD) with a 3-inch In₂O₃/SnO₂ (90/10 wt %) target (99.99% purity, Kurt J. Lesker Company GmbH, Dresden, Germany). The thicknesses of ITO are varied according to the template type: 3 nm for Type 2/TiO₂-70_ITO-3, 6 nm for Type 3/TiO₂-70_ITO-6, 10 nm for Type 4/TiO₂-70_ITO-10, and 30 nm for Type 5/TiO₂-70_ITO-30. Following ITO deposition, a 70 nm-thick layer of TiO₂ is sputtered onto each substrate, mirroring the process used for Type 1/TiO₂-70_ITO-0. The lift-off procedure is executed in the same manner, ensuring the removal of excess resist and leaving behind the desired TiO₂ patterns on the ITO layers.

Type 6/TiO₂-70_ITO-6-unstr. begins with ITO deposition over the entire substrate, applying a uniform layer of 6 nm thickness. The subsequent lithography process follows the previously detailed method, leading to the sputtering of a 70 nm-thick TiO₂ layer. The lift-off process for Type 6/TiO₂-70_ITO-6-unstr. also adheres to the methods established for the earlier types. The schematic in Figure 9b shows the steps and shapes of the templates after deposition.

To convert the TiO₂ thin films to the anatase phase, a heat treatment is uniformly applied to all six template types. The substrates are heated in a muffle furnace at 400 °C for 90 min and then cooled promptly using a metal plate. This step is critical for achieving the desired crystalline structure in the TiO₂.

4.2. Photocatalytic Gold Growth Experiment

The photocatalytic gold growth process was conducted on all six types of substrates using a consistent approach. The photocatalytic reduction of precursor ions from a HAuCl₄ solution was facilitated by UV-illuminated TiO₂ and ITO patterns.

To prepare the precursor solution, 99.99 % pure gold (III) chloride (HAuCl_4) powder, sourced from Sigma-Aldrich, was mixed with deionized water in a concentration of 15 mg in 60 mL of water. This mixture was thoroughly blended to achieve a homogeneous solution.

Each substrate was positioned at the bottom of a 5 cm diameter glass beaker, and 15 mL of the prepared gold precursor solution was added. A UV LED (Nichia) emitting light at a wavelength of 365 nm was then positioned approximately 7 cm above the beaker, providing an intensity of approximately 3.7 mJ/cm^2 , as measured using a Newport optical power meter.

The illumination process for all six types of substrates was carried out in two distinct steps. The first step involved an initial illumination period of 150 min, after which each substrate was carefully washed and dried. Following this, the precursor solution was refreshed, and a second illumination step of 60 min was conducted. After each illumination period, the substrates were consistently washed and dried to ensure optimal conditions for gold particle growth. This cyclic illumination process allowed for the effective photocatalytic reduction of the gold ions, leading to the deposition of gold particles on the substrate surfaces.

4.3. Template Type 3/ TiO_2 -70_ITO-6: TiO_2 Pattern Fabrication with Manual Scratching

In this work, a template similar to Template Type 3 (TiO_2 -70_ITO-6) was created to investigate the localized growth of gold on TiO_2 surfaces. The fabrication process followed the same steps as previously outlined for Type 3, with a 6 nm ITO layer deposited beneath the TiO_2 patterns. To further investigate the growth of gold particles, manual scratching was employed using tweezers. Various micro-scale scratches of different widths were created on the TiO_2 surface, allowing us to observe the effects of such modifications on gold nanoparticle growth. These manually introduced surface features provided an additional level of control over the gold deposition, enabling a deeper understanding of how localized electron transfer and surface morphology influence the growth behavior of gold particles.

5. Conclusions

This study explored the effects of varying ITO thickness beneath TiO_2 on the morphological characteristics and growth dynamics of gold particles via photocatalytic growth. Through systematic analysis using scanning electron microscopy (SEM), it was determined that Template Type 3/ TiO_2 -70_ITO-6, featuring a 6 nm ITO layer, provided the most favorable conditions for achieving uniform gold lines along the edges of the TiO_2 patterns.

The introduction of the ITO- TiO_2 heterojunction significantly enhanced the growth and coverage of gold particles, while specific morphological features such as the emergence of 3D flower-shaped structures were noted in the appropriate contexts. Conductance measurements further indicated that the gold lines exhibited a conductance of 23 mS, suggesting their potential applicability in bio-inspired electronics aimed at mimicking the electrical signaling of neurons.

One of the key characteristics of biological neural networks is the reorganization of axons and synapses during the learning process. Training of an artificial intelligence system is typically conducted by programming an existing network during the learning process. This is very different from nature, where networks reorganize in the learning process. In an infant's brain, dendrites grow and dendrite density increases from birth to the age of two years old, while connection density subsequently decreases to the age of four [30]. Our ultimate aim is to realize a physical platform that mimics this biological network connection growth and destruction. In this paper, we focus on the network growth under stimulus as the first important step in mimicking biology. Different gold wire thicknesses lead to changing conductivity. Thus, we propose that parts of the network with the highest UV stimulus will have the highest conductivity. The strength of the signal at each connection in an artificial neural network is determined by a weight, which adjusts during the learning process. In our neuromorphic approach, this weight is represented by the conductivity. It is not programmed, but "grown" during metal line formation. In future research, we will

also consider the destruction of unused connections to mimic network pruning in biology on a physical platform.

The findings of this research contribute valuable insights into the optimization of gold line growth technique for applications in neuromorphic engineering and bioelectronics, highlighting the importance of substrate configuration and material properties in facilitating effective electrical communication in synthetic neural networks. Further research may focus on refining these techniques including other factors that influence the gold growth such as illumination wavelength and power, substrate type, and modification of the solution with additives such as isopropanol or surfactants. Additionally, the long-term stability and functionality of the gold patterns in dynamic environments shall be investigated.

Author Contributions: Conceptualization, F.A. and M.G.; methodology, F.A. and M.G.; software, F.A., M.P. and M.G.; validation, F.A. and M.G.; formal analysis, F.A., S.V., A.V. and M.G.; investigation, F.A., S.V., A.V. and M.G.; resources, M.G.; data curation, F.A. and M.G.; writing—original draft preparation, F.A.; writing—review and editing, F.A., M.P., S.V., A.V. and M.G.; visualization, F.A.; supervision, M.G.; project administration, M.G.; funding acquisition, M.G. All authors have read and agreed to the published version of the manuscript.

Funding: This work was supported by the Deutsche Forschungsgemeinschaft (DFG, German Research Foundation)—Project-ID 434434223—SFB 1461.

Data Availability Statement: The original contributions presented in this study are included in the article. Further inquiries can be directed to the corresponding author(s).

Conflicts of Interest: The authors declare no conflict of interest.

References

1. Kendall, J.D.; Kumar, S. The building blocks of a brain-inspired computer. *Appl. Phys. Rev.* **2020**, *7*, 011305. [\[CrossRef\]](#)
2. Du, N.; Zhao, X.; Chen, Z.; Choubey, B.; Di Ventra, M.; Skorupa, I.; Bürger, D.; Schmidt, H. Synaptic Plasticity in Memristive Artificial Synapses and Their Robustness Against Noisy Inputs. *Front. Neurosci.* **2021**, *15*, 660894. [\[CrossRef\]](#) [\[PubMed\]](#)
3. Strukov, D.B.; Snider, G.S.; Stewart, D.R.; Williams, R.S. The missing memristor found. *Nature* **2008**, *453*, 80–83. [\[CrossRef\]](#) [\[PubMed\]](#)
4. Wright, C.D. Precise computing with imprecise devices. *Nat. Electron.* **2018**, *1*, 212–213. [\[CrossRef\]](#)
5. Sangwan, V.K.; Hersam, M.C. Neuromorphic nanoelectronic materials. *Nat. Nanotechnol.* **2020**, *15*, 517–528. [\[CrossRef\]](#) [\[PubMed\]](#)
6. Zhu, X.; Lee, S.H.; Lu, W.D.; Zhu, X.; Lee, S.H.; Lu, W.D. Nanoionic Resistive-Switching Devices. *Adv. Electron. Mater.* **2019**, *5*, 1900184. [\[CrossRef\]](#)
7. Tang, J.; Yuan, F.; Shen, X.; Wang, Z.; Rao, M.; He, Y.; Sun, Y.; Li, X.; Zhang, W.; Li, Y.; et al. Bridging Biological and Artificial Neural Networks with Emerging Neuromorphic Devices: Fundamentals, Progress, and Challenges. *Adv. Mat.* **2019**, *31*, 1902761. [\[CrossRef\]](#)
8. Vahl, A.; Milano, G.; Kuncic, Z.; Brown, S.A.; Milani, P. Brain-inspired computing with self-assembled networks of nano-objects. *J. Phys. D Appl. Phys.* **2024**, *57*, 3001. [\[CrossRef\]](#)
9. Veziroglu, S.; Paulsen, M.; Schardt, J.; Adejube, B.; Aktas, C.; Vahl, A.; Gerken, M. Photocatalytic Deposition for Metal Line Formation. In *Bio-Inspired Information Pathways: From Neuroscience to Neurotronics*; Springer International Publishing: New York, NY, USA, 2024; Volume 16, pp. 241–263.
10. Gkoupidenis, P.; Koutsouras, D.A.; Malliaras, G.G. Neuromorphic device architectures with global connectivity through electrolyte gating. *Nat. Commun.* **2017**, *8*, 15448. [\[CrossRef\]](#) [\[PubMed\]](#)
11. Irfan, F.; Tanveer, M.U.; Moiz, M.A.; Husain, S.W.; Ramzan, M. TiO₂ as an effective photocatalyst mechanisms, applications, and dopants: A review. *Eur. Phys. J. B.* **2022**, *95*, 184. [\[CrossRef\]](#)
12. Conings, B.; Baeten, L.; Jacobs, T.; Dera, R.; D’Haen, J.; Manca, J.; Boyen, H.G. An easy-to-fabricate low-temperature TiO₂ electron collection layer for high efficiency planar heterojunction perovskite solar cells. *APL Mater* **2014**, *2*, 081505. [\[CrossRef\]](#)
13. Abshari, F.; Veziroglu, S.; Adejube, B.; Vahl, A.; Gerken, M. Photocatalytic edge growth of conductive gold lines on microstructured TiO₂–ITO substrates. *Langmuir* **2024**, *40*, 19051–19059. [\[CrossRef\]](#) [\[PubMed\]](#)
14. Yu, Y.; He, T.; Guo, L.; Yang, Y.; Guo, L.; Tang, Y.; Cao, Y. Efficient visible-light photocatalytic degradation system assisted by conventional Pd catalysis. *Sci. Rep.* **2015**, *5*, 9561. [\[CrossRef\]](#)
15. Safajou, H.; Khojasteh, H.; Salavati-Niasari, M.; Mortazavi-Derazkola, S. Enhanced photocatalytic degradation of dyes over graphene/Pd/TiO₂ nanocomposites: TiO₂ nanowires versus TiO₂ nanoparticles. *J. Colloid Interface Sci.* **2017**, *498*, 423–432. [\[CrossRef\]](#) [\[PubMed\]](#)
16. Vahl, A.; Veziroglu, S.; Henkel, B.; Strunskus, T.; Polonskyi, O.; Aktas, O.C.; Faupel, F. Pathways to tailor photocatalytic performance of TiO₂ thin films deposited by reactive magnetron sputtering. *Materials* **2019**, *12*, 2840. [\[CrossRef\]](#)

17. Kusmieriek, E. A CeO₂ semiconductor as a photocatalytic and photoelectrocatalytic material for the remediation of pollutants in industrial wastewater: A review. *Catalysts* **2020**, *10*, 1435. [[CrossRef](#)]
18. Kedves, E.Z.; Pap, Z.; Hernadi, K.; Baia, L. Significance of the surface and bulk features of hierarchical TiO₂ in their photocatalytic properties. *Ceram. Int.* **2021**, *47*, 7088–7100. [[CrossRef](#)]
19. Binas, V.; Venieri, D.; Kotzias, D.; Kiriakidis, G. Modified TiO₂ based photocatalysts for improved air and health quality. *J. Mater.* **2017**, *3*, 3–16. [[CrossRef](#)]
20. Salomatina, E.V.; Fukina, D.G.; Koryagin, A.V.; Titaev, D.N.; Suleimanov, E.V.; Smirnova, L.A. Preparation and photocatalytic properties of titanium dioxide modified with gold or silver nanoparticles. *J. Environ. Chem. Eng.* **2021**, *9*, 106078. [[CrossRef](#)]
21. Veziroglu, S.; Obermann, A.L.; Ullrich, M.; Hussain, M.; Kamp, M.; Kienle, L.; Leißner, T.; Rubahn, H.G.; Polonskyi, O.; Strunskus, T.; et al. Photodeposition of Au nanoclusters for enhanced photocatalytic dye degradation over TiO₂ thin film. *ACS Appl. Mater. Interfaces* **2020**, *12*, 14983–14992. [[CrossRef](#)] [[PubMed](#)]
22. Guo, Y.; Siretanu, I.; Zhang, Y.; Mei, B.; Li, X.; Mugele, F.; Huang, H.; Mul, G. pH-dependence in facet-selective photo-deposition of metals and metal oxides on semiconductor particles. *J. Mater. Chem. A* **2018**, *6*, 7500–7508. [[CrossRef](#)]
23. Veziroglu, S.; Ghor, M.Z.; Kamp, M.; Kienle, L.; Rubahn, H.G.; Strunskus, T.; Fiutowski, J.; Adam, J.; Faupel, F.; Aktas, O.C. Photocatalytic growth of hierarchical Au needle clusters on highly active TiO₂ thin film. *Adv. Mater. Interfaces* **2018**, *5*, 1800465. [[CrossRef](#)]
24. Mendoza-Diaz, M.I.; Cure, J.; Djafari Rouhani, M.; Tan, K.; Patnaik, S.G.; Pech, D.; Quevedo-Lopez, M.; Hungria, T.; Rossi, C.; Estève, A. On the UV-visible light synergetic mechanisms in Au/TiO₂ hybrid model nanostructures achieving photoreduction of water. *J. Phys. Chem. C* **2020**, *124*, 25421–25430. [[CrossRef](#)]
25. Shi, Q.; Zhang, X.; Li, Z.; Raza, A.; Li, G. Plasmonic Au nanoparticle of a Au/TiO₂–C₃N₄ heterojunction boosts up photooxidation of benzyl alcohol using LED light. *ACS Appl. Mater. Interfaces* **2023**, *15*, 30161–30169. [[CrossRef](#)] [[PubMed](#)]
26. Dai, W.; Wang, X.; Liu, P.; Xu, Y.; Li, G.; Fu, X. Effects of electron transfer between TiO₂ films and conducting substrates on the photocatalytic oxidation of organic pollutants. *J. Phys. Chem. B* **2006**, *110*, 13470–13476. [[CrossRef](#)] [[PubMed](#)]
27. Zhong, Y.; Peng, C.; He, Z.; Chen, D.; Jia, H.; Zhang, J.; Ding, H.; Wu, X. Interface engineering of heterojunction photocatalysts based on 1D nanomaterials. *Catal. Sci. Technol.* **2021**, *11*, 27–42. [[CrossRef](#)]
28. Tangeysh, B.; Moore Tibbetts, K.; Odhner, J.H.; Wayland, B.B.; Levis, R.J. Triangular gold nanoplate growth by oriented attachment of Au seeds generated by strong field laser reduction. *Nano Lett.* **2015**, *15*, 3377–3382. [[CrossRef](#)] [[PubMed](#)]
29. Zhang, X.; Wang, J.; Dong, X.X.; Lv, Y.K. Functionalized metal-organic frameworks for photocatalytic degradation of organic pollutants in environment. *Chemosphere* **2020**, *242*, 125144. [[CrossRef](#)] [[PubMed](#)]
30. Seung, S. *Connectome: How the Brain's Wiring Makes Us Who We Are*; Houghton Mifflin Harcourt: New York, NY, USA, 2012; p. 108.

Disclaimer/Publisher's Note: The statements, opinions and data contained in all publications are solely those of the individual author(s) and contributor(s) and not of MDPI and/or the editor(s). MDPI and/or the editor(s) disclaim responsibility for any injury to people or property resulting from any ideas, methods, instructions or products referred to in the content.

3.3. Mimicking Axon Growth and Pruning by Photocatalytic Growth and Chemical Dissolution of Gold on Titanium Dioxide Patterns

3.3.1. Introduction

F. Abshari, M. Paulsen, S. Veziroglu, A. Vahl, and M. Gerken, “Mimicking Axon Growth and Pruning by Photocatalytic Growth and Chemical Dissolution of Gold on Titanium Dioxide Patterns,” *Molecules*, vol. 30, no. 1, p. 99, Dec. 2024, doi: 10.3390/molecules30010099.

Copyright © 2024 by the authors. Published by MDPI, Basel, Switzerland. This article is an open access article distributed under the terms and conditions of the Creative Commons Attribution (CC BY) license (<https://creativecommons.org/licenses/by/4.0/>).

Statement about the own contribution:

For this publication, I collected the data, wrote the manuscript, conducted the data analysis, prepared the samples, and performed the SEM and conductance measurements. Additionally, I contributed to developing the research idea.

Conceptualization	Planning	Implementation	Manuscript Preparation
Medium	High	High	High

3.3.2. Abstract

This paper aimed to advance neuromorphic engineering by demonstrating the sequential processes of axon-like growth and pruning using material-based techniques. Specifically, it sought to emulate the biological mechanisms of axonal growth and pruning through the photocatalytic deposition and chemical dissolution of gold structures on titanium dioxide (TiO₂) patterns. By integrating these processes, the study established a framework for dynamic, reconfigurable networks that closely mimic the adaptability and plasticity of

biological neural systems, a key step toward developing advanced neuromorphic architectures.

The overarching goal of the project is to explore adaptive and reconfigurable neuromorphic systems through innovative material-based methodologies. This paper aligns with this objective by presenting an approach that integrates growth and pruning, fundamental processes underpinning plasticity in biological neural networks. The study demonstrates how these processes can be effectively emulated using photocatalytic and chemical techniques, establishing a connection between biological principles and material science advancements.




This paper directly contributes to the thesis by presenting a well-defined experimental framework for the sequential growth and pruning of gold structures. It emphasizes how controlled material processes can replicate the adaptability of neural networks, offering valuable insights for the design of advanced neuromorphic devices. This work builds upon the findings of the previous studies by incorporating the dynamic interaction between growth and pruning, a crucial step in mimicking the functional plasticity of biological neural systems.

To achieve the objectives, this study utilized patterned TiO_2 templates combined with an underlying indium tin oxide (ITO) layer to enhance photocatalytic activity. UV illumination initiated gold deposition along the TiO_2 patterns, effectively mimicking axonal growth. The pruning process was simulated through the selective dissolution of gold structures using a potassium iodide (KI) solution. Real-time monitoring of the processes was conducted with optical microscopy, while scanning electron microscopy (SEM) provided detailed morphological analyses. This integrated approach ensured precise control and thorough examination of both growth and dissolution, establishing a foundation for practical applications in neuromorphic systems.

3.3.3. Published Paper

Article

Mimicking Axon Growth and Pruning by Photocatalytic Growth and Chemical Dissolution of Gold on Titanium Dioxide Patterns

Fatemeh Abshari ^{1,*} , Moritz Paulsen ¹, Salih Veziroglu ^{2,3} , Alexander Vahl ^{2,3,4} and Martina Gerken ^{1,3,*} 

¹ Chair for Integrated Systems and Photonics, Department of Electrical and Information Engineering, Faculty of Engineering, Kiel University, Kaiserstr. 2, 24143 Kiel, Germany

² Chair for Multicomponent Materials, Department of Materials Science, Faculty of Engineering, Kiel University, Kaiserstr. 2, 24143 Kiel, Germany

³ Kiel Nano, Surface and Interface Science (KiNSIS), Kiel University, Christian-Albrechts-Platz 4, 24118 Kiel, Germany

⁴ Leibniz Institute for Plasma Science and Technology, Felix-Hausdorff-Str. 2, 17489 Greifswald, Germany

* Correspondence: fa@tf.uni-kiel.de (F.A.); mge@tf.uni-kiel.de (M.G.); Tel.: +49-4318806255 (F.A.); +49-431886250 (M.G.)

Abstract: Biological neural circuits are based on the interplay of excitatory and inhibitory events to achieve functionality. Axons form long-range information highways in neural circuits. Axon pruning, i.e., the removal of exuberant axonal connections, is essential in network remodeling. We propose the photocatalytic growth and chemical dissolution of gold lines as a building block for neuromorphic computing mimicking axon growth and pruning. We predefine photocatalytic growth areas on a surface by structuring titanium dioxide (TiO₂) patterns. Placing the samples in a gold chloride (HAuCl₄) precursor solution, we achieve the controlled growth of gold microstructures along the edges of the indium tin oxide (ITO)/TiO₂ patterns under ultraviolet (UV) illumination. A potassium iodide (KI) solution is employed to dissolve the gold microstructures. We introduce a real-time monitoring setup based on an optical transmission microscope. We successfully observe both the growth and dissolution processes. Additionally, scanning electron microscopy (SEM) analysis confirms the morphological changes before and after dissolution, with dissolution rates closely aligned to the growth rates. These findings demonstrate the potential of this approach to emulate dynamic biological processes, paving the way for future applications in adaptive neuromorphic systems.

Keywords: photocatalytic deposition; chemical dissolution; gold; titanium dioxide; potassium iodide solution; indium tin oxide; neuromorphic engineering; transmission optical microscopy



Academic Editor: Sugang Meng

Received: 30 November 2024

Revised: 20 December 2024

Accepted: 23 December 2024

Published: 30 December 2024

Citation: Abshari, F.; Paulsen, M.; Veziroglu, S.; Vahl, A.; Gerken, M. Mimicking Axon Growth and Pruning by Photocatalytic Growth and Chemical Dissolution of Gold on Titanium Dioxide Patterns. *Molecules* **2025**, *30*, 99. <https://doi.org/10.3390/molecules30010099>

Copyright: © 2024 by the authors. Licensee MDPI, Basel, Switzerland. This article is an open access article distributed under the terms and conditions of the Creative Commons Attribution (CC BY) license (<https://creativecommons.org/licenses/by/4.0/>).

1. Introduction

Neuromorphic engineering focuses on developing advanced computational systems by drawing inspiration from the structure and processes of biological neural networks, with the goal of achieving improved efficiency [1]. In neural networks, neuronal connections are dynamically and continuously reorganized. These connections evolve over different time scales: rapid synaptic plasticity results in localized adjustments at synapses between neurons, while slower processes, such as axon growth and pruning, occur throughout the broader network. Building on the dynamic reorganization of neuronal connections, axon growth represents a critical phase of neural network development, where intrinsic genetic programs and extracellular signals work in concert to extend axons toward their target regions, forming the foundational pathways for neural circuitry [2,3]. Many studies

have focused on replicating rapid synaptic plasticity using memristive devices, given their unique ability to enable in-memory computing [4,5]. Ongoing research continues to investigate neuronal connections at a global scale within biological neural networks, while simultaneously developing innovative methods to integrate these mechanisms into next-generation bio-inspired systems [6].

Recent advances in neuromorphic engineering have increasingly focused on nanowire networks that exhibit memristive properties, which are being explored for their ability to emulate the dynamic and adaptable behavior of synapses in biological neural networks. These networks are gaining attention for their potential to enhance computational efficiency by replicating both short-term synaptic plasticity and long-term memory storage, paving the way for the integration of such systems into bio-inspired computing architecture [7–9]. These networks are naturally self-organizing, with nanowires forming conductive, one-dimensional (1D) pathways. The intricate topology of these networks results in collective switching behaviors, making them highly compatible with memristive architecture. In biological neural networks, the ability to dynamically regulate stimuli and control the formation and dissolution of connections is a key feature for adaptive functionality [10–12].

Axonal pruning is a critical process in the development and remodeling of neural networks, wherein excess or improperly connected axons are selectively eliminated to refine the neural circuitry, ensuring the optimal function of the nervous system [13]. This process occurs primarily during developmental stages, but also plays a role in adult neuroplasticity, where axonal pruning helps to fine-tune neural pathways based on learning, experience, and environmental stimuli [13]. Mechanistically, axonal pruning is regulated by molecular signals that induce synaptic weakening and the targeted retraction of axons, a process that parallels cellular processes, like apoptosis, ultimately contributing to the structural and functional optimization of neural circuits [14]. In the early stages, attempts to replicate the global interactions within neuronal assemblies were made by exploring global connectivity through electrolyte gating in liquid media [15].

We focus on the gradual formation of one-dimensional, long-range connections, which have the potential to enable adaptive modifications in network topology. This aspect of the research aims to mimic axonal growth through the photocatalytic deposition of conductive gold lines onto ultraviolet (UV) light-activated titanium dioxide (TiO₂) substrates. Additionally, we explore the pruning of these axonal-like structures by the chemical dissolution of the grown gold lines using a potassium iodide (KI) solution, simulating the axonal pruning process. Chemical dissolution was chosen as it allows for a gradual loss of conductivity in continuous gold lines due to the reduction in the gold line diameter. Once the gold coverage falls below the percolation threshold, conductivity is lost completely. With gold growth, the percolation threshold may be reached again, regaining conductivity. Therefore, this approach promises a reversible, stimulus-dependent growth and pruning of network connections during the learning process mimicking the situation in biological neural networks. Here, it is recognized that the density of the human dendrite network increases from birth to the age of 2 years old [16]. Subsequently, the density decreases again, which is associated with network consolidation during learning.

TiO₂ is widely utilized as a semiconductor photocatalyst due to its high photocatalytic efficiency, ease of fabrication, cost-effectiveness, non-toxic nature, and robust chemical stability [17–19]. Considering the critical role of TiO₂ as a semiconductor photocatalyst with excellent optical properties, recent studies have demonstrated its ability to facilitate photocatalytic processes under UV light, particularly for structural modifications and degradation mechanisms [20]. It was recently shown that the co-precipitation of TiO₂ with terbium and manganese effectively improves its photocatalytic performance by lowering the band gap energy and enhancing electron-hole separation, which facilitates the efficient

degradation of tetracycline antibiotics under both UV- and visible-light conditions [21]. The deposition of gold onto TiO₂ thin films has been successfully achieved through the photoreduction of gold chloride (HAuCl₄) under UV illumination [22–24]. It has been reported that the addition of isopropanol to the HAuCl₄ solution can significantly accelerate the photoreduction process by acting as a hole scavenger, thereby enhancing the speed of gold nanoparticle growth under UV light [25]. In addition to the use of isopropanol, other parameters have been shown to significantly influence the morphology and coverage of the deposited gold structures. These include factors such as the crystal structure and surface morphology of the underlying TiO₂ thin film, the composition and pH of the precursor solution, as well as the intensity and duration of UV illumination [26,27].

Through UV illumination, TiO₂ facilitates the generation of electron-hole pairs, with electrons migrating to the conduction band. These electrons reduce Au³⁺ ions from the HAuCl₄ solution, leading to the formation of neutral gold atoms. The gold atoms form solid nuclei on the TiO₂ surface, which then grow through the consecutive addition of gold atoms into gold nano- and microparticles. Simultaneously, the holes oxidize nearby molecules, completing the photocatalytic reaction [28]. The efficiency of photocatalytic processes, such as gold growth on TiO₂ surfaces, is strongly influenced by light intensity, as higher UV intensities enhance the generation of electron-hole pairs, accelerating reaction rates and structural formation [29]. These findings provide valuable insights into how UV illumination affects both the growth and morphological evolution of gold particles [30].

In this study, photocatalysis is utilized to grow gold lines on TiO₂ thin films patterned using lithography. A thin indium tin oxide (ITO) sublayer is incorporated beneath the TiO₂. Given that ITO has a higher work function compared to TiO₂, a Schottky barrier forms at the TiO₂-ITO interface, which affects the overall photocatalytic performance [31,32]. In a recent study, we demonstrated that a 6 nm ITO layer beneath TiO₂ effectively promotes localized gold growth along the edges of the TiO₂ patterns resulting in electrically conductive gold lines [33]. This study builds on these previous findings by using a consistent template with a 6 nm ITO layer beneath the TiO₂ for all experiments. Here, we investigate the sequential processes of photocatalytic gold growth followed by chemical dissolution mimicking axon growth and pruning. The schematic in Figure 1 demonstrates the abstraction process for mimicking neuronal network dynamics through a material-based approach. Figure 1a on the left presents a simplified schematic representation of a neural network, illustrating the interconnectivity between neurons in a network. This is not a true 3D neuronal network, but rather a simplified projection to communicate the idea of neuronal connectivity. Moving to the right, the neural network is translated into a 2D schematic geometry on a surface. This 2D representation simplifies the complex volumetric arrangement while retaining the essential connectivity, making it accessible for technical implementation.

Figure 1b introduces the technical methodology used to mimic axon-like connections in a proposed material system. First, a patterned template is designed to define specific regions for selective gold growth. This template mimics synapse-like nodes connected by axon-like linear pathways. Under UV illumination, the photocatalytic growth of gold structures is induced along these defined pathways, simulating the formation of axon-like connections. The resulting gold pathways provide a physical basis for mimicking neuronal connectivity in a controllable manner. Finally, the grown gold structures undergo a targeted chemical dissolution process, emulating the natural phenomenon of axonal pruning. This selective removal of gold pathways enables dynamic modifications of the network, reflecting the adaptive and self-organizing properties of biological neural circuits. This approach represents a proposed material system to mimic the formation and dissolution of axon-like connections in a simplified, reproducible framework. By combining photocatalytic growth and chemical dissolution processes, this study introduces

a methodology for investigating adaptive, neuromorphic systems, laying the groundwork for further exploration in network remodeling.

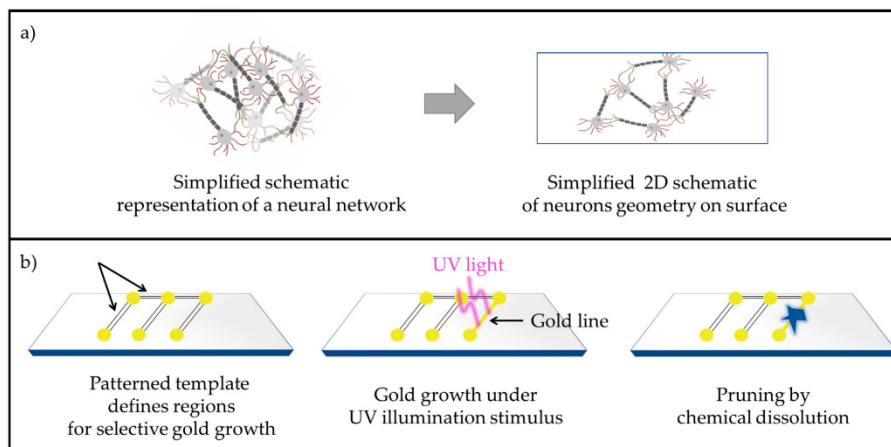


Figure 1. (a) Simplified schematic representation of a neural network (left) and its abstraction into 2D schematic geometry on a surface (right), retaining the essential connectivity of the network. (b) Process for mimicking axon-like connections: (left) a patterned template defines regions for selective gold growth, (center) UV illumination induces photocatalytic gold growth along predefined pathways, forming axon-like structures, and (right) chemical dissolution selectively prunes the gold connections, mimicking axonal pruning.

To further clarify this, the abstraction process depicted in Figure 1 bridges the gap between biological complexity and material implementation. The transition from a neural network to a patterned material system involves translating the functional principles of connectivity and adaptability into a simplified, physical framework. This includes using the patterned template to mimic axonal pathways, where gold deposition represents axonal growth and its selective removal represents pruning. By replicating these key features, the proposed system provides a versatile platform to study the dynamic remodeling of networks, offering insights into neuromorphic engineering and adaptive material systems.

The chemical dissolution of gold using the KI solution has proven to be an effective method for removing gold from various substrates. KI acts as a complexing agent, forming soluble gold–iodine complexes, which enable the controlled removal of gold lines grown during photocatalytic processes [34]. This dissolution process mimics the axonal pruning in neural networks, allowing for repeated cycles of growth and removal, essential for dynamic neuromorphic systems. In this paper, we aim to investigate the UV-stimulated photocatalytic growth of gold on titanium dioxide patterns, followed by chemical dissolution using KI solutions. By analyzing both real-time optical monitoring data and post-experiment scanning electron microscopy (SEM) imaging, we provide insights into the mechanisms governing these processes and their potential for precise microstructure manipulation.

2. Results

2.1. Analysis of Gold Growth Dynamics on the Edge and Surface of TiO₂

In this section, the photocatalytic growth of gold lines on TiO₂ edges is analyzed in real-time using optical transmission microscope data. As described in Section 4, a beaker was filled with 20 mL of a gold chloride precursor solution, mixed with isopropanol in a 10:1 ratio to enhance the deposition rate. The substrate was submerged in this solution and exposed to UV illumination ($\lambda = 365$ nm) for 30 min. The growth process was monitored through a transmission microscope by capturing images every 4 s over a total duration

of 30 min. A certain region around the TiO₂ edge was selected where the gold structures predominantly grew. The selected region included the TiO₂ surface on the left side and the glass substrate on the right side of the TiO₂ edge located in the center. Figure 2a presents optical microscope images of the selected region taken at different times during the growth process: $t = 0$, $t = 10$, $t = 20$, and $t = 30$ min. A supplementary video (Video S1) is provided to offer a clearer visualization of the growth dynamics.

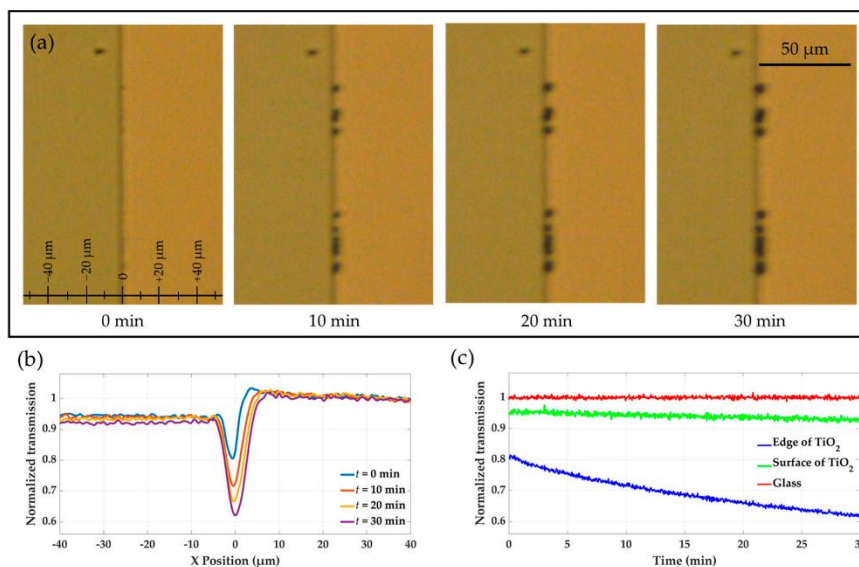


Figure 2. Real-time monitoring of gold growth (a) Sequential optical microscope images of a selected region around the TiO₂ edge, including the TiO₂ surface on the left side and the glass substrate on the right side, taken at various time points, $t = 0$, $t = 10$, $t = 20$, and $t = 30$ min, illustrating the gradual growth of gold structures over 30 min. (b) Transmission profiles across the TiO₂ edge at $t = 0$, $t = 10$, $t = 20$, and $t = 30$ min, normalized to the reference transmission on the glass substrate. (c) Time-dependent transmission curves showing dissolution progress at the TiO₂ edge and surface compared to the glass substrate.

For every pixel of the selected region, we measured a distinct transmitted light intensity. At each x -coordinate, we averaged the measured intensity values over all pixels with different y -coordinates to generate transmission profiles across the x -span of the selected region. These transmission curves, showing the variation in intensity as a function of x -span, are plotted in Figure 2b for four different time points: $t = 0$, $t = 10$, $t = 20$, and $t = 30$ min. All transmission values are normalized relative to the reference transmission on the bare glass substrate, located far from the TiO₂ edge at $x = 40\ \mu\text{m}$.

At the beginning of the growth process ($t = 0$), the transmission at the TiO₂ edge ($x = 0$) was lower than those of the TiO₂ surface ($x < 0$) and the glass substrate ($x > 0$). This difference is attributed to light scattering at the TiO₂ edge, which creates a narrow dark line in the middle of the selected area, as displayed in the optical microscopy images (Figure 2a). Furthermore, the transmission on the TiO₂ surface ($x < 0$) was slightly lower than that of the glass substrate ($x > 0$). During the growth process, a decrease in the transmitted light intensity is observed for $x = 0$ and $x < 0$, corresponding to the growth of gold particles along the edge and on the surface of TiO₂ over time. At the end of the growth experiment ($t = 30$ min), the normalized transmission at the edge ($x = 0$) was significantly reduced compared to the beginning time ($t = 0$), with a total change of $\Delta T_{\text{Edge}} \approx 0.19$ over 30 min. On the surface of the TiO₂ ($x < 0$), the transmission was slightly reduced, with $\Delta T_{\text{Surface}} \approx 0.03$ after 30 min of growth. While a significant growth rate is achieved along

the edge of TiO_2 , little changes in transmission are observed on the left and right sides of the edge, confirming the selective formation of gold lines along the edge.

The dissolution process of gold structures on the TiO_2 edge and surface was analyzed by monitoring transmission changes over time. The glass substrate served as a reference, as it remained unaffected throughout the experiment. The transmission at the TiO_2 edge and surface increased during dissolution, indicating the gradual removal of gold structures. Figure 2 part (c) of the figure presents the time-dependent transmission curves for these regions, highlighting the sharper rise in transmission at the TiO_2 edge compared to the surface, reflecting the higher density of gold structures at the edge.

2.2. Analysis of Gold Dissolution Dynamics on the Edge and Surface and TiO_2

Following the growth process, a KI solution diluted in DI water at a ratio of 1:300 was utilized to initiate chemical dissolution of the gold structures. The dissolution process was monitored using the same method as described for the growth process. Figure 3a displays the optical microscope images of a certain area around the TiO_2 edge taken at different times during the dissolution process: $t = 0$, $t = 5$, $t = 10$, and $t = 30$ min. For a better visualization of the dissolution dynamics, a supplementary video (Video S2) is provided. Similar to the growth analysis, the TiO_2 edge is located in the center, with the TiO_2 surface and the glass substrate on the left and right sides, respectively. Figure 3b presents the transmission curves across the x -span of the selected region at four different time points: $t = 0$, $t = 10$, $t = 20$, and $t = 30$ min. All transmission values were normalized relative to the reference transmission on the bare glass substrate, located far from the TiO_2 edge at $x = 40 \mu\text{m}$.

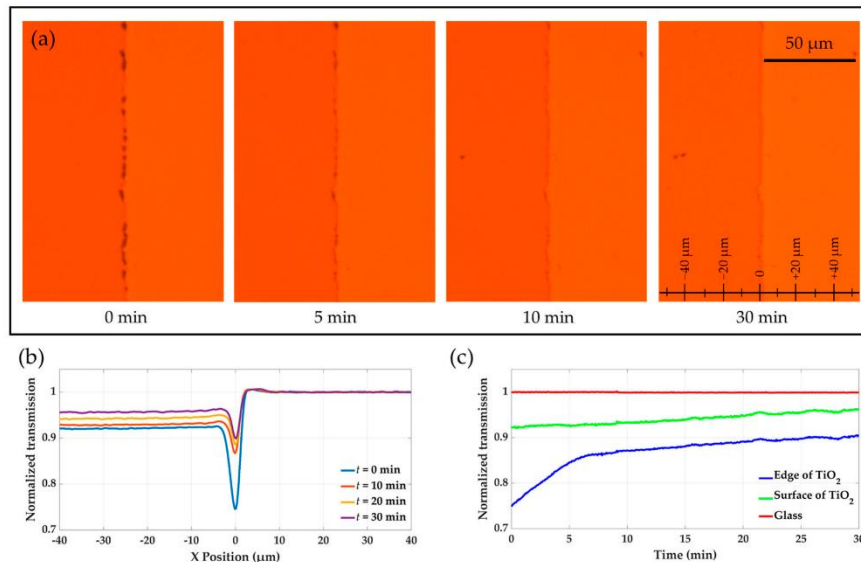


Figure 3. Real-time monitoring of gold dissolution (a) Sequential optical microscope images of a selected region around the TiO_2 edge, including the TiO_2 surface on the left side and the glass substrate on the right side, taken at various time points, $t = 0$, $t = 5$, $t = 10$, and $t = 30$ min, illustrating the gradual dissolution of gold structures over 30 min. (b) Transmission profiles across the TiO_2 edge at $t = 0$, $t = 10$, $t = 20$, and $t = 30$ min, normalized to the reference transmission on the glass substrate. (c) Time-dependent transmission curves showing dissolution progress at the TiO_2 edge and surface compared to the glass substrate.

At the start of the dissolution experiment ($t = 0$), the transmission at the TiO_2 edge ($x = 0$) was nearly 0.25 lower than that of the adjacent glass substrate ($x > 0$). This difference

indicates that gold was substantially deposited along the edge of the TiO₂. On the surface of the TiO₂ ($x < 0$), the normalized transmission value was approximately 0.08 lower compared to the glass substrate, suggesting partial gold growth on the TiO₂ surface. As dissolution proceeded, the gold structures dissolved at varying rates on the edge and surface of TiO₂. While the transmission over the glass substrate remained constant throughout the experiment, a significant increase in transmission was observed on the TiO₂ edge and surface as the gold structures dissolved.

The dissolution process was tracked on Figure 3c by monitoring transmission changes over time, with the glass substrate as a constant reference. Figure 3c shows time-dependent transmission curves, with a sharper increase at the TiO₂ edge, indicating higher initial gold density, similar to the previous analysis.

2.3. Morphological Examination Using Scanning Electron Microscopy

In this section, the morphology of gold particles on a single sample was examined at different stages using SEM. The SEM imaging was performed using a Carl Zeiss Supra 55VP instrument (ZEISS AG, Oberkochen, Germany), operated at an acceleration voltage of 3 kV and a working distance of 3 mm. This technique provides high-resolution images that allow for a detailed visualization of the particles, revealing their size, shape, and distribution along the TiO₂ patterns. By applying SEM, the structural characteristics of the gold particles could be analyzed, both after growth and after dissolution.

SEM analysis was first conducted to observe the morphology of the gold particles formed along the edges of the titanium dioxide patterns after 30 min of UV illumination. The photocatalytic growth experiment used a precursor solution of gold chloride mixed with isopropanol in a 10:1 ratio to enhance growth. After the growth phase, SEM was also performed following the chemical dissolution of the gold particles, where the KI solution was diluted with 300 mL of deionized water to assess the effects of dissolution.

2.3.1. SEM Analysis of Grown Gold Particles on TiO₂ Edges

The SEM images in Figure 4 provide detailed insights into the selective growth of gold microstructures on the edge of TiO₂ patterns. Notably, no visible particle growth is observed on the glass substrate, confirming that the photocatalytic deposition occurred exclusively on the TiO₂. This result is significant, as the addition of isopropanol to the precursor solution, combined with the controlled intensity of the UV LEDs, prevented any unwanted nucleation or deposition on the glass, ensuring that growth was confined to the TiO₂ regions, which is consistent with the in-situ microscopy measurements where the transmission intensity on the glass substrate remained unchanged during the growth process.

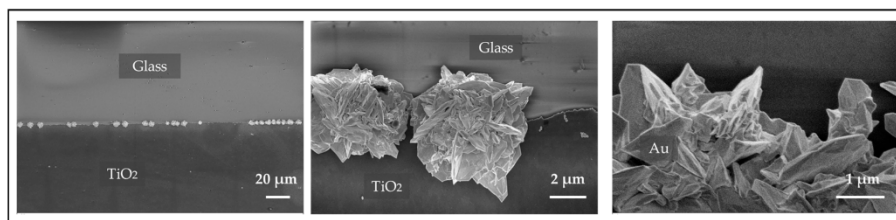


Figure 4. SEM images of the template post-growth, illustrating the formation of gold particles along the edges of the TiO₂ patterns.

The gold microstructures display a distinct 3D flower-like morphology, primarily concentrated along the edges of the TiO₂ patterns. These structures are composed of sharp, crossed plates, forming intricate flower-shaped formations. While the growth is focused along the edges, the microstructures do not form a continuous line; instead, they appear as

separate clusters. This is due to the limited illumination time of 30 min in this experiment, as the focus was on studying the spontaneous growth and dissolution processes rather than forming a continuous line. With extended illumination times, a uniform and continuous gold line along the edges can be achieved [33]. In certain areas, however, the flower-shaped particles grow close together, nearly forming a connected structure along the edge. This unique morphology and spatial distribution suggest that the edges of the ITO-TiO₂ patterns serve as preferential nucleation sites, promoting the formation of well-defined, three-dimensional gold structures.

2.3.2. SEM Analysis After the Chemical Dissolution of Gold Structures

The SEM images in Figure 5, illustrate the morphological changes in the gold structures after the chemical dissolution process for 30 min. In some regions on the TiO₂ surface, clusters of flower-shaped gold particles were observed to have grown, though these areas were limited both in number and in size. Figure 5a shows one of these small regions on the surface where the characteristic flower-shaped gold particles had formed prior to the dissolution experiment.

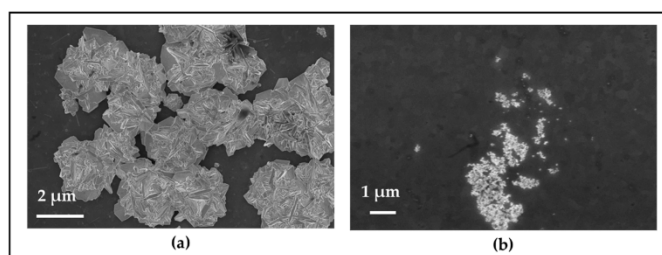


Figure 5. SEM images of gold particles on TiO₂: (a) Before dissolution, with flower-shaped particles on the surface; (b) After dissolution, showing reduced and irregularly shaped particles, though not fully removed.

Following chemical dissolution using the KI solution, SEM imaging of the same area in Figure 5b reveals noticeable changes. The previously well-formed, flower-like gold particles appear etched and reduced in size, suggesting the dissolution process was partially successful. The gold structures seem to have been broken down into smaller fragments, though complete dissolution was not achieved, as some remnants of gold particles are still visible. The decrease in particle size and the etched morphology indicate that the KI solution effectively initiated the dissolution, but did not fully dissolve the gold structures.

This partial etching highlights the ability of the KI solution to interact with and reduce the size of gold particles, although further refinement of the dissolution conditions may be required to achieve full removal. Additionally, the size of the gold particles noticeably decreased, and their morphology transformed from the original flower-like shapes into more irregular, amorphous spots, indicating significant structural alteration during the dissolution process.

3. Discussion

Reconfigurable long-range connections with stimulus-induced formation and stimulus-free, spontaneous dissolution over time are in high demand to implement axon-like dynamic connection schemes. Possible technical implementations range from guided wiring upon metal filament formation in liquid media upon an electrochemical redox reaction [11] toward the electrophoretic reorganization of metallic nanoparticles into anisotropic long-range nanoparticle agglomerates along electrical field gradients in nanofluids [35]. In contrast to these earlier studies, which reported on material systems for the electrically

stimulated growth of long-range connections, in this study, UV illumination is applied as a stimulus. To mimic a biological neural network, growth and dissolution rates should be compatible with each other. Photocatalytic gold growth allows for UV-stimulus activated connection formation. The rate may be tailored by adjusting the chemical composition of the precursor solution or by changing the UV wavelength or intensity. We enhanced the growth rate in this experiment by using isopropanol as a hole scavenger in the precursor solution. Additionally, the implementation of two UV LEDs, positioned at an angle for even illumination, further accelerated the growth process. We decreased the gold dissolution rate by diluting the KI solution. This had the additional benefit that a higher transparency is achieved, allowing for the real-time monitoring of the dissolution with the optical transmission microscope. Based on the results of a dilution series, the 1:300 dilution was chosen. The dissolution process in this setup was slightly slower than the gold growth. This is desired as the gold lines should grow under UV stimulus and dissolve without stimulus.

The incomplete dissolution of gold structures observed in this study is attributed to the slower dissolution rate relative to the growth rate under the chosen experimental conditions. While this resulted in residual gold particles, the dissolution process can be fully completed by increasing the concentration of KI in the DI water mixture. This adjustment would accelerate the dissolution, ensuring the complete removal of gold when required. However, in the context of mimicking axon-like behaviors in neuromorphic systems, achieving a fully resolved state may not be desired. Instead, the most interesting operation point is at the percolation threshold of the gold lines. By analyzing changes in conductance during the growth and dissolution processes, the system can effectively replicate the dynamic behavior of neural connections. This conductance-based approach provides insights into dynamic behaviors without necessitating complete dissolution, highlighting the versatility of the proposed system for neuromorphic and adaptive material applications.

The SEM observations confirmed gold growth and incomplete dissolution for 30 min of each process. Small amounts of gold residue remaining after the dissolution experiment confirm the lower dissolution rate compared to the growth rate. The time scales on the minutes to hours range align well with the remodeling times of biological systems. Further tuning of the rates is possible. Regarding long-range metal connection formation and dissolution, it has to be considered that a longer gold growth is necessary to achieve a conductive gold line without gaps. On the other hand, as soon as gaps appear, the electrical conductivity is lost. In future experiments, instead of pre-grown metal lines, a photo-forming step could be utilized to initiate long-range gold connections, similar to the electroforming process in filamentary memristive devices. Once a proto-filament is formed through the photo-forming step, subsequent cycles of UV illumination and dissolution can lead to dynamic reconfigurable states, mimicking axon-like connections. This approach aligns with the foundational role of forming steps in early memristive devices, as discussed in the reviews [36].

The diameter of the gold lines in our work is comparable to the diameter of biological axons in the micrometer range [37]. In biology, the plasticity of white matter is of high importance for learning and memory [38]. The conduction time of axons is not simply regulated by the axon diameter, but myelin formation and remodeling play a key role [39]. The inhomogeneous conductivity of biological axons may be compared to the inhomogeneous nature of our grown gold lines. The dissolution mimics the reversible and localized nature of axon pruning, focusing on the functional principles of dynamic connectivity rather than the molecular complexity of biological systems. Different to biology, our two-dimensional implementation has a much lower line density and total length. In a human brain, the combined length of myelinated axons reaches approximately 160,000 km [38]. Biological network reconfiguration times are on the time scale of hours to days and longer [38]. In

our study, we considered growth or pruning sequences of half-hour durations for partial growth and partial dissolution. This is comparable to biological time frames. In summary, our proposed two-dimensional approach offers a similar line diameter as well as similar reconfiguration time scales, but a much shorter overall length. While acknowledging the significant differences, stimulus-adaptive gold “axon” formation and pruning are much closer to the biological situation than the fixed conductivity of electrical connections in standard electronics.

As in biology, this neuromorphic building block only functions in a liquid environment. This is highly unusual for electronic systems and definitely poses challenges regarding system stability, leakage, etc. Nevertheless, it is an intriguing thought to mimic axonal long-range connection growth and pruning, and the system opens the possibility to study the interaction of local UV stimuli and a homeostatic environment. Different than in biology, the liquid has to be exchanged between growth and dissolution. This poses an additional challenge for further development toward applications. We envision a microfluidic realization, where the liquid is exchanged in short intervals in a flow cell. Thus, this system is in principle suitable as a building block for neuromorphic engineering, allowing for sequential growth and dissolution cycles.

The findings of this study demonstrate a controlled approach to the photocatalytic growth and chemical dissolution of gold structures on a substrate, opening potential applications in neuromorphic systems. This study represents an effort to mimic axonal dynamics on a larger scale, providing a foundation for future work aimed at achieving finer and more biologically comparable structures [7]. The ability to dynamically grow and dissolve axon-like connections reflects fundamental biological processes, such as axonal growth and pruning, which are essential for synaptic plasticity and learning [10]. This capability could eventually lead to adaptive hardware systems that reconfigure in response to stimuli, offering a pathway toward more flexible and biologically inspired artificial neural networks.

Beyond neuromorphic systems, this method holds promise for bioelectronics, particularly for the development of reconfigurable sensor arrays. Dynamically adjustable conductive pathways could enable sensors to adapt in real time to changing environmental or physiological conditions [11]. Additionally, this approach offers a platform for studying synaptic behaviors in artificial systems, enabling controlled investigations of neural processes at a larger, more accessible scale.

While there are limitations in terms of achieving the high density of three-dimensional biological systems, the versatility of the proposed system lays a foundation for adaptive and responsive material systems. By bridging biological functionality and synthetic implementation, this work represents an important step toward biologically inspired material systems that operate on scales compatible with current fabrication technologies.

4. Materials and Methods

4.1. Substrate Preparation

In this study, a single type of substrate template was used for all experiments to investigate the photocatalytic growth and dissolution processes. Soda-lime glass substrates were precisely diced into 10 mm × 10 mm squares using a Wafer Dicing System (model DAD3350, Aurotech, Santa Rosa, Philippines) to ensure uniformity and provide a consistent surface area for material deposition. The substrates were then cleaned thoroughly to remove contaminants that could interfere with the photocatalytic reactions. The cleaning process involved sequential sonication in acetone and isopropanol (both of 99% purity, Sigma-Aldrich, St. Louis, MO, USA) in an ultrasonic bath (Martin Walter Ultraschalltechnik AG,

Straubenhardt, Germany), followed by complete drying with high-purity nitrogen gas to ensure the removal of all solvent residues.

A 6 nm layer of ITO was deposited onto the cleaned glass substrates using physical vapor deposition (PVD) with an $\text{In}_2\text{O}_3/\text{SnO}_2$ (90/10 wt%) target (99.99% purity, Kurt J. Lesker Company GmbH, Dresden, Germany). The ITO layer, selected for its higher work function relative to TiO_2 , was critical for achieving photocatalytic growth along the TiO_2 edges [33]. The deposition of this thin, uniform, ITO layer formed a heterojunction TiO_2 -ITO interface, facilitating electron transfer and optimizing the conditions for gold growth during subsequent experiments.

Following ITO deposition, a 70 nm-thick layer of TiO_2 was sputtered onto the ITO-coated substrates. This was achieved using a 3-inch TiO_2 target (99.99% purity, Kurt J. Lesker Company GmbH) to ensure high-quality, uniform TiO_2 coverage across the entire substrate. The TiO_2 was deposited in its amorphous form, requiring further processing to transform it into its active photocatalytic anatase phase.

To pattern the TiO_2 layer, a standard photolithography technique was employed. The substrates were first spin-coated with AZ5214E photoresist (Microchemicals GmbH, Ulm, Germany) at 3000 rpm for 30 s to achieve a uniform resist layer. Hexamethyldisiloxane (HMDS) was used as an adhesion promoter before applying the photoresist to ensure reliable patterning. After spin coating, the substrates were prebaked at 110 °C for 50 s to solidify the resist layer.

UV exposure was performed using a mask aligner (SUSS MicroTec, Garching, Germany), with a 5-inch photomask containing reflective chromium structures for line patterns as small as 50 μm (Rose Fotomasken, Bergisch Gladbach, Germany). The exposure energy was set to 32 mJ/cm^2 . Following exposure, a reversal bake at 120 °C for 2 min was performed to create the desired resist pattern, and a flood UV exposure with 320 mJ/cm^2 was applied. The unexposed areas were developed using the AZ726 developer (Microchemicals GmbH) for 1 min, after which the substrates were rinsed with deionized water and dried with nitrogen gas.

The lift-off process, used to remove the unwanted TiO_2 and ITO, involved immersing the substrates in acetone with ultrasonic agitation for 10 min, followed by a 5-min rinse in isopropanol. This process ensured that only the desired patterned regions of TiO_2 remained on the ITO layer.

Finally, to convert the sputtered TiO_2 from its amorphous state to the photocatalytically active anatase phase, the substrates were annealed in a muffle furnace at 400 °C for 90 min. This heat treatment was critical for achieving the desired crystalline structure and ensuring optimal photocatalytic properties for the TiO_2 . After annealing, the substrates were rapidly cooled on a metal plate to lock in the anatase phase, preparing them for subsequent photocatalytic growth and dissolution experiments. The preparation process of the substrates, including lithographic patterning and material deposition, is schematically illustrated in Figure 6 to provide a clear overview of the procedural steps.

4.2. Photocatalytic Growth Experiment

After completing the heat treatment to convert the TiO_2 to its anatase phase, the photocatalytic growth of gold lines along the edges of the TiO_2 patterns was performed in a beaker. The precursor solution was prepared by dissolving 99.99% pure gold (III) chloride (HAuCl_4) powder (Sigma-Aldrich) in deionized water, with a concentration of 15 mg in 60 mL of water. This solution was thoroughly mixed to ensure the complete dissolution of the gold chloride and to create a homogeneous precursor solution, essential for consistent photocatalytic growth across the entire surface of the substrates.

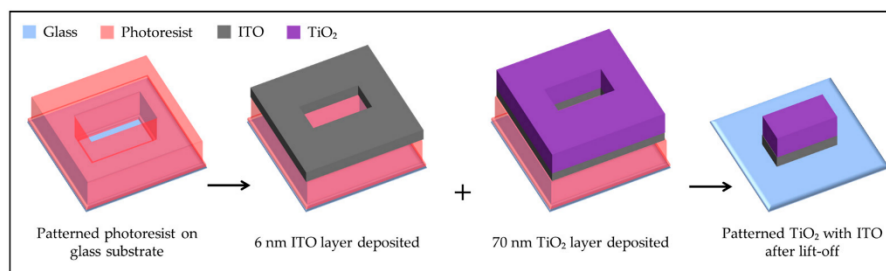


Figure 6. Schematic representation of the substrate preparation process. The glass substrate is negatively patterned with AZ5214E photoresist after lithography. A 6 nm ITO layer and a 70 nm TiO₂ layer are then deposited via sputtering. After the lift-off process, the final patterned TiO₂ structures with the underlying ITO layer are revealed.

To enhance the growth rate of the gold particles and improve the efficiency of the photocatalytic process, the precursor solution was mixed with isopropanol in a 10:1 ratio. The addition of isopropanol, which acts as a hole scavenger, plays a critical role by accelerating the reduction of Au³⁺ ions under UV illumination.

Each substrate was positioned at the bottom of a glass beaker with the TiO₂ facing upward. A total of 20 mL of the prepared precursor solution was added to the beaker, completely submerging the substrate. Two UV LEDs (Nichia, Tokushima, Japan), each emitting light at a wavelength of 365 nm, were positioned at opposite sides of the beaker with roughly 7 cm distance to the beaker, illuminating the template at an angle. The intensity of the UV light was measured using a Newport optical power meter and was found to be approximately 5 mJ/cm². The total illumination time was set to 30 min, ensuring sufficient energy input for the reduction of Au³⁺ ions and the subsequent formation of gold lines along the edges of the TiO₂ patterns. The schematic of the illumination experiment setup is shown in Figure 7. The setup is placed in a transmission microscope (DMi8 inverted microscope, Leica, Wetzlar, Germany) to allow for optical image recording of the gold growth and dissolution on the transparent substrates.

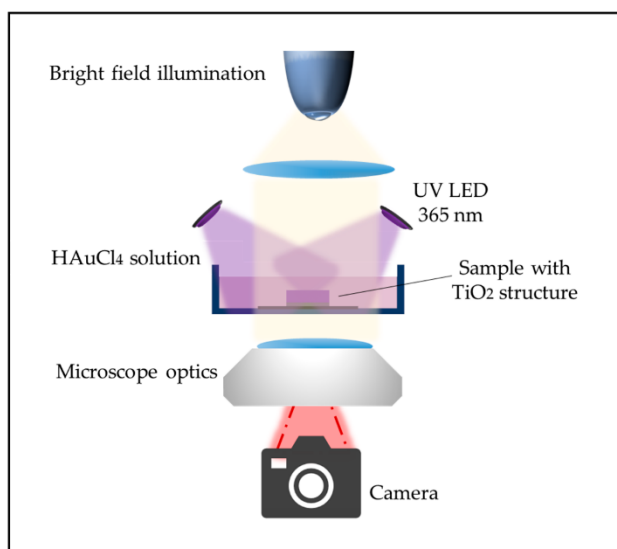


Figure 7. Schematic of the photocatalytic illumination setup. The sample with TiO₂ structures is submerged in the HAuCl₄ solution and illuminated by two angled UV LEDs (365 nm) under a transmission microscope connected to a camera.

4.3. Dissolution Experiment Using a KI Solution Mixed in Different Ratios with DI Water

To investigate the chemical dissolution of gold lines grown on the edge of TiO_2 patterns, a KI solution was prepared by mixing KI (Sigma-Aldrich, product number 204102) and iodine (I_2) (Sigma-Aldrich) in a ratio of 1:4:40 (DI water), which is a commonly used ratio for gold dissolution in similar chemical systems [40]. After thoroughly mixing the KI and I_2 with deionized water, the prepared solution was further diluted to different concentrations for the dissolution experiments.

Three distinct dilutions of KI solution were prepared by mixing 1 mL of the stock solution with 200 mL, 300 mL, and 400 mL of DI water. These varying concentrations were chosen to explore how different KI solution strengths impact the dissolution rate of the gold lines. The prepared solutions, exhibiting different shades of color due to varying concentrations of KI in DI, are shown in Figure 8. As the KI solution is diluted with DI water, the color transitions from dark brown to a lighter reddish hue, becoming progressively lighter with increasing amounts of DI water.

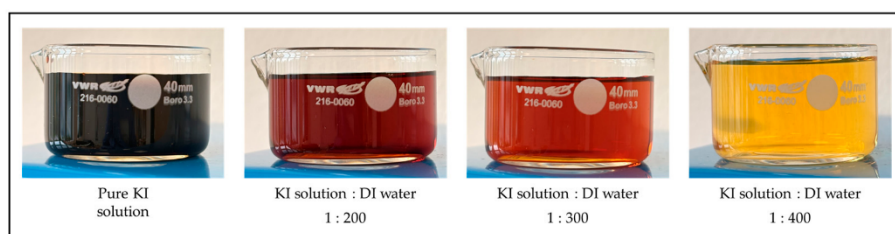


Figure 8. Visual representation of the KI solution diluted with DI water at different ratios. From left to right: pure KI solution, 1:200 KI solution to DI water, 1:300 KI solution to DI water, and 1:400 KI solution to DI water.

After preparing the KI solutions, two substrates were used for the dissolution experiments. Both substrates first underwent the photocatalytic gold growth process as described in Section 4.2. For the dissolution experiment, one of the gold-grown substrates was immersed in the KI solution diluted with 300 mL of DI water, and the other substrate was immersed in the solution mixed with 400 mL of DI water. Both samples were kept in the solution for 30 min to allow sufficient dissolution of the gold lines. The dissolution experiments were conducted under a transmission microscope connected to a camera, enabling the real-time visualization and recording of the process.

4.4. Photocatalytic Growth and Chemical Dissolution Sequence

The experiment was conducted on the substrate described in Section 4.1, using a transmission microscope for the continuous real-time observation of both the photocatalytic growth and subsequent chemical dissolution processes. The substrate was fixed in place throughout the experiment, eliminating the need for repositioning during the solution exchange steps.

In the first step, the beaker was filled with 20 mL of a HAuCl_4 precursor solution, which had been mixed with isopropanol in a 10:1 ratio to enhance the growth rate of the gold lines. The substrate, submerged in this solution, was then illuminated using two UV LEDs (365 nm), placed at an angle, for 30 min. This illumination initiated the photocatalytic growth of gold lines along the edges of the TiO_2 patterns on the substrate. After the growth phase, the beaker and substrate were thoroughly rinsed with deionized water to remove any residual gold precursor solution, and the substrate was dried using nitrogen gas to prepare for the next step.

In the second step, the photocatalytically grown gold Structures were subjected to chemical dissolution. The beaker was filled with 20 mL of KI solution, diluted in 30 mL of DI water. During this phase, the UV LEDs were turned off to avoid any photocatalytic effects that could interfere with the dissolution process. The substrate remained in the KI solution for 30 min, allowing the KI solution to dissolve the gold lines by forming a soluble gold–iodide complex [40]. Following the dissolution, the substrate was again rinsed with deionized water to ensure the complete removal of the KI solution, and the substrate was dried using nitrogen gas.

5. Conclusions

In this study, we demonstrated the sequential photocatalytic growth and chemical dissolution of gold structures on a patterned ITO/TiO₂ template. By optimizing the precursor solution, we achieved controlled gold growth along the edges of the ITO/TiO₂ patterns and subsequently carried out the dissolution process in an optimized KI solution. The kinetics of the growth and dissolution processes were explored through real-time monitoring using optical transmission microscopy and image processing. Although a uniform gold line was not formed within the 30 min illumination, the focus of this study was on the sequential growth and dissolution processes rather than achieving continuous lines. While the current setup did not allow simultaneous growth and dissolution, the findings suggest potential for future microfluidic systems that enable dynamic solution exchange for UV-driven growth and dissolution cycles, mimicking biological processes such as axonal growth and pruning in bio-inspired networks. This work provides a robust methodology for optimized photocatalytic growth and dissolution processes, contributing to the development of dynamic, reconfigurable material systems for neuromorphic engineering and adaptive technologies.

Supplementary Materials: The following supporting information can be downloaded at: <https://www.mdpi.com/article/10.3390/molecules30010099/s1>, Video S1: Gold growth dynamics in 30 min; Video S2: Gold dissolution dynamics in 30 min.

Author Contributions: Conceptualization, F.A. and M.G.; methodology, F.A. and M.G.; software, F.A., M.P. and M.G.; validation, F.A. and M.G.; formal analysis, F.A., S.V., A.V. and M.G.; investigation, F.A., S.V., A.V. and M.G.; resources, M.G.; data curation, F.A. and M.G.; writing—original draft preparation, F.A.; writing—review and editing, F.A., M.P., S.V., A.V. and M.G.; visualization, F.A.; supervision, M.G.; project administration, M.G.; funding acquisition, M.G. All authors have read and agreed to the published version of the manuscript.

Funding: This work was supported by the Deutsche Forschungsgemeinschaft (DFG, German Research Foundation)—Project-ID 434434223—SFB 1461.

Data Availability Statement: The data supporting the conclusions of this article will be made available by the corresponding authors on request.

Conflicts of Interest: The authors declare no conflict of interest.

References

1. Kendall, J.D.; Kumar, S. The Building Blocks of a Brain-Inspired Computer. *Appl. Phys. Rev.* **2020**, *7*, 011305. [CrossRef]
2. Goldberg, J.L. How Does an Axon Grow? *Genes. Dev.* **2003**, *17*, 941–958. [CrossRef]
3. Riccomagno, M.M.; Kolodkin, A.L. Sculpting Neural Circuits by Axon and Dendrite Pruning. *Annu. Rev. Cell Dev. Biol.* **2015**, *31*, 779–805. [CrossRef]
4. Strukov, D.B.; Snider, G.S.; Stewart, D.R.; Williams, R.S. The Missing Memristor Found. *Nature* **2008**, *453*, 80–83, Erratum in *Nature* **2009**, *453*, 7191. [CrossRef] [PubMed]
5. Asif, M.; Singh, Y.; Thakre, A.; Singh Ab, V.N.; Kumar, A. Synaptic Plasticity and Learning Behaviour in Multilevel Memristive Devices. *RSC Adv.* **2023**, *13*, 13292–13302. [CrossRef] [PubMed]
6. Wright, C.D. Precise Computing with Imprecise Devices. *Nat. Electron.* **2018**, *1*, 212–213. [CrossRef]

7. Vahl, A.; Milano, G.; Kuncic, Z.; Brown, S.A.; Milani, P. Brain-Inspired Computing with Self-Assembled Networks of Nano-Objects. *J. Phys. D Appl. Phys.* **2024**, *57*, 503001. [[CrossRef](#)]
8. Milano, G.; Pedretti, G.; Montano, K.; Ricci, S.; Hashemkhani, S.; Boarino, L.; Ielmini, D.; Ricciardi, C. In Materia Reservoir Computing with a Fully Memristive Architecture Based on Self-Organizing Nanowire Networks. *Nat. Mater.* **2021**, *21*, 195–202. [[CrossRef](#)] [[PubMed](#)]
9. Loeffler, A.; Diaz-Alvarez, A.; Zhu, R.; Ganesh, N.; Shine, J.M.; Nakayama, T.; Kuncic, Z. Neuromorphic Learning, Working Memory, and Metaplasticity in Nanowire Networks. *Sci. Adv.* **2023**, *9*, eadg3289. [[CrossRef](#)] [[PubMed](#)]
10. Ziegler, M.; Mussenbrock, T.; Kohlstedt, H. *Bio-Inspired Information Pathways*; Springer: Cham, Switzerland, 2023.
11. Terasa, M.I.; Birkoben, T.; Noll, M.; Adejube, B.; Madurawala, R.; Carstens, N.; Strunskus, T.; Kaps, S.; Faupel, F.; Vahl, A.; et al. Pathways towards Truly Brain-like Computing Primitives. *Mater. Today* **2023**, *69*, 41–53. [[CrossRef](#)]
12. Milano, G.; Pedretti, G.; Fretto, M.; Boarino, L.; Benfenati, F.; Ielmini, D.; Valov, I.; Ricciardi, C.; Milano, G.; Ricciardi, C.; et al. Brain-Inspired Structural Plasticity through Reweighting and Rewiring in Multi-Terminal Self-Organizing Memristive Nanowire Networks. *Adv. Intell. Syst.* **2020**, *2*, 2000096. [[CrossRef](#)]
13. Cusack, C.L.; Swahari, V.; Hampton Henley, W.; Ramsey, J.M.; Deshmukh, M. Distinct Pathways Mediate Axon Degeneration during Apoptosis and Axon-Specific Pruning. *Nat. Commun.* **2013**, *4*, 1876. [[CrossRef](#)] [[PubMed](#)]
14. Mear, Y.; Enjalbert, A.; Thirion, S.; Malagón, M.M.; Kineman, R.D. GHS-R1a Constitutive Activity and Its Physiological Relevance. *Front. Neurosci.* **2013**, *7*, 87. [[CrossRef](#)]
15. Gkoupidenis, P.; Koutsouras, D.A.; Malliaras, G.G. Neuromorphic Device Architectures with Global Connectivity through Electrolyte Gating. *Nat. Commun.* **2017**, *8*, 15448. [[CrossRef](#)]
16. Seung, S. *Connectome: How the Brain's Wiring Makes Us Who We Are*; Houghton Mifflin Harcourt: New York, NY, USA, 2012.
17. Safajou, H.; Khojasteh, H.; Salavati-Niasari, M.; Mortazavi-Derazkola, S. Enhanced Photocatalytic Degradation of Dyes over Graphene/Pd/TiO₂ Nanocomposites: TiO₂ Nanowires versus TiO₂ Nanoparticles. *J. Colloid. Interface Sci.* **2017**, *498*, 423–432. [[CrossRef](#)]
18. Vahl, A.; Veziroglu, S.; Henkel, B.; Strunskus, T.; Polonskyi, O.; Aktas, O.C.; Faupel, F. Pathways to Tailor Photocatalytic Performance of TiO₂ Thin Films Deposited by Reactive Magnetron Sputtering. *Materials* **2019**, *12*, 2840. [[CrossRef](#)] [[PubMed](#)]
19. Kusmirek, E. A CeO₂ Semiconductor as a Photocatalytic and Photoelectrocatalytic Material for the Remediation of Pollutants in Industrial Wastewater: A Review. *Catalysts* **2020**, *10*, 1435. [[CrossRef](#)]
20. Pan, X.; Tang, S.; Chen, X.; Liu, H.; Yu, C.; Gao, Q.Z.; Zhao, X.; Yang, H.; Gao, H.; Wang, S. Temperature-Controlled Synthesis of TiO₂ Photocatalyst with Different Crystalline Phases and Its Photocatalytic Activity in the Degradation of Different Mixed Dyes. *Russ. J. Phys. Chem. A* **2022**, *96*, S210–S218. [[CrossRef](#)]
21. You, C.S.; Jung, S.C. Photo-Catalytic Destruction of Tetracycline Antibiotics Using Terbium and Manganese Co-Precipitated TiO₂ Photocatalyst. *J. Environ. Chem. Eng.* **2024**, *12*, 111666. [[CrossRef](#)]
22. Kedves, E.Z.; Pap, Z.; Hernadi, K.; Baia, L. Significance of the Surface and Bulk Features of Hierarchical TiO₂ in Their Photocatalytic Properties. *Ceram. Int.* **2021**, *47*, 7088–7100. [[CrossRef](#)]
23. Binas, V.; Venieri, D.; Kotzias, D.; Kiriakidis, G. Modified TiO₂ Based Photocatalysts for Improved Air and Health Quality. *J. Mater.* **2017**, *3*, 3–16. [[CrossRef](#)]
24. Salomatina, E.V.; Fukina, D.G.; Koryagin, A.V.; Titaev, D.N.; Suleimanov, E.V.; Smirnova, L.A. Preparation and Photocatalytic Properties of Titanium Dioxide Modified with Gold or Silver Nanoparticles. *J. Environ. Chem. Eng.* **2021**, *9*, 106078. [[CrossRef](#)]
25. Veziroglu, S.; Obermann, A.L.; Ullrich, M.; Hussain, M.; Kamp, M.; Kienle, L.; Leißner, T.; Rubahn, H.G.; Polonskyi, O.; Strunskus, T.; et al. Photodeposition of Au Nanoclusters for Enhanced Photocatalytic Dye Degradation over TiO₂ Thin Film. *ACS Appl. Mater. Interfaces* **2020**, *12*, 14983–14992. [[CrossRef](#)] [[PubMed](#)]
26. Guo, Y.; Siretanu, I.; Zhang, Y.; Mei, B.; Li, X.; Mugele, F.; Huang, H.; Mul, G. PH-Dependence in Facet-Selective Photo-Deposition of Metals and Metal Oxides on Semiconductor Particles. *J. Mater. Chem. A Mater.* **2018**, *6*, 7500–7508. [[CrossRef](#)]
27. Veziroglu, S.; Ghor, M.Z.; Kamp, M.; Kienle, L.; Rubahn, H.G.; Strunskus, T.; Fiutowski, J.; Adam, J.; Faupel, F.; Aktas, O.C. Photocatalytic Growth of Hierarchical Au Needle Clusters on Highly Active TiO₂ Thin Film. *Adv. Mater. Interfaces* **2018**, *5*, 1800465. [[CrossRef](#)]
28. Mendoza-Diaz, M.I.; Cure, J.; Rouhani, M.D.; Tan, K.; Patnaik, S.G.; Pech, D.; Quevedo-Lopez, M.; Hungria, T.; Rossi, C.; Estève, A. On the UV-Visible Light Synergetic Mechanisms in Au/TiO₂ Hybrid Model Nanostructures Achieving Photoreduction of Water. *J. Phys. Chem. C* **2020**, *124*, 25421–25430. [[CrossRef](#)]
29. Sari, Y.; Garesio, P.L.; Armynah, B.; Tahir, D. A Review of TiO₂ Photocatalyst for Organic Degradation and Sustainable Hydrogen Energy Production. *Int. J. Hydrogen Energy* **2024**, *55*, 984–996. [[CrossRef](#)]
30. Stampelcoskie, K.G.; Swint, A. Optimizing Molecule-like Gold Clusters for Light Energy Conversion. *J. Mater. Chem. A* **2015**, *4*, 2075–2081. [[CrossRef](#)]
31. Dai, W.; Wang, X.; Liu, P.; Xu, Y.; Li, G.; Fu, X. Effects of Electron Transfer between TiO₂ Films and Conducting Substrates on the Photocatalytic Oxidation of Organic Pollutants. *J. Phys. Chem. B* **2006**, *110*, 13470–13476. [[CrossRef](#)]

32. Irfan, F.; Tanveer, M.U.; Moiz, M.A.; Husain, S.W.; Ramzan, M. TiO₂ as an Effective Photocatalyst Mechanisms, Applications, and Dopants: A Review. *Eur. Phys. J. B* **2022**, *95*, 184. [[CrossRef](#)]
33. Abshari, F.; Veziroglu, S.; Adejube, B.; Vahl, A.; Gerken, M. Photocatalytic Edge Growth of Conductive Gold Lines On Microstructured TiO₂–ITO Substrates. *Langmuir* **2024**, *40*, 22. [[CrossRef](#)] [[PubMed](#)]
34. Tomic, P. Method for Metallization Stripping of Gold Interconnected Semiconductors Using an Aqueous Potassium Iodide Solution. *Microsc. Today* **2002**, *10*, 18–19. [[CrossRef](#)]
35. Nikitin, D.; Biliak, K.; Pleskunov, P.; Ali-Ogly, S.; Červenková, V.; Carstens, N.; Adejube, B.; Strunskus, T.; Černochová, Z.; Štěpánek, P.; et al. Resistive Switching Effect in Ag-Poly(Ethylene Glycol) Nanofluids: Novel Avenue Toward Neuromorphic Materials. *Adv. Funct. Mater.* **2024**, *34*, 2310473. [[CrossRef](#)]
36. Zhu, J.; Zhang, T.; Yang, Y.; Huang, R. A Comprehensive Review on Emerging Artificial Neuromorphic Devices. *Appl. Phys. Rev.* **2020**, *7*, 011312. [[CrossRef](#)]
37. Barazany, D.; Basser, P.J.; Assaf, Y. In Vivo Measurement of Axon Diameter Distribution in the Corpus Callosum of Rat Brain. *Brain* **2009**, *132*, 1210–1220. [[CrossRef](#)]
38. Sampaio-Baptista, C.; Johansen-Berg, H. White Matter Plasticity in the Adult Brain. *Neuron* **2017**, *96*, 1239–1251. [[CrossRef](#)] [[PubMed](#)]
39. Seidl, A.H. Regulation of Conduction Time along Axons. *Neuroscience* **2014**, *276*, 126–134. [[CrossRef](#)] [[PubMed](#)]
40. Nakao, Y.; Soneb, K. Reversible Dissolutioddeposition of Gold in Iodine-Iodide-Acetonitrile Systems. *Chem. Commun.* **1996**, *8*, 897–898. [[CrossRef](#)]

Disclaimer/Publisher’s Note: The statements, opinions and data contained in all publications are solely those of the individual author(s) and contributor(s) and not of MDPI and/or the editor(s). MDPI and/or the editor(s) disclaim responsibility for any injury to people or property resulting from any ideas, methods, instructions or products referred to in the content.

Chapter 4

4. Conference Contributions

4.1. Photocatalytic Conductive Gold Deposition on Titanium Dioxide Templates Mimicking Axonal growth

This work was presented as a poster at the MRS Spring Meeting, April 10–14, 2023, San Francisco, California. This research explores the light-stimulated photocatalytic growth of conductive gold lines on titanium dioxide substrates as a means of mimicking long-range axonal connections in neuromorphic systems. By leveraging the photocatalytic properties of titanium dioxide, the study demonstrates how controlled growth processes can emulate the formation of neural pathways. This work contributes to the thesis by addressing a key aspect of neuromorphic network engineering: the creation of adaptive and reconfigurable conductive pathways that mimic biological systems, advancing the integration of growth mechanisms for artificial neuronal architectures.

4.1.1. Abstract

Nanoionic memristive devices that are based on the field driven migration of metal cations and oxygen vacancies have gathered high interest in the scientific community for their capability to technically mimic synaptic connections. Less attention has been given to long-range global plasticity in artificial neuronal networks. The aim of our research is to use light-stimulated growth of gold metal lines to technically mimic the growth of long-range axonal connections for neuromorphic computing architectures. To mimic the growth of axons


we investigated the formation of metal lines by UV-light-stimulus-driven photocatalytic deposition of gold on titanium dioxide layers. The growth process was conducted in a beaker by reduction from aqueous gold chloride precursor (HAuCl_4) and observed by transmission optical measurements in an inverted-microscope setup. We analyze the surface properties by 3D laser interference microscopy and scanning electron microscopy (SEM) and electrical conduction measurements are taken.

We fabricated the photoactive titanium dioxide layers with the thickness of 40-100 nm on quartz glass by DC sputtering. The substrates were then heat treated for 1h at 300°C and subsequently cooled on a metal plate to achieve the photocatalytically active anatase phase of titanium dioxide. In the growth process the substrates are placed in a beaker containing 15 ml of the precursor. The solution is obtained by dissolving 15 mg of HAuCl_4 crystalline powder in 60 ml of deionized water. We utilize a UV LED with the wavelength peak of 365 nm to illuminate the sample in the beaker. The illumination time and UV-intensity are crucial for this dynamic process. Here we illuminated for 3h and replaced the solution every hour. Furthermore, we repeated this experiment by adding a surfactant to the solution to achieve faster growth and better surface coverage as proposed by literature.


In-situ characterization of the growth process is possible by placing the beaker in an optical microscope with transmission configuration. While the sputtered titanium dioxide and the quartz glass substrate show high transparency, the grown gold will absorb and reflect the transmitted light and thus yield an observable change in transmission. We also analyzed the morphology of the grown gold layers by 3D laser interference microscopy and scanning electron microscopy (SEM) after the growth procedure. The measurements show the formation of gold clusters on the surface of the titanium dioxide layers. Sufficient growth time is needed to reach the percolation threshold and attain a conductive gold layer which is crucial for our aim of mimicking axonal connections. We recorded electrical current-voltage characteristics to investigate the electrical conductivity of the grown gold. Our measurements revealed a value of electrical conductivity $\sigma=0.015\text{ S}$ for areas with high surface coverage. It

was obvious from 3D laser interference microscopy that the thickness of gold clusters is not uniform throughout the surface of titanium dioxide. Therefore, the conductivity across the 2D surface of the TiO_2/Au composite varies. With its potential capability to locally control the growth of long-range metallic connections, photodegradation is a promising approach towards mimicking the dynamic formation of long-range axonal connections in neural networks.


4.1.2. Presented Poster



CRC 1461 Neurotronics



MATERIALS RESEARCH SOCIETY®
Advancing materials. Improving the quality of life.



Christian-Albrechts-Universität zu Kiel
Technische Fakultät

Photocatalytic conductive gold growth on titanium dioxide line mimicking axonal growth

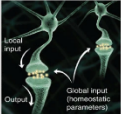
F. Abshari¹, M. Paulsen¹, J. Schardt¹, B. Adejube², A. Vahl², and M. Gerken¹

¹Chair for Integrated Systems and Photonics, Faculty of Engineering, Kiel University, ²Chair for Multicomponent Materials, Faculty of Engineering, Kiel University

Motivation

- Neuronal networks offer more efficient performance in complex tasks like image recognition than traditional silicon-based hardware.
- Our research aims to use light-stimulated growth to replicate the growth of long-range axonal connections in networks.

Here, we investigate the growth of gold connections on top of plain and structured TiO_2 thin films.

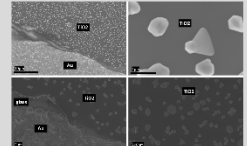


Neuronal network with local and global inputs [1].

Template Fabrication


- Lithography to create contacts negative pattern
- Au sputtering, 20nm
- Lift-off
- Lithography to create line negative pattern
- TiO_2 sputtering, 60nm
- Lift-off
- Heat treatment, 90min @400°C

Scanning electron microscopy images



Photocatalytic growth experiment

- First Au growth in HAuCl_4 for 2h
- Replace by fresh solution
- Second Au growth in HAuCl_4 for 2h



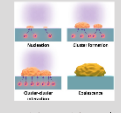
Dynamic growth experiment on TiO_2

Template:
 TiO_2 sputtered in glass thickness: 60nm
 Heat treatment, 90min @400°C

Red rectangles are on TiO_2 and greens are on quartz

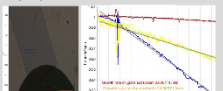
Photocatalysis Process

Au nanoclusters (NCs) deposited on TiO_2 by photoreduction [2]:



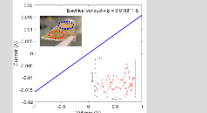
Scheme depicting the photocatalytic deposition of Au NCs on TiO_2 under UV light

Dynamic growth experiment on TiO_2 line



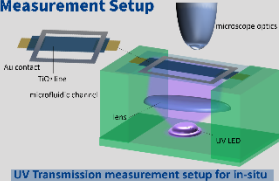
blue rectangle is on TiO_2 line, yellow on gold contact and red rectangle on glass substrate

Electric Conductivity of Au



Electrical conductivity of 0.015811 S is achieved. (Inset: I-V diagram of TiO_2 film without gold growth)

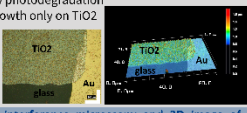
Measurement Setup



UV Transmission measurement setup for in-situ monitoring of Au growth on TiO_2

Template Characterization

- Successful growth of Au structures by photodegradation
- Growth only on TiO_2



Laser interference microscopy and 3D image of template after growth experiment

Outlook

- Photocatalytic gold growth in microfluidics
- Electrical characterization on TiO_2 line
- More localized growth

References

- Paschalis Gkoupidenis, Dimios A. Koutsouras, and George G. Malliaras, "Neuromorphic device architectures with global connectivity through electrolyte gating," *Nature communications* 5, no. 1 (2017): 1-5.
- Salih Vezirgolu, Anna-Lena Obermann, Marie Ullrich, Majid Hussain, Marius Kamp, Lorenz Kienle, Till Leibner et al, "Photodeposition of Au nanoclusters for enhanced photocatalytic dye degradation over TiO_2 thin film," *ACS applied materials & interfaces* 12, no. 13 (2020): 14953-14952.

Speaker's abstract:
 E-Mail: fabshari@kif.uni-kiel.de
 Phone: +49 431 880-6256

Invited by: B. Gerken
 E-Mail: bgerken@kif.uni-kiel.de
 Phone: +49 431 880-6256

Technische Fakultät
 Raum 001/010
 24143 Kiel

Chair for Integrated Systems and Photonics
<https://www.kif.uni-kiel.de>

4.2. Optical Probes for Resonance-Enhanced Gold Growth on Nano optical Substrates

This work was presented at the 245th ECS Meeting, May 26–30, 2024, in San Francisco, California. In this work, we focused on developing wavelength- and angle-dependent growth of gold metal lines on photoactive titanium dioxide layers, drawing inspiration from the neuronal connectivity of biological systems, such as the Hydra. Utilizing nano optical templates featuring hexagonal designs and periodic nanostructures, the research demonstrated how optical resonance effects could enhance photocatalytic processes. By integrating nanoimprint lithography, advanced characterization techniques, and resonant optical enhancement, this study aligns closely with the thesis objectives of creating adaptive and reconfigurable neuromorphic networks. The innovative approach highlights the role of precise optical templating in achieving efficient axonal pathway formation for neuromorphic applications.

4.2.1. Abstract

We investigate light-stimulated growth of gold metal lines to technically mimic the growth of long-range axonal connections for neuromorphic computing architectures. Photocatalytic gold growth from an aqueous gold chloride precursor solution (HAuCl_4) on a photoactive titanium dioxide layer is used. It is known that local gold growth may be obtained by UV illumination through a shadow mask [27]. To obtain a wavelength and angle dependent growth of metal lines – and thus stimulus-dependent resistances – we suggest to employ a nano-optical template. Inspired by the typical number of 2 to 10 connections to a node found, e.g., in the neuronal system of the biological species Hydra, we decided on the implementation of a hexagonal design. The edges are formed by periodic grating nanostructures with 10 to 20 periods and a grating pitch of 170 nm to 210 nm for excitation in the UV. In order to investigate the resonant optical enhancement, we employ optical probes. It is well known that colloidal quantum dots show enhanced fluorescence emission on photonic crystal surfaces due to resonant excitation and resonant outcoupling [89]. In our initial experiments for investigation of the resonant enhancement, we use 4,4'-Bis(2,2-

diphenylvinyl)-1,1'-biphenyl (DPVBi) as the emitter material. Its absorption maximum matches the excitation laser at 355 nm and fluorescence in the visible spectrum around 455 nm may be monitored with our camera and spectrometer setup.

The nanostructure master was fabricated by electron-beam lithography (Kelvin Nanotechnology Ltd.) according to our design. We transfer the nanostructure pattern onto 1.1 mm thick soda-lime glass substrates by UV-nanoimprint lithography. Subsequently, a 100 nm titanium dioxide layer is deposited. The 150 nm emissive DBVBi layer is then added by thermal evaporation. The samples are characterized optically with a camera setup and magnifying optics on an in-plane rotatable *xy*-stage. We use a Cobolt Zouk 355 nm 10 mW laser to excite the emissive layer. The output power of the laser is set to 2 mW and its output beam is widened with a collimating lens setup to a diameter of approximately 1.5 mm². The widened beam is essential to obtain a homogeneous excitation. We observe the successful resonant excitation by the higher emission intensity of DPVBi in specific regions of the nanostructure at specific excitation angles. Already for 10 periods of the grating structure resonance effects are observed. A stronger enhancement is obtained for 20 periods. Further, the enhancement depends on the grating pitch as connections with nanograting pitches below 190 nm are no longer visible. They do not meet the criteria for resonant excitation.

This method of using optical probes on the nano-optical template works well for initial characterization of the resonance enhancement at different excitation angles. Now the setup is ready for performing gold growth under different excitation conditions. Without the additional emissive layer, the waveguide thickness change needs to be compensated with an increased titanium dioxide layer thickness. For online monitoring of the resonant enhancement during growth optical probes may be employed below the photoactive titanium dioxide layer. It is expected that the resonance enhancement is reduced with the addition of gold due to the increased absorption and thus reduced quality factor as was previously studied in the context of nanostructured OLEDs [90].

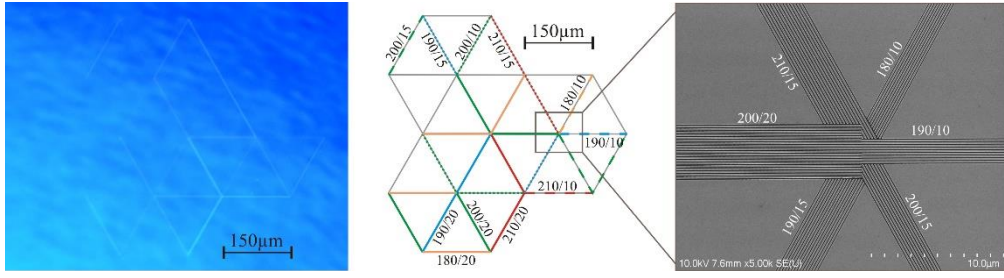


Figure 3. (Left) Fluorescence image of optical probe layer on nano-optical substrate for 355 nm laser excitation. (Middle) Schematic of nano-optical substrate with grating pitch (in nm) and number of periods given. Same colors represent identical grating features. (Right) Field emission scanning electron microscopy (FESEM) image of one node with 6 connections.

4.3. Mimicking Axons by Conductive Metal Lines Formed by Photocatalytically Grown Gold

4.3.1. Abstract

Nanoionic memristive devices based on the field-driven migration of metal cations and oxygen vacancies have gathered high interest in the scientific community for their capability to technically mimic synaptic connections. Less attention has been given to long-range global plasticity in artificial neuronal networks. The aim of our research is to use light-stimulated growth of gold metal lines to technically mimic the growth of long-range axonal connections for neuromorphic computing architectures. For this purpose, we investigate the formation of metal lines by UV-light-stimulus-driven photocatalytic deposition of gold on titanium dioxide layers.

0.8-mm wide photoactive titanium dioxide lines are defined by photolithography on a Sodalime glass substrate. We deposited a 70 nm thick titanium dioxide line on a 10 nm thick indium tin oxide adhesion layer by DC sputtering. The substrate was then heat treated for 90 minutes at 400°C and subsequently cooled on a metal plate to achieve the photocatalytically active anatase phase of titanium dioxide [27]. The growth process is conducted in a beaker by reduction from an aqueous gold chloride precursor solution (HAuCl_4). In each step of the growth process, the substrate is placed in a beaker containing 15 ml

of the precursor. The solution is obtained by dissolving 15 mg of HAuCl_4 powder in 60 ml of deionized water. We utilize a UV LED with the peak wavelength of 365 nm and an approximate intensity of 1.8 - 2.7 mW/cm^2 to illuminate the sample in the beaker. The illumination time and UV intensity are crucial for this dynamic process. Here, we illuminated the sample for 12 hours and refreshed the solution every 2 hours. After each refreshment of the solution, the substrate is washed thoroughly with deionized (DI) water and is dried under nitrogen gas. We analyze the surface properties of grown gold utilizing scanning electron microscopy (SEM) and measure the conductance of the grown lines by applying voltage via the needles of a hard contact probe station.

In the first experiments the growth of gold clusters on the surface is observed instead of the homogeneous gold coverage of the photolithographically defined titanium dioxide lines, which are needed for long-range electrical connections. Then, we coincidentally observed that the presence of a scratch on the titanium dioxide line led to the growth of continuous gold lines on the damaged area. Subsequently, deliberate scratches were introduced manually using tweezers, varying in both size and thickness. SEM images depict islands and covered areas, with notable growth observed on the scratched regions. Remarkably, wider scratches exhibit a proportionally increased width of the grown lines, and a uniform line devoid of any gaps is distinctly visible on broader scratches. We observed particle growth on thinner lines. However, unlike the uniform alignment observed in wider scratches, these particles did not coalesce into a continuous line. Instead, they remained separated from each other, exhibiting small gaps between individual particles. The morphological analysis of the grown gold line using SEM reveals a crystalline morphology of particles.

As the primary objective of this research is to mimic axons with gold lines, ensuring conductivity is crucial for obtaining long-range electrical connections mimicking axons. To achieve this, voltage was applied using the needles of a hard contact probe station, and the resulting current was measured. The linear behavior observed in the I-V diagram of the wider line serves as a confirmation of its conductance ($\approx 0.003 \text{ S}$).

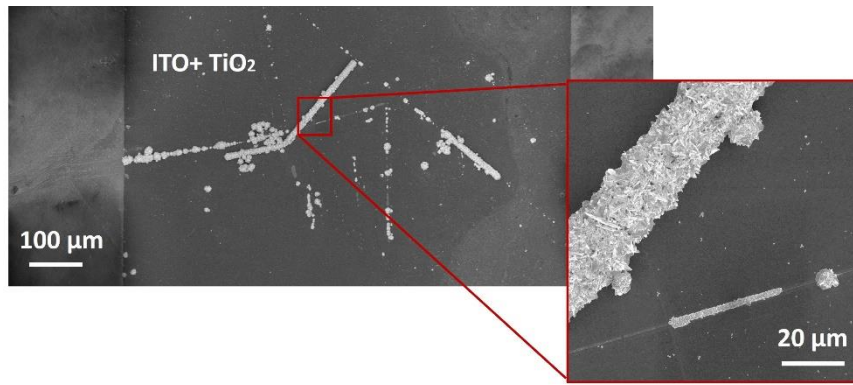


Figure 4. SEM images of the template after growth: Grown lines on scratches with varying widths.

4.4. Photocatalytic Growth and Chemical Dissolution of Gold Nanoparticles on TiO₂ Patterns

The conference presentation titled "Photocatalytic Growth and Chemical Dissolution of Gold Nanoparticles on TiO₂ Patterns" was delivered at the FMNT&NIBS-2024 Conference in Tartu, Estonia. This work focused on the dynamic processes of gold nanoparticle growth and dissolution, aiming to mimic the adaptive connectivity of axons in neuromorphic computing architectures. By investigating the rates of UV-stimulated photocatalytic growth and chemical dissolution on photolithographically patterned TiO₂ substrates, the study contributes to the development of techniques for creating and pruning axon-like structures in artificial neural networks. This research aligns with the broader goals of the thesis by exploring methods to balance growth and dissolution processes, enabling adaptive and reconfigurable neuromorphic systems.

4.4.1. Abstract

Our research targets the stimulus-driven formation of gold connections and the loss of connections for longer stimulus absence. We aim to extend the toolbox of neuromorphic computing by a method for growing and pruning of axon-like connections. We investigate the rates of UV-stimulated photocatalytic growth in HAuCl₄ solution and chemical dissolution in KI solution of gold nanoparticles. Photolithographically patterned 70 nm TiO₂ lines on glass are

used as substrates. For irradiation with a 365-nm LED rather slow growth is observed and attributed to the low absorption. The rate of chemical dissolution is adapted by changing the KI concentration in order to achieve a balance resembling the biological situation.

Chapter 5

5. Conclusion and Proposed Future Research

This chapter encapsulates the core findings and contributions of this research, alongside a forward-looking discussion on potential avenues for further exploration. In the first section, Thesis Summary and Conclusions, the key achievements and insights derived from the research are detailed, emphasizing their significance in advancing the understanding of neuromorphic systems. The second section, Proposed Improvements, delves into possible enhancements to the experimental methodologies and theoretical frameworks presented in this thesis. These refinements are aimed at overcoming existing challenges and broadening the applicability of photocatalytic growth and chemical dissolution methods in adaptive material systems. Collectively, these discussions underscore the innovative nature of this research, its role in bridging gaps in current knowledge, and its potential to guide future advancements in dynamic, bio-inspired technologies.

5.1. Summary and Conclusions

In summary, this dissertation presents a detailed investigation of photocatalytic growth and chemical dissolution processes as foundational steps toward the development of adaptive neuromorphic systems. The study focuses on titanium dioxide (TiO_2) as a photocatalytic substrate to facilitate the growth of conductive gold structures and their controlled removal. By exploring mechanisms that emulate biological processes such as synaptic connectivity and axonal dynamics, this work contributes to the fundamental understanding of

material-based approaches for neuromorphic engineering. While the findings underline the potential of these processes to enable plasticity and adaptability in engineered systems, they are positioned as exploratory steps toward developing building blocks for future neuromorphic networks.

The work begins with a systematic investigation of the photocatalytic gold deposition mechanisms on TiO_2 substrates. Experimental studies focus on critical parameters such as UV light intensity, precursor concentration, and reaction time, providing essential insights into controlling growth patterns and morphology. By understanding these interactions, the study offers a framework for directing the growth process to create structured, high-resolution gold formations. These structures serve as fundamental building blocks, advancing the exploration of adaptive configurations required for neuromorphic applications, without yet reaching the stage of practical system integration.

Additionally, this dissertation explores the concept of chemical pruning using KI as a means to selectively remove redundant or undesired connections in neuromorphic networks. The findings highlight how balancing growth and dissolution cycles allows for the dynamic reconfiguration of these networks. This balance, while foundational in its exploration, provides insights into creating systems capable of adaptive responses to stimuli and functional optimization, reflecting the potential for mimicking biological neural plasticity.

The integration of these processes was examined to demonstrate their potential in contributing to the formation of long-range, reconfigurable networks that emulate aspects of biological axonal pathways. Techniques such as photocatalytic lithography and patterned growth were utilized to create structured, application-specific designs. While these methods underscore the adaptability of the approaches developed in this research, they are positioned as exploratory steps toward enhancing the versatility and functionality of neuromorphic systems.

Through its comprehensive approach, this thesis establishes a foundational framework for exploring the growth and pruning of gold structures on TiO_2 substrates, aimed at advancing neuromorphic systems. The findings provide valuable insights into the feasibility and potential scalability of

photocatalytic methods for neuromorphic applications. While the results demonstrate significant progress in understanding and controlling these processes, they serve as a stepping stone for further research and development in this emerging field.

5.2. Proposed Improvements

Building on the findings of this dissertation, several promising directions for future research are suggested to deepen the understanding and broaden the applicability of photocatalytic growth and chemical dissolution processes for neuromorphic systems. These proposals include exploring diverse material configurations, investigating alternative growth techniques, and developing dynamic systems that enable simultaneous growth and pruning. Such advancements could enhance the adaptability and precision of neuromorphic device fabrication, paving the way for more efficient and responsive network designs tailored to specific computational needs.

One promising direction involves the investigation of multilayered substrate configurations to study how complex interfaces affect photocatalytic activity and gold growth patterns. By incorporating alternating layers of titanium dioxide (TiO_2) and indium tin oxide (ITO) with varied thicknesses and sequences, future research could examine the impact of multilayer designs on electron transfer dynamics, light absorption efficiency, and growth uniformity. This approach may uncover unique properties and behaviors not achievable with single-layer configurations, offering opportunities to optimize substrate designs for enhanced performance in advanced neuromorphic architectures.

Another innovative approach involves employing microfluidic systems to replace the static beaker method for photocatalytic gold growth. Delivering the gold chloride precursor solution through microfluidic channels offers precise control over flow rates, potentially impacting the deposition kinetics and the morphology of the resulting gold structures. By varying flow rates, researchers could investigate how hydrodynamic parameters influence the distribution, density, and size of gold particles, providing valuable insights into photocatalytic processes. Additionally, this method enables the creation of highly

localized and tunable growth conditions, enhancing the resolution and functionality of conductive pathways in neuromorphic systems.

An extension of the microfluidic approach could involve the simultaneous introduction of gold chloride and KI solutions into the system. By precisely controlling the concentrations and flow rates of these solutions, researchers could explore the concurrent processes of gold nanoparticle growth and dissolution under UV illumination. This approach would enable investigation into whether UV light, in the presence of both solutions, promotes deposition, dissolution, or establishes a dynamic equilibrium, providing critical insights into the mechanisms of adaptive material processes. Such a dual-flow system could model real-time adaptive networks, wherein the balance between connection growth and pruning dynamically responds to environmental stimuli, further advancing the development of neuromorphic systems.

These proposed directions are intended to expand the methodologies available in neuromorphic engineering by utilizing advanced substrate configurations, pioneering growth techniques, and integrated dynamic control systems. By focusing on these areas, future research has the potential to enable the development of neuromorphic devices that are not only highly adaptable and efficient but also scalable, thereby better replicating the intricate and dynamic functionalities of biological neural networks.

6. Bibliography

- [1] J. J. Hopfield, “Neural networks and physical systems with emergent collective computational abilities.,” *Proceedings of the National Academy of Sciences*, vol. 79, no. 8, pp. 2554–2558, Apr. 1982, doi: 10.1073/PNAS.79.8.2554.
- [2] C. Mead, “Neuromorphic Electronic Systems,” *Proceedings of the IEEE*, vol. 78, no. 10, pp. 1629–1636, 1990, doi: 10.1109/5.58356.
- [3] Z. Jakšić and O. Jakšić, “Biomimetic Nanomembranes: An Overview,” *Biomimetics*, vol. 5, no. 2, p. 24, May 2020, doi: 10.3390/BIOMIMET-ICS5020024.
- [4] Y. Van De Burgt and P. Gkoupidenis, “Organic materials and devices for brain-inspired computing: From artificial implementation to biophysical realism,” *MRS Bulletin*, vol. 45, no. 8, pp. 631–640, Aug. 2020, doi: 10.1557/MRS.2020.194.
- [5] S. Seung, *Connectome: How the Brain’s Wiring Makes Us Who We Are*, Houghton Mifflin Harcourt: New York, NY, USA, 2012.
- [6] J. D. Kendall and S. Kumar, “The building blocks of a brain-inspired computer,” *Applied Physics Reviews*, vol. 7, no. 1, Mar. 2020, doi: 10.1063/1.5129306/997408.
- [7] V. K. Sangwan and M. C. Hersam, “Neuromorphic nanoelectronic materials,” *Nature Nanotechnology*, vol. 15, no. 7, pp. 517–528, Mar. 2020, doi: 10.1038/s41565-020-0647-z.
- [8] M. Ziegler, T. Mussenbrock and H. Kohlstedt, *Bio-Inspired Information Pathways*, Springer: Cham, Switzerland, 2023.
- [9] F. Abshari, S. Veziroglu, B. Adejube, A. Vahl, and M. Gerken, “Photocatalytic Edge Growth of Conductive Gold Lines on Microstructured TiO₂–ITO Substrates,” *Langmuir*, vol. 40, p. 22, 2024, doi: 10.1021/acs.langmuir.4c02106.
- [10] A. Vahl *et al.*, “Pathways to Tailor Photocatalytic Performance of TiO₂ Thin Films Deposited by Reactive Magnetron Sputtering,” *Materials*, vol. 12, no. 17, p. 2840, Sep. 2019, doi: 10.3390/MA12172840.
- [11] G. Indiveri, and S. C. Liu, “Memory and Information Processing in Neuromorphic Systems,” *Proceedings of the IEEE*, vol. 103, no. 8, pp. 1379–1397, Jul. 2015, doi: 10.1109/JPROC.2015.2444094.
- [12] J. Tang *et al.*, “Bridging Biological and Artificial Neural Networks with Emerging Neuromorphic Devices: Fundamentals, Progress, and Challenges,” *Advanced Materials*, vol. 31, no. 49, p. 1902761, Dec. 2019, doi: 10.1002/ADMA.201902761.
- [13] I. Boybat *et al.*, “Neuromorphic computing with multi-memristive synapses”, *Nature Communications*, vol. 9, no. 1, p. 2514, Jun. 2018, doi: 10.1038/s41467-018-04933-y.

- [14] A. Naldoni *et al.*, “Photocatalysis with Reduced TiO₂: From Black TiO₂ to Cocatalyst-Free Hydrogen Production,” *ACS Catalysis*, vol. 9, no. 1, pp. 345–364, Nov. 2018, doi: 10.1021/acscatal.8b04068.
- [15] R. Attri, I. Mondal, B. Yadav, G. U. Kulkarni, and C. N. R Rao ab, “Neuromorphic devices realised using self-forming hierarchical Al and Ag nanostructures: towards energy-efficient and wide-ranging synaptic plasticity,” *Materials Horizons*, vol. 11, no. 3, pp. 737–746, 2024, doi: 10.1039/d3mh01367g.
- [16] B. J. Choi *et al.*, “Electrical Performance and Scalability of Pt Dispersed SiO₂ Nanometallic Resistance Switch,” *Nano Letters*, vol. 13, no. 7, pp. 3213–3217, Jul. 2013, doi: 10.1021/nl401283q.
- [17] D. B. Strukov, G. S. Snider, D. R. Stewart, and R. S. Williams, “The missing memristor found,” *Nature*, vol. 453, no. 7191, pp. 80–83, May 2008, doi: 10.1038/nature06932.
- [18] P. Gkoupidenis, D. A. Koutsouras, and G. G. Malliaras, “Neuromorphic device architectures with global connectivity through electrolyte gating,” *Nature Communications*, vol. 8, no. 1, pp. 1–8, May 2017, doi: 10.1038/ncomms15448.
- [19] J. Grollier, D. Querlioz, and M. D. Stiles, “Spintronic Nanodevices for Bioinspired Computing”, *Proceedings of the IEEE*, vol. 104, no. 10, pp. 2024–2039, Sep. 2016, doi: 10.1109/JPROC.2016.2597152.
- [20] M. Hamza Pervez *et al.*, “Recent Developments on Novel 2D Materials for Emerging Neuromorphic Computing Devices,” *Small Structures*, p. 2400386, 2024, doi: 10.1002/ssr.202400386.
- [21] M. K. Song *et al.*, “Recent Advances and Future Prospects for Memristive Materials, Devices, and Systems,” *ACS Nano*, vol. 17, no. 13, pp. 11994–12039, Jul. 2023, doi: 10.1021/ACS.NANO.3C03505.
- [22] K. C. Kwon, J. H. Baek, K. Hong, S. Y. Kim, and H. W. Jang, “Memristive Devices Based on Two-Dimensional Transition Metal Chalcogenides for Neuromorphic Computing,” *Nano-Micro Letters*, vol. 14, no. 1, pp. 1–30, Feb. 2022, doi: 10.1007/S40820-021-00784-3.
- [23] Q. Xu *et al.*, “Hierarchical Spiking-Based Model for Efficient Image Classification with Enhanced Feature Extraction and Encoding,” *IEEE Transactions on Neural Networks and Learning Systems*, vol. 35, no. 7, pp. 9277–9285, 2024, doi: 10.1109/TNNLS.2022.3232106.
- [24] K. Roy, A. Jaiswal, and P. Panda, “Towards spike-based machine intelligence with neuromorphic computing,” *Nature*, vol. 575, no. 7784, pp. 607–617, Nov. 2019, doi: 10.1038/s41586-019-1677-2.
- [25] X. Zhu, S. H. Lee, and W. D. Lu, “Nanoionic Resistive-Switching Devices,” *Advanced Electronic Materials*, vol. 5, no. 9, p. 1900184, Sep. 2019, doi: 10.1002/AELM.201900184.
- [26] G. Milano, E. Miranda, and C. Ricciardi, “Connectome of memristive nanowire networks through graph theory,” *Neural Networks*, vol. 150, pp. 137–148, Jun. 2022, doi: 10.1016/J.NEUNET.2022.02.022.
- [27] S. Veziroglu *et al.*, “Photocatalytic Growth of Hierarchical Au Needle Clusters on Highly Active TiO₂ Thin Film,” *Advanced Materials*

- Interfaces*, vol. 5, no. 15, p. 1800465, Aug. 2018, doi: 10.1002/ADMI.201800465.
- [28] S. Yu, W. Shim, X. Peng, and Y. Luo, “RRAM for Compute-in-Memory: From Inference to Training,” *IEEE Transactions on Circuits and Systems I: Regular Papers*, vol. 68, no. 7, pp. 2753–2765, Jul. 2021, doi: 10.1109/TCSI.2021.3072200.
 - [29] B. Sun *et al.*, “Synaptic devices based neuromorphic computing applications in artificial intelligence,” *Materials Today Physics*, vol. 18, p. 100393, May 2021, doi: 10.1016/J.MTPHYS.2021.100393.
 - [30] W. Qin, B. H. Kang, J. Bin An, and H. J. Kim, “Indium oxide nanomesh-based electrolyte-gated synaptic transistors,” *Journal of Information Display*, vol. 22, no. 3, pp. 179–185, Jul. 2021, doi: 10.1080/15980316.2021.1911866.
 - [31] A. Emboras *et al.*, “Atomic Scale Photodetection Enabled by a Memristive Junction,” *ACS Nano*, vol. 12, no. 7, pp. 6706–6713, Jul. 2018, doi: 10.1021/ACSNANO.8B01811.
 - [32] S. Y. Li *et al.*, “In-sensor neuromorphic computing using perovskites and transition metal dichalcogenides,” *Journal of Physics: Materials*, vol. 7, no. 3, p. 032002, Jun. 2024, doi: 10.1088/2515-7639/AD5251.
 - [33] E. R. W. Van Doremaele, P. Gkoupidenis, and Y. Van De Burgt, “Towards organic neuromorphic devices for adaptive sensing and novel computing paradigms in bioelectronics,” *Journal of Materials Chemistry C*, vol. 7, no. 41, pp. 12754–12760, 2019, doi: 10.1039/C9TC03247A.
 - [34] Z. Xiao *et al.*, “Preparation of MXene-based hybrids and their application in neuromorphic devices,” *International Journal of Extreme Manufacturing*, vol. 6, no. 2, p. 022006, Jan. 2024, doi: 10.1088/2631-7990/AD1573.
 - [35] H. Zhang and Y. Hu, “A constitutive model that couples light propagation direction and deformation for photo-responsive polymers and polymeric gels,” *Journal of the Mechanics and Physics of Solids*, vol. 191, p. 105786, Oct. 2024, doi: 10.1016/J.JMPS.2024.105786.
 - [36] J. L. de Deus, O. S. Faborode, and S. Nandi, “Synaptic Pruning by Microglia: Lessons from Genetic Studies in Mice,” *Developmental Neuroscience*, pp. 1–21, Sep. 2024, doi: 10.1159/000541379.
 - [37] F. Wang, T. Zhang, C. Dou, Y. Shi, and L. Pan, “Neuromorphic Devices, Circuits, and Their Applications in Flexible Electronics,” *IEEE Journal on Flexible Electronics*, vol. 3, no. 1, pp. 42–56, Oct. 2023, doi: 10.1109/JFLEX.2023.3321256.
 - [38] L. Yang *et al.*, “Deep-UV-photo-excited synaptic Ga₂O₃ nano-device with low-energy consumption for neuromorphic computing,” *Journal of Semiconductors*, vol. 45, no. 11, p. 1, doi: 10.1088/1674-4926/24050037.
 - [39] V. Likodimos, “Advanced photocatalytic materials,” *Materials*, vol. 13, no. 4, Feb. 2020, doi: 10.3390/MA13040821.

- [40] M. R. Hoffmann, S. T. Martin, W. Choi, D. W. Bahnemann, and W. M. Keck, "Environmental Applications of Semiconductor Photocatalysis," *Chemical Reviews*, vol. 95, pp. 69–96, Jan. 1995.
- [41] S. Gonuguntla, R. Kamesh, U. Pal, and D. Chatterjee, "Dye sensitization of TiO₂ relevant to photocatalytic hydrogen generation: Current research trends and prospects," *Journal of Photochemistry and Photobiology C: Photochemistry Reviews*, vol. 57, p. 100621, Dec. 2023, doi: 10.1016/J.JPHOTOCHEMREV.2023.100621.
- [42] J. Tao *et al.*, "Highly Transparent, Highly Thermally Stable Nanocellulose/Polymer Hybrid Substrates for Flexible OLED Devices," *ACS Applied Materials Interfaces*, vol. 12, no. 8, pp. 9701–9709, Feb. 2020, doi: 10.1021/ACSAMI.0C01048.
- [43] M. Shahrezaei *et al.*, "Ultrasound-Driven Defect Engineering in TiO₂-x Nanotubes—Toward Highly Efficient Platinum Single Atom-Enhanced Photocatalytic Water Splitting," *ACS Applied Materials Interfaces*, vol. 15, no. 31, pp. 37976–37985, Aug. 2023, doi: 10.1021/ACSAMI.3C04811.
- [44] P. V. Kamat, "Photophysical, photochemical and photocatalytic aspects of metal nanoparticles," *Journal of Physical Chemistry B*, vol. 106, no. 32, pp. 7729–7744, Aug. 2002, doi: 10.1021/JP0209289.
- [45] A. Fujishima, T. N. Rao, and D. A. Tryk, "Titanium dioxide photocatalysis," *Journal of Photochemistry and Photobiology C: Photochemistry Reviews*, vol. 1, no. 1, pp. 1–21, Jun. 2000, doi: 10.1016/S1389-5567(00)00002-2.
- [46] A. L. Linsebigler, G. Lu, and J. T. Yates, "Photocatalysis on TiO₂ Surfaces: Principles, Mechanisms, and Selected Results," *Chemical Reviews*, vol. 95, pp. 735–758, May 1995.
- [47] X. Chen and S. S. Mao, "Titanium dioxide nanomaterials: Synthesis, properties, modifications and applications," *Chemical Reviews*, vol. 107, no. 7, pp. 2891–2959, Jul. 2007, doi: 10.1021/CR0500535.
- [48] O. Carp, C. L. Huisman, and A. Reller, "Photoinduced reactivity of titanium dioxide," *Progress in Solid State Chemistry*, vol. 32, no. 1–2, pp. 33–177, Jan. 2004, doi: 10.1016/J.PROGSOL-IDSTCHEM.2004.08.001.
- [49] Y. Sun and Y. Xia, "Shape-controlled synthesis of gold and silver nanoparticles," *Science*, vol. 298, no. 5601, pp. 2176–2179, Dec. 2002, doi: 10.1126/SCIENCE.1077229.
- [50] M. C. Daniel and D. Astruc, "Gold Nanoparticles: Assembly, Supramolecular Chemistry, Quantum-Size-Related Properties, and Applications toward Biology, Catalysis, and Nanotechnology," *Chemical Reviews*, vol. 104, no. 1, pp. 293–346, Jan. 2004, doi: 10.1021/CR030698.
- [51] Z. Ma and S. Dai, *Heterogeneous Gold Catalysts and Catalysis*, The Royal Society of Chemistry, Cambridge, UK, 2014.
- [52] E. Grabowska *et al.*, "Modification of Titanium (IV) Dioxide with Small Silver Nanoparticles: Application in Photocatalysis," *The Journal of Physical Chemistry C*, vol. 117, no. 4, pp. 1955–1962, Jan. 2013, doi: 10.1021/jp3112183.

- [53] C. Gu, C. Cheng, H. Huang, T. Wong, N. Wang, and T.-Y. Zhang, “Growth and Photocatalytic Activity of Dendrite-like ZnO@Ag Heterostructure Nanocrystals”, *Crystal Growth and Design*, vol. 9, no. 7, pp. 3278-3285, Jul. 2009, doi: 10.1021/cg900043k.
- [54] D. Aureau, Y. Varin, K. Roodenko, O. Seitz, O. Pluchery, and Y. J. Chabal, “Controlled Deposition of Gold Nanoparticles on Well-Defined Organic Monolayer Grafted on Silicon Surfaces”, *The Journal of Physical Chemistry C*, vol. 114, no. 33, pp. 14180-14186, Aug. 2010, doi: 10.1021/jp104183m.
- [55] S. Ge *et al.*, “A Review on the Progress of Optoelectronic Devices Based on TiO₂ Thin Films and Nanomaterials,” *Nanomaterials*, vol. 13, no. 7, p. 1141, Mar. 2023, doi: 10.3390/nano13071141.
- [56] H. Li, Q. Li, T. Sun, Y. Zhou, and S. T. Han, “Recent advances in artificial neuromorphic applications based on perovskite composites,” *Materials Horizons*, 2024, doi: 10.1039/d4mh00574k.
- [57] Z. Sun, X. Huang, and G. Zhang, “TiO₂-based catalysts for photothermal catalysis: Mechanisms, materials and applications,” *Journal of Cleaner Production*, vol. 381, p. 135156, Dec. 2022, doi: 10.1016/j.jclepro.2022.135156.
- [58] J. J. Kelley, M. L. Jespersen, and R. A. Vaia, “Self-limiting gold nanoparticle surface assemblies through modulation of pH and ionic strength,” *Journal of Nanoparticle Research*, vol. 20, no. 11, pp. 1–13, Nov. 2018, doi: 10.1007/S11051-018-4388-Y.
- [59] V. A. Holovatsky, “Effect of magnetic and electric fields on optical properties of semiconductor spherical layer,” *Semiconductor Physics Quantum Electronics and Optoelectronics*, vol. 17, no. 1, pp. 7–13, Mar. 2014, doi: 10.15407/SPQEO17.01.007.
- [60] C. J. Murphy *et al.*, “Anisotropic metal nanoparticles: Synthesis, assembly, and optical applications,” *Journal of Physical Chemistry B*, vol. 109, no. 29, pp. 13857–13870, Jul. 2005, doi: 10.1021/JP0516846.
- [61] C. Tossi *et al.*, “Size- and density-controlled photodeposition of metallic platinum nanoparticles on titanium dioxide for photocatalytic applications,” *Journal of Materials Chemistry A*, vol. 7, no. 24, pp. 14519–14525, Jun. 2019, doi: 10.1039/C8TA09037H.
- [62] H. Notsu, W. Kubo, I. Shitanda, and T. Tatsuma, “Super-hydrophobic/super-hydrophilic patterning of gold surfaces by photocatalytic lithography,” *Journal of Materials Chemistry*, vol. 15, no. 15, pp. 1523–1527, Feb. 2005, doi: 10.1039/B418884E.
- [63] S. A. Bansal, V. Kumar, J. Karimi, A. P. Singh, and S. Kumar, “Role of gold nanoparticles in advanced biomedical applications,” *Nanoscale Advances*, vol. 2, no. 9, pp. 3764–3787, Sep. 2020, doi: 10.1039/D0NA00472C.
- [64] R. Sayago-Carro, L. J. Jiménez-Chavarriga, E. Fernández-García, A. Kubacka, and M. Fernández-García, “Efficiency in photocatalytic production of hydrogen: energetic and sustainability implications,” *Energy Advances*, vol. 3, no. 11, pp. 2738–2757, Nov. 2024, doi: 10.1039/D4YA00361F.

- [65] K. Maeda and K. Domen, “Photocatalytic water splitting: Recent progress and future challenges,” *Journal of Physical Chemistry Letters*, vol. 1, no. 18, pp. 2655–2661, Sep. 2010, doi: 10.1021/JZ1007966.
- [66] H. Beygi, S. A. Sajjadi, A. Babakhani, J. F. Young, and F. C. J. M. van Veggel, “Surface chemistry of as-synthesized and air-oxidized PbS quantum dots,” *Applied Surface Science*, vol. 457, pp. 1–10, Nov. 2018, doi: 10.1016/J.APSUSC.2018.06.152.
- [67] A. Facchetti, M. H. Yoon, and T. J. Marks, “Gate Dielectrics for Organic Field-Effect Transistors: New Opportunities for Organic Electronics,” *Advanced Materials*, vol. 17, no. 14, pp. 1705–1725, Jul. 2005, doi: 10.1002/ADMA.200500517.
- [68] J. Molina-Reyes *et al.*, “Study on the photocatalytic activity of titanium dioxide nanostructures: Nanoparticles, nanotubes and ultra-thin films,” *Catalysis Today*, vol. 341, pp. 2–12, Feb. 2020, doi: 10.1016/J.CAT-TOD.2018.05.033.
- [69] Y. Li, J. Li, C. Lu, J. Kou, and Z. Xu, “Facile fabrication of large-area hierarchical plasmonic cavities with broadband plasmon resonance for enhanced photocatalytic hydrogen evolution,” *Nano Research*, vol. 17, no. 11, pp. 9573–9584, Nov. 2024, doi: 10.1007/S12274-024-6964-Z.
- [70] V. N. Nguyen *et al.*, “Surface-Modified Titanium Dioxide Nanofibers with Gold Nanoparticles for Enhanced Photoelectrochemical Water Splitting,” *Catalysts*, vol. 10, no. 2, p. 261, Feb. 2020, doi: 10.3390/CATAL10020261.
- [71] A. Pringkasemchai, F. Hoshyargar, B. Lertanantawong, and A. P. O’Mullane, “Lightweight ITO Electrodes Decorated with Gold Nanostructures for Electrochemical Applications,” *Electroanalysis*, vol. 31, no. 11, pp. 2095–2102, Nov. 2019, doi: 10.1002/ELAN.201900152.
- [72] M. Berdakin *et al.*, “Dynamical evolution of the Schottky barrier as a determinant contribution to electron–hole pair stabilization and photocatalysis of plasmon-induced hot carriers,” *Nanoscale*, vol. 14, no. 7, pp. 2816–2825, Feb. 2022, doi: 10.1039/D1NR04699C.
- [73] M. U. Rashid *et al.*, “Role of Ti interfacial layer in the stability of TiO₂ based transparent synaptic device,” *Current Applied Physics*, vol. 64, pp. 16–24, Aug. 2024, doi: 10.1016/J.CAP.2024.05.005.
- [74] N. Yang *et al.*, “TiO₂-based heterojunctions for photocatalytic hydrogen evolution reaction,” *Microstructures*, vol. 4, no. 4, Jul. 2024, doi: 10.20517/MICROSTRUCTURES.2024.06.
- [75] S. Oh *et al.*, “Band restructuring of ordered/disordered blue TiO₂ for visible photocatalyst,” arXiv preprint, arXiv:2010.09328, Oct. 2020.
- [76] F. Wu and T.-Y. Tseng, “All-Optically Regulated ITO/Cu₂O/WO₃/ITO Memristor for Optoelectronic Neuromorphic Computing,” *ACS Applied Electronic Materials*, vol. 6, p. 5221, Jul. 2024, doi: 10.1021/acsaelm.4c00726.
- [77] F. Abshari, M. Paulsen, S. Veziroglu, A. Vahl, and M. Gerken, “ITO-TiO₂ Heterojunctions on Glass Substrates for Photocatalytic Gold

- Growth Along Pattern Edges,” *Catalysts*, vol. 14, no. 12, p. 940, Dec. 2024, doi: 10.3390/CATAL14120940.
- [78] H. Jiang *et al.*, “Considerably Improved Photovoltaic Performances of ITO/Si Heterojunction Solar Cells by Incorporating Hydrogen into Near-Interface Region,” *IEEE Journal of Photovoltaics*, vol. 12, no. 5, pp. 1102–1108, Sep. 2022, doi: 10.1109/JPHOTOV.2022.3179940.
 - [79] X. Wu *et al.*, “Gold nanoparticles modified ITO anode for enhanced PLEDs brightness and efficiency,” *Journal of Materials Chemistry C*, vol. 1, no. 42, pp. 7020–7025, Oct. 2013, doi: 10.1039/C3TC31237B.
 - [80] R. Amin *et al.*, “An ITO-graphene heterojunction integrated absorption modulator on Si-photonics for neuromorphic nonlinear activation,” *APL Photonics*, vol. 6, no. 12, Dec. 2021, doi: 10.1063/5.0062830/1024558.
 - [81] W. Guo, M. E. Fouda, H. E. Yantir, A. M. Eltawil, and K. N. Salama, “Unsupervised Adaptive Weight Pruning for Energy-Efficient Neuromorphic Systems,” *Frontiers in Neuroscience*, vol. 14, p. 598876, Nov. 2020, doi: 10.3389/FNINS.2020.598876.
 - [82] L. Tan *et al.*, “Fine-tuning growth in gold nanostructures from achiral 2D to chiral 3D geometries,” *Nano Research*, vol. 17, no. 7, pp. 6654–6660, Jul. 2024, doi: 10.1007/S12274-024-6582-9.
 - [83] W. Guo, H. E. Yantir, M. E. Fouda, A. M. Eltawil, and K. N. Salama, “Towards efficient neuromorphic hardware: Unsupervised adaptive neuron pruning,” *Electronics*, vol. 9, no. 7, pp. 1–15, Jul. 2020, doi: 10.3390/ELECTRONICS9071059.
 - [84] T. A. Green, “Gold etching for microfabrication,” *Gold Bulletin*, vol. 47, no. 3, pp. 205–216, May 2014, doi: 10.1007/S13404-014-0143-Z.
 - [85] J. Ryland, “Modeling Axonal Plasticity in Artificial Neural Networks,” *Neural Processing Letters*, vol. 53, no. 2, pp. 1119–1146, Apr. 2021, doi: 10.1007/S11063-021-10433-W/TABLES/5.
 - [86] F. Abshari, M. Paulsen, S. Veziroglu, A. Vahl, and M. Gerken, “Mimicking Axon Growth and Pruning by Photocatalytic Growth and Chemical Dissolution of Gold on Titanium Dioxide Patterns,” *Molecules*, vol. 30, no. 1, p. 99, Dec. 2024, doi: 10.3390/MOLECULES30010099.
 - [87] J. Schardt, M. Paulsen, and M. Gerken, “Nanooptical Substrates for Resonance-Enhanced Gold Growth,” *24th International Conference on Transparent Optical Networks (ICTON)*, pp. 1–4, Sep. 2024, doi: 10.1109/ICTON62926.2024.10647239.
 - [88] D. R. Chialvo, “Emergent complex neural dynamics,” *Nature Physics*, vol. 6, no. 10, pp. 744–750, Oct. 2010, doi: 10.1038/NPHYS1803.
 - [89] A. Levina, J. M. Herrmann, and T. Geisel, “Dynamical synapses causing self-organized criticality in neural networks,” *Nature Physics*, vol. 3, no. 12, pp. 857–860, Nov. 2007, doi: 10.1038/NPHYS758.
 - [90] N. Ganesh *et al.*, “Enhanced fluorescence emission from quantum dots on a photonic crystal surface,” *Nature Nanotechnology*, vol. 2, no. 8, pp. 515–520, Jul. 2007, doi: 10.1038/nnano.2007.216.
 - [91] J. Buhl, H. Lüder, G. Bichmann, T. Nolte, A. Petraru, and M. Gerken, “Resonance-Based Directional Light Emission from Organic Light-

Emitting Diodes: Comparing Integrated Nanopatterns and Color Conversion Waveguide Gratings,” *Advanced Photonics Research*, vol. 4, no. 2, Feb. 2023, doi: 10.1002/ADPR.202370003.